Photocatalyst-Independent Photoredox Ring-Opening Polymerization of *O*-Carboxyanhydrides: Stereocontrol and Mechanism

Yongliang Zhong, [a] Quanyou Feng, [a,b] Xiaoqian Wang, [a] Lei Yang, [b] Andrew G. Korovich, [c] Louis A. Madsen, [c] Rong Tong [a,*]

[a] Department of Chemical Engineering, Virginia Polytechnic Institute and State University, 635 Prices Fork Road, Blacksburg, Virginia, 24061, United States

[b] Key Laboratory for Organic Electronics and Information Displays, Jiangsu Key Laboratory for Biosensors, Institute of Advanced Materials, Jiangsu National Synergetic Innovation Center for Advanced Materials, Nanjing University of Posts and Telecommunications, 9 Wenyuan Road, Nanjing, 210023, China

[c] Department of Chemistry, Virginia Polytechnic Institute and State University, 1040 Drillfield Drive, Blacksburg, Virginia, 24061, United States

* Correspondence to: rtong@vt.edu

Supplementary information

Table of Contents

S1. Materials

S1.1 General

Bis(1,5-cyclooctadiene) nickel(0) (Ni(COD)$_2$), 2,2'-bipyridine (bpy), (1*R*,2*R*)-(-)-1,2-cyclohexanediamino-*N*,*N*''-bis(3,5-di-*t*-butylsalicylidene), bis[2-(2,4-difluorophenyl)-5-(trifluoromethyl)pyridine] iridium(III) hexafluorophosphate (**Ir-1**), chlorotris(triphenylphosphine) cobalt(I), (1*R*,2*R*)-(-)-1,2-cyclohexanediamino-*N*,*N*'-bis(3,5-di-t-butylsalicylidene) cobalt(II), cyclopentadienylcobalt dicarbonyl, dichloro[1,1'-bis(diphenylphosphino)ferrocene] cobalt(II), cobalt(II) dibromo(1,2-dimethoxyethane), anhydrous cobalt(II) chloride and *meso*-tetraphenylporphyrin cobalt(II) were purchased from Strem Chemicals (Newbury port, MA). *O*-benzyl-L-serine, *O*-benzyl-D-serine, L-glutamic acid-γ-benzyl ester and D-glutamic acid-γ-benzyl ester were purchased from Chem-Impex (Wood Dale, IL). L-phenylalanine and D-phenylalanine were purchased from Alfa Aesar (Haverhill, MA). Anhydrous tetrahydrofuran (THF) was dried by alumina columns and stored with 4Å molecular sieve in the dark bottle in the glove box (MBraun, Labstar Pro, < 1 ppm oxygen and moisture). Anhydrous THF-d_8, benzyl alcohol, hexane, benzene, toluene, diethyl ether, diisopropyl ether, pyridine and dichloromethane were dried and stored by 4Å molecular sieves in the glove box. All other chemicals were purchased from Sigma-Aldrich (St. Louis, MO) unless otherwise noted. All metal catalysts were synthesized in the glove box, characterized by NMR (except Ni and Co complexes), and stored in the glove box freezer (-30 °C).

S1.2 OCA monomers

L-PheOCA (L-**1**) and D-PheOCA (D-**1**),[1] L-Ser(Bn)OCA (L-**2**) and D-Ser(Bn)OCA (D-**2**),[2] L-Glu(Cbz)OCA (L-**3**) and D-Glu(Cbz)OCA (D-**3**),[3] L-LacOCA (L-**4**) and D-LacOCA (D-**4**),[4] and L-ManOCA (L-**5**) and D-ManOCA (D-**5**),[5] were synthesized and recrystallized according to the literature. [$^{13}C_2$]-**1** was prepared using phosgene-^{13}C in toluene solution (20 wt%, Sigma-Aldrich). [$^{13}C_5$]-**1** was synthesized from L-phenylalanine-1-^{13}C (Cambridge Isotope). All OCA monomers were recrystallized three times and stored in -30 °C freezer in the glove box.

S1.3 Zn complexes

Zn(HMDS)$_2$ (**Zn-1**) was prepared and distilled according to the literature.[6] (**NNO-1**)ZnN(TMS)$_2$ (**Zn-2**) was prepared according to the literature.[7, 8] β-diiminate Zn complexes (**Zn-3, Zn-4** and

Zn-5) were synthesized according to the literature.[9] All Zn complexes were stored in the glove box freezer (-30 °C).

S1.4 Ni complex

The Ni complex solution was prepared freshly prior to the reaction. In a glove box, Ni(COD)$_2$ (5.5 mg, 0.02 mmol) was mixed with bipyridyl ligand (e.g., bpy, 3.1 mg, 0.02 mmol) or tricyclophosphine (11.2 mg, 0.04 mmol) in THF solution (300 μL) at room temperature and stirred for 1-2 hour to ensure all Ni(COD)$_2$ dissolved. The Ni complex solution could be stored in the glove box freezer (-30 °C) no longer than seven days.

S1.5 Co(II) complexes

Co(HMDS)$_2$ was prepared and distilled according to the literature.[10, 11] The Co(II) complexes were prepared freshly prior to the polymerization. In general, Co(HMDS)$_2$ (2.9 mg, 7.6 μmol) was mixed with the ligand (e.g., bpy, 1.2 mg, 7.6 μmol; [Co]/[ligand] = 1/1) in toluene solution (1 mL) at room temperature and stirred for 2 hours to ensure all Co(HMDS)$_2$ dissolved. The Co complex solution could be stored in the glove box freezer (-30 °C) no longer than seven days. Note that both **Co-1** and **Co-2** can be recrystallized;[10, 11] and we do not observe significant reactivity between the recrystallized solid and freshly prepared solution.

S1.5.1 Synthesis of Co-1

In a glove box, Co(HMDS)$_2$ (2.9 mg, 7.6 μmol) was mixed with the bpy (1.2 mg, 7.6 μmol) in toluene solution (1 mL) at room temperature and stirred for 2 hours to ensure all Co(HMDS)$_2$ dissolved. The **Co-1** complex solution could be stored in the glove box freezer (-30 °C) no longer than seven days.

S1.5.2 Synthesis of Co-2

In a glove box, 5.0 mg (5.1 μL) anhydrous pyridine was mixed with toluene to prepare 1 mL solution. Co(HMDS)$_2$ (1.5 mg, 3.9 μmol) was mixed with 62.5 μL above pyridine in toluene solution, and was further diluted to 1 mL by adding 937.5 μL toluene at room temperature. The mixture was stirred for 2 hours to ensure all Co(HMDS)$_2$ dissolved. The **Co-2** complex solution could be stored in the glove box freezer (-30 °C) no longer than seven days.

S1.6 Hf and Zr complexes

Zr-1,[12] **Hf-1,**[12] **Hf-2,**[12] **Hf-3**[13] and **Hf-4**[14] complexes were synthesized according to the literature.

S2. Instrument and Characterization

S2.1 NMR spectroscopy

All room temperature NMR and homodecoupling ^{1}H NMR spectra were recorded on Agilent U4-DD2 (400 MHz) or Bruker Avance II (500 MHz). Low temperature ^{1}H and ^{13}C NMR spectra were measured on Bruker Avance III (600 MHz) after the inner temperature of the NMR machine reached -20 ^{o}C for 20 min. The samples were kept at -20 ^{o}C $\pm$ 5 ^{o}C with a dry ice/ethylene glycol bath before the low-temperature NMR acquisition. All ^{13}C NMR spectra are proton decoupled.

Diffusion Ordered NMR Spectroscopy (DOSY-NMR)

DOSY-NMR experiments were performed on a Bruker 400 MHz Avance III spectrometer using a Micro5 XYZ gradient probe, using a convection-compensated double stimulated echo sequence (Bruker dstegp3s), with a diffusion gradient pulse time (δ) of 4 ms, a diffusion encoding time (Δ) of 50 ms, and a linear gradient list of 16 points from 11.3 G*cm^{-1} to 141 G*cm^{-1}. The DOSY processing for each spectrum was performed using the Bayesian fit function in Mestrelab MestreNova, with a resolution factor of 0.10, 0 repetitions, and 64 points in the diffusion dimension. The identical diffusion peaks observed for the α-carbons of each of the two polymer block species (for all synthesized samples) confirm the successful synthesis of the block copolymers.

S2.2 FTIR spectroscopy

Fourier-transform infrared spectra were recorded on an Agilent Cary 630 FTIR spectrometer (Agilent Technologies Inc., Santa Clara, CA, USA) equipped with Diamond ATR and transmission sampling accessory.

Monomer conversion measurement:

A small aliquot of polymer solution (20 µL) was removed out of the glove box and quenched with 5% acetic acid / THF solution (20 µL). The mixture (~10 µL) was immediately dropped onto the FTIR-ATR diamond sampler and formed a film within 10-20 seconds for the spectra measurement. The peak at 1800 cm^{-1} is assigned as the anhydride bond stretch in OCA; the peak at 1760 cm^{-1} corresponds to the formation of the ester bond in the polymer. The monomer conversion was determined by the intensity ratio between 1760 cm^{-1} and 1800 cm^{-1}: conversion%

= I_{1760} / (I_{1760}+ I_{1800}). Note that the method is verified by the use of monomer/polymer mixture with predetermined concentrations (see Figure S40).

S2.3 Gel permeation chromatography (GPC)

GPC experiments were performed on a system equipped with an isocratic pump with degasser (Agilent 1260 series, Agilent Technologies, Santa Clara, CA, USA), Wyatt DAWN HELEOS multiangle laser light scattering (MALS) detector (GaAs 30 mW laser at λ=690nm), and an Wyatt Optilab rEX differential refractive index (DRI) detector with a 690 nm light source (Wyatt Technology, Santa Barbara, CA, USA). Separations were performed using serially connected size exclusion columns (100 Å, 500 Å, 10^3 Å, and 10^4 Å Phenogel columns, 5 μm, 300 × 4.6 mm, Phenomenex, Torrance, CA, USA) at 35 °C using THF as the mobile phase with a flow rate of 0.35 mL/min. The polymer molecular weight (MW) and molecular weight distribution (Đ) were determined using Zimm model fit of MALS-DRI data by ASTRA software (Version 6.1, Wyatt Technology). Data collection interval: 0.5 sec.

The refractive index increment dn/dc value was determined by the Wyatt Optilab rEX refractive index detector using ASTRA software dn/dc template (Version 6.1, Wyatt Technology). Five polymer / THF solutions with different concentrations were sequentially injected into the refractive index detector and the refractive index values were plotted versus concentration in ASTRA software. The slope of the linear fitting data is the dn/dc value.

The dn/dc values: poly(L-**1**), 0.1670; poly(L-**2**), 0.1377; poly(L-**3**), 0.1057; poly(L-**4**), 0.042; poly(L-**5**), 0.084.

S2.4 DSC

Differential scanning calorimetry (DSC) measurements were performed on TA Instruments DSC Q2000 instrument equipped with photocalorimeter accessory and RCS90 cooling system. Polymer samples in crimped aluminum pans were analyzed under nitrogen at a heating rate of 10 °C/min from 0 to 220 °C. Glass transition temperature (T_g) and melting temperature (T_m) were obtained and reported from the second heating run.

S2.5 ESI-MS

The ESI-MS analysis of air-sensitive samples followed the literature.[15] In brief, in a glove box, a 100 μL aliquote of the sample containing air-sensitive Co / Zn complexes were taken up into the 250 μL Hamilton gastight syringe. The syringe was punched into a 1 mL LC sampler vial capped with rubber septum to avoid the contact between needle and air, and was sealed in a zip bag. The zip bag was removed from the glove box and immediately analyzed by ESI-MS (Agilent 6220 Accurate-Mass Time-of-Flight LC/MS).

S2.6 Magnetic moment measurement

The magnetic moment μ of the cobalt complex was determined by Evans method on a Bruker Advance II 500 MHz NMR machine at 298 K in benzene/deuterated benzene or chloroform/CDCl$_3$.[16] Concentrations of cobalt complexes in benzene solution ranged from 5 to 10 mg/mL.

S2.7 Cyclic voltammetry

Cyclic voltammetries (CVs) were performed in a three-electrode measurement setup in a glove box with a Gamry Interface 1010 potentiostat/galvanostat at a potential sweep rate of 50 mV/s (the setup was previously described).[17] The measurements were carried out in a 20 mL Gamry Dr. Bob's electrochemical cell with approximately 1 mM concentration of Co complex in 0.1 M tetra-*n*-butylammonium hexafluorophosphate (TBAH) in anhydrous THF, fitted with a glassy carbon working electrode (3 mm in diameter, Gamry), a Ag/AgNO$_3$ reference electrode (a silver wire in 0.01 M AgNO$_3$ and 0.1 M TBAH in anhydrous acetonitrile), and a platinum wire (Gamry) counter electrode. Ferrocene (Fc) was measured as an internal standard,[18] and all potentials versus Fc$^+$/Fc were subsequently referenced to SCE (adding 380 mV) based on the reported method.[19]

S2.8 Calculation of redox properties of photocatalysts from electrochemical and photophysics studies

After calibrating the E_{ox} value (onset potential of oxidation; unit: V) against Fc$^+$/Fc in CV experiments, the HOMO energy (E_{HOMO}) value was evaluated according to the following equations:

E_{HOMO} (eV) = $-(E_{ox}(\text{vs Fc}^+/\text{Fc}) + 4.8)$ (eq. 1)

The LUMO energy of excited species can be determined using the following equations:

E_{LUMO} (eV) = $-(E_{HOMO} + E_g^{opt})$ (eq. 2)

where the E_g^{opt} indicates the optical energy gap. To calculate E_g^{opt}, the longest absorption wavelength λ_{onset} (nm) is used usually and is converted to eV according to the equation:

$E_g^{opt} = 1242/\lambda_{onset}$ (eq. 3)

As an approximation, the excited-state potentials of a photocatalyst (PC) are related to its ground state potentials and its zero–zero excitation energy ($E_{0,0}$).[20] $E_{0,0}$ can be approximated by the maximum emission wavelength (λ_{em}, nm) of the catalyst and is converted to eV according to the equation:

$E_{0,0} = 1242/\lambda_{em}$ (eq. 4)

Given the reduction potentials of the PC ($E_{1/2}[PC^{+1}/PC]$ and $E_{1/2}[PC/PC^{-1}]$) that can be measured by CVs, the excited-state of the photocatalyst (*PC) reduction potential can be calculated:

$E_{1/2}[PC^{+1}/*PC] = E_{1/2}[PC^{+1}/PC] - E_{0,0}$ (eq. 5)

$E_{1/2}[*PC/PC^{-1}] = E_{1/2}[PC/PC^{-1}] + E_{0,0}$ (eq. 6)

The equation (eq. 5) is used in the oxidative quenching cycle, equation (eq. 5) the reductive quenching cycle.[20, 21]

S3. Polymerization Procedures

S3.1 The photoredox polymerization of L-1 mediated by Co-1 / Zn-1 / BnOH

In a glove box, prior to the polymerization, all reagents were cooled in the cold trap equipped with a thermometer at -20 °C, which was cooled by the liquid nitrogen and ethanol in a dewar. The monomer **1** (15 mg, 150 μL of 100 mg/mL in THF, 0.078 mmol, 700 equiv.) was mixed with **Co-1** (9.9 μL of 3.7 mg/mL in toluene, 0.112 μmol, 1 equiv.), **Zn-1** (9.0 μL of 4.2 mg/mL in THF, 0.112 μmol, 1 equiv.), and BnOH (2.8 μL of 3.7 mg/mL in THF, 0.112 μmol, 1 equiv.) in a 7-mL glass vial equipped with a magnetic stir bar. The solution was stirred and irradiated with a 34 W blue LED lamp (Kessil KSH150B LED Grow Light 150) at -15 ± 5 °C (with a cooling fan to keep the reaction temperature) over 1-2 hours. The OCA monomer conversion was monitored by FTIR (see S2.2). The resulted polymer's MW and Đ were directly measured by GPC after the polymerization.

S3.2 The photoredox block copolymerization of L-1 and L-2 mediated by Co-1 / Zn-1 / BnOH

In a glove box, L-**1** (15 mg, 150 μL of 100 mg/mL in THF, 0.078 mmol, 400 equiv.) was mixed with **Co-1** (21.2 μL toluene solution, 0.195 μmol, 1 equiv.), **Zn-1** (23.8 μL of 3.2 mg/mL in THF, 0.195 μmol, 1 equiv.), and BnOH (13.2 μL of 1.6 mg/mL in THF, 0.195 μmol, 1 equiv.) in a 7-mL glass vial equipped with a magnetic stir bar at room temperature. The solution was stirred and irradiated with a 34 W blue LED lamp (Kessil KSH150B LED Grow Light 150) around -20 °C (with a cooling fan to keep the reaction temperature) for 30 min. Upon the quantitative conversion of **1** was achieved, measured by FTIR, an aliquot of poly(L-**1**) solution (50 μL) was taken out of the box for GPC characterization. The monomer L-**2** (32.5 μL of 100 mg/mL in THF, 14.6 μmol, 100 equiv.) was added into the remaining mixture and stirred at -15 °C ± 5 °C with irradiation over another 1-3 hours. The monomer conversion was measured by FTIR. The obtained copolymer's MW and Đ were measured by GPC, and ^{1}H NMR. The copolymer's MW from NMR was calculated based on the integration ratio between α-proton of two OCAs and the M_n of poly(**1**) obtained from GPC.

S3.3 The photoredox polymerization of racemic OCA (*rac*-1) mediated by Co-1 / Hf-1

In a glove box, prior to the polymerization, all reagents were cooled in the cold trap equipped with a thermometer at -15 to -20 °C, which was cooled by the liquid nitrogen and ethanol in a dewar. L-**1** (15 mg, 150 μL of 100 mg/mL, 0.078 mmol, 200 equiv.) and D-**1** (15 mg, 150 μL of 100 mg/mL, 0.078 mmol, 200 equiv.) were mixed **Co-1** (51.1 μL of 2.9 mg/mL in toluene, 0.391 μmol, 1 equiv.) and **Hf-1** (28.1 μL of 12.2 mg/mL in THF, 0.391 μmol, 1 equiv.) in a 7-mL glass vial equipped with a magnetic stir bar at -15 °C. The solution was stirred and irradiated with a 34 W blue LED lamp (Kessil KSH150B LED Grow Light 150) around -15 °C ± 5 °C (with a cooling fan to keep the reaction temperature) over 1 hour. The OCA monomer conversion was monitored by FTIR. The resulted polymer's MW and $Đ$ were directly measured by GPC after the polymerization. The P_r or P_m values of poly(*rac*-**1**) were determined by ^{1}H and ^{13}C NMR spectra.

S3.4 Other ring-opening polymerization techniques

The ring-opening polymerizations of OCAs initiated by (bpy)Ni(COD) / Zn(HMDS)$_2$ / BnOH / **Ir-1** was reported in our previous work.[22]

S3.5 Kinetic study of the photoredox polymerization of OCA

In a glove box, the monomer L-**1** (10 mg, 100 μL of 100 mg/mL in THF, 52.1 μmol, 600 equiv.) was mixed with **Co-1** (6.6 μL of 5.0 mg/mL in toluene, 86.8 nmol, 1 equiv.), **Zn-1** (7.3 μL of 4.6 mg/mL in THF, 86.8 nmol, 1 equiv.), and BnOH (3.0 μL of 3.1 mg/mL in THF, 86.8 nmol, 1 equiv.) in a 7-mL glass vial equipped with a magnetic stir bar. The mixture was stirred at -15 °C ± 5 °C with irradiation in a manner similar to that in **S3.1**. At the predetermined time point, 20 μL of the polymer solution was taken out and immediately analyzed by FTIR.

All the catalysts' concentrations were varied, and the semi-logarithmic plots were drawn to calculate the kinetic constants and reaction orders according to the kinetic laws:

$-d[\mathbf{1}]/dt = k_{app}\cdot[\mathbf{1}]$ (eq. 7)

where k_{app} is the apparent first-order rate constant. For eq.7 it equals to

$\ln[\mathbf{1}]_0/\ln[\mathbf{1}]_t = k_{app}\cdot t + C$ (eq. 8)

thus $\ln[\mathbf{1}]_0/\ln[\mathbf{1}]_t$ versus t was plotted.

S4. Computation studies

All calculations were carried out using the Gaussian 09 D.01 program. Geometry optimization was performed with hybrid density functional theory (DFT) using Becke's three-parameter hybrid exchange-correlation functional (B3LYP) 6-31G(d) basis set for C, H, N, Si, whereas for Co the pseudo potential LanL2Dz was used. Thermodynamic corrections were also applied to determine the energies of the species at a temperature of 298.15 K. Linear response time dependent DFT (TD-DFT) calculations were carried out based on B3LYP. All computation results see S7.

S5. Supplementary Tables

Table S1. Optimization of reaction conditions for photoredox ring-opening polymerization of L-1. [a]
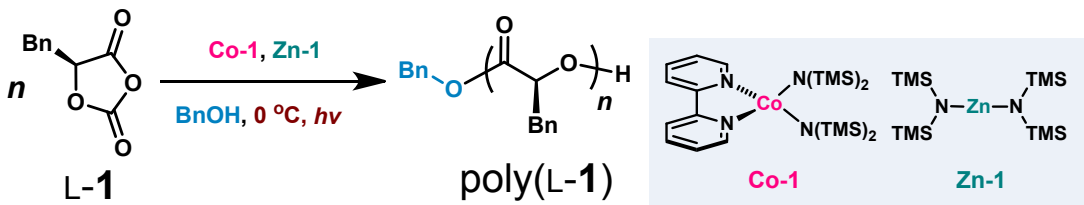
[L-**1**]/[**Zn-1**]/[**Co-1**]/[BnOH] = 700/1/1/1; 1 h. Expected MW: 103.7 kDa

Entry	Conditions	Conv. (%) [b]	M_n (kDa) [c]	MW_{theo} (kDa)	Đ [c]
1	As shown	100	119.3	103.7	1.04
2	−15 °C	100	124.8	103.7	1.08
3	r.t., 2 h	100	84.3	103.7	1.04
4	No **Co-1**	33	81.7	34.2	1.09
5	No **Zn-1**	19	16.9	19.7	1.41
6	Only **Co-1**	11	23.6	11.4	1.35
7	Only **Zn-1**	39	84.3	40.4	1.08
8	**Co-1** + light	13	14.5	13.5	3.50
9	No BnOH	67	108.7	69.5	1.05
10	No light	69	96.9	71.6	1.06
11	No light, -30 °C, 12 h	80	110.1	82.9	1.11
12	No light, 3 h [d]	51	49.1	68.0	2.83
13	Sunlight instead of LED	100	100.7	103.7	1.03

a Abbreviations: Conv., monomer conversion; Temp., temperature; M_n, number-average molecular weight; MW_{theo}, molecular weights calculated on the basis of monomer conversion; Đ, molecular weight distribution. For all polymerization reactions, [**Co-1**] = [**Zn-1**] = [BnOH].

b Determined from the intensity of the Fourier transform infrared peak at 1805 cm^{-1}, which corresponds to the anhydride group of the *O*-carboxyanhydride.

c Determined by gel-permeation chromatography.

d [L-**1**]/[**Zn-1**]/[**Co-1**]/[BnOH] = 900/1/1/1.

Discussion:

Only Zn complex (Table S1, entry 7), or Zn alkoxide (entry 4) could initiate ROP with a conversion of 39% or 33%, respectively. The ROP also proceeded to some extent without light (entries 10-12), with incomplete monomer conversions over the time (polymerization likely stopped). It seems that Co/Zn complexes could initiate ROP in an uncontrolled manner without any external stimulus. Based on our previous reports,[22, 23] Zn itself initiates ROP of OCAs via conventional coordination-insertion mechanism of ROP. Co complex may mediate oxidative insertion as Ni or Co complexes for NCA polymerization but in an inefficient way (entry 5).[24, 25] However, Co-mediated decarboxylation is necessary for the chain propagation especially for high-MW polymer synthesis, as shown in Figure 1a. The inefficient decarboxylation, as previously investigated,[22, 23] is the problem for chain propagation in the ROP of OCAs to synthesize high-MW polyesters; and such problem can be overcome using our photoredox ROP approach.

Table S2. Measurement of residue metal concentrations in polymers after purification by inductively coupled plasma mass spectrometry (ICP-MS) [a]

	[Co] (ppb)	[Zn] (ppb)
HNO₃	0	18.6
Co-1/Zn-1 mediated Photoredox ROP of L-**1**	7.4	8.3

[a] Abbreviations: ROP, ring-opening polymerizations; ppb: parts per billion, that equals to μg/L. For ICP-MS studies, the polymer was dissolved in 10% HNO₃ at 70-80 ℃ at a concentration of 1 mg/mL for three days in order to complete degrade the polymer. The obtained polymer solution was analyzed by ICP-MS.

**Table S3. Photoredox ring-opening polymerization of various *O*-carboxyanhydride monomers mediated by Co-1/Zn-1** [a]

Entry	Monomer	FR	Temp. (°C)	Time (h)	Conv. (%) [b]	M_n (kDa) [c]	MW_{cal} (kDa)	Đ [c]
1	L-**2**	400	r.t.	3	100	77.4	71.3	1.09
2	L-**2**	300	-15	1	100	55.7	35.7	1.01
3	L-**2**	400	-15	1.5	100	79.6	53.4	1.03
4	L-**2**	500	-15	2	100	92.9	71.3	1.01
5	L-**3**	400	r.t.	1	100	90.4	88.1	1.04
6	L-**3**	300	-15	0.5	100	72.6	66.1	1.08
7	L-**3**	500	-15	1	100	122.8	110.1	1.08
8	L-**3**	700	-15	3	100	151.4	154.1	1.04
9	L-**4**	400	r.t.	1	100	33.2	28.9	1.02
10	L-**4**	200	-15	0.5	100	13.9	14.5	1.01
11	L-**4**	300	-15	1	100	19.5	21.7	1.01
12	L-**4**	400	-15	1.5	100	34.6	28.9	1.05
13	L-**5**	200	-15	1	100	23.7	26.9	1.08
14	L-**5**	300	-15	1.5	100	37.7	40.3	1.02
15	L-**5**	400	-15	2.5	100	55.2	53.7	1.07

[a] Abbreviations: FR, the feeding ratio of [OCA]/[Zn]; Conv., monomer conversion; Temp., temperature; M_n, number-average molecular weight; MW_{cal}, molecular weight calculated from the ratio of the amount of monomer to the amount of catalyst; Đ, molecular weight distribution; r.t., room temperature. For all polymerization reactions, [**Co-1**] = [**Zn-1**] = [BnOH].

[b] Determined from the intensity of the Fourier transform infrared peak at 1805 cm^{-1}, which corresponds to the anhydride group of the OCA.

[c] Determined by gel-permeation chromatography.

Table S4. Photoredox block copolymerization of various _O_-carboxyanhydrides [a]
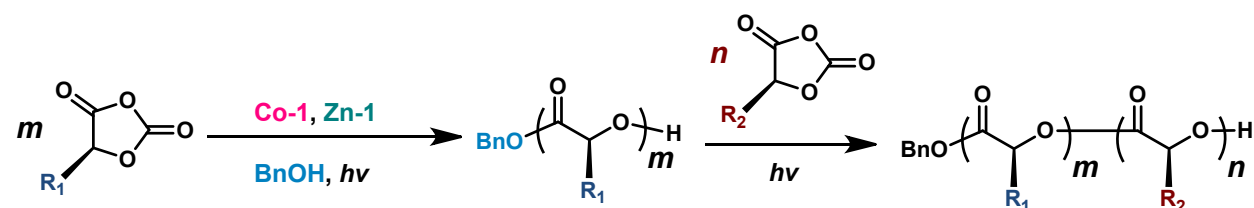
| Entry	Monomers	FR	Temp. (°C)	Time (h)	Conv. (%) [b]	M_n (M_n-b1) (kDa) [c]	MW$_{cal}$ (MW$_{cal}$-b1) (kDa)	Đ (Đ-b1) [c]
1	**1/2**	400/100	r.t.	0.5/3	100	78.2 (67.0)	77.1 (59.3)	1.07 (1.03)
2	**1/3**	400/100	r.t.	0.5/3	100	75.3 (67.0)	81.3 (59.3)	1.07 (1.03)
3	**1/4**	400/200	r.t.	0.5/3	100	75.8 (67.0)	73.7 (59.3)	1.04 (1.03)
4	**1/5**	400/100	-15	0.5/3	100	82.4 (63.5)	72.6 (59.3)	1.01 (1.02)
5	**2/4**	400/100	r.t.	3/3	100	78.6 (77.4)	78.5 (71.3)	1.05 (1.03)
6	**3/2**	400/100	r.t.	1/3	100	130.9 (90.4)	105.9 (88.1)	1.02 (1.04)
7	**4/3**	400/100	r.t.	1/3	100	56.3 (33.2)	50.9 (28.9)	1.05 (1.02)
8	**1/3/4**	400/100/100	r.t.	0.5/3/3	100	90.7 (60.5)	88.5 (59.3)	1.02 (1.03)

[a] Abbreviations: OCA, _O_-carboxyanhydride; FR, the feeding ratio of [OCA]/[Zn]; Conv., monomer conversion; Temp., temperature; M_n, number-average molecular weight; MW$_{cal}$, molecular weight calculated from the ratio of the amount of monomer to the amount of catalyst; Đ, molecular weight distribution; r.t., room temperature. M_n-b1 and Đ-b1 refer to the molecular weight and molecular weight distribution of the first block polymer. For all polymerization reactions, [**Co-1**] = [**Zn-1**] = [BnOH].

[b] Determined from the intensity of the Fourier transform infrared peak at 1805 cm^{-1}, which corresponds to the anhydride group of the OCA.

[c] For copolymers, M_n-b1, Đ, and Đ-b1 were determined by gel-permeation chromatography; M_n of the block copolymer was calculated on the basis of the ^{1}H NMR integration ratio of the α-methine peaks of the different blocks.

Table S5. Effects of the addition of precious-metal photocatalysts and radical scavengers into the photoredox ring-opening polymerization of L-1 [a]
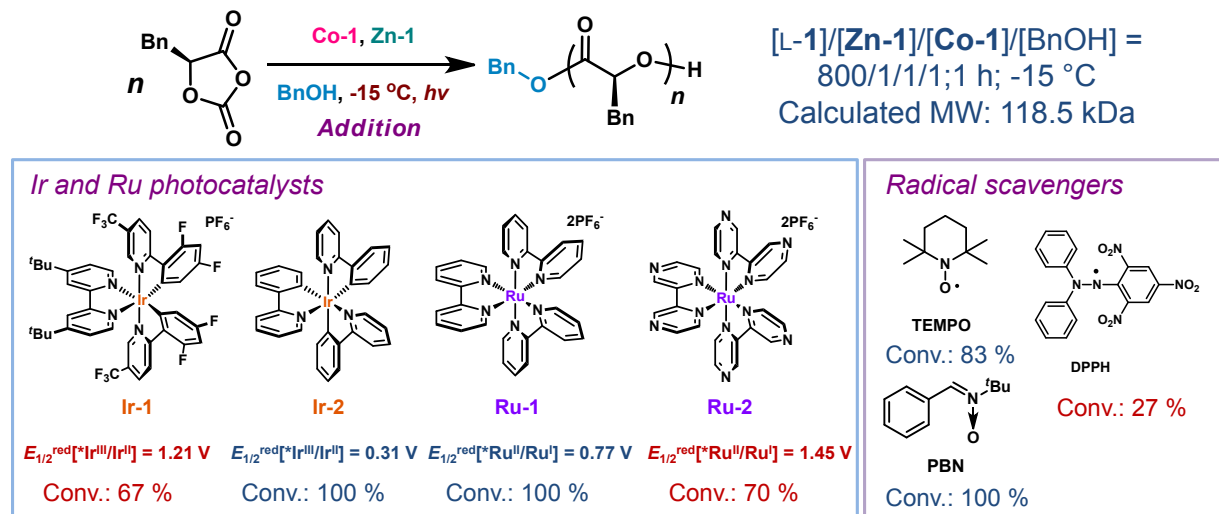
Entry	Addition (eq.)	Conv. (%) [b]	M_n (kDa) [c]	MW$_{theo}$ (kDa)	Đ [c]
1	None	100	141.3	118.5	1.08
2	**Ir-1** (0.1)	67.0	90.0	79.4	1.03
3	**Ir-2** (0.1)	100	158.4	118.5	1.03
4	**Ru-1** (0.1)	100	132.2	118.5	1.09
5	**Ru-2** (0.1)	70.2	118.9	83.2	1.13
6	**TEMPO** (10)	83.1	159.5	98.4	1.02
7	**PBN** (10)	100	167.0	118.5	1.04
8	**DPPH** (10)	26.9	N.D	31.9	N.D.

[a] Abbreviations: Conv., monomer conversion; Temp., temperature; M_n, number-average molecular weight; MW$_{theo}$, molecular weights calculated on the basis of monomer conversion; Đ, molecular weight distribution. TEMPO, 2,2,6,6-tetramethylpiperidine-N-oxyl; PBN, N-$tert$-butyl-α-phenylnitrone; DPPH, 2,2-diphenyl-1-picrylhydrazyl. For all polymerization reactions, [**Co-1**] = [**Zn-1**] = [BnOH]. $E_{1/2}^{red}$ values for photocatalysts are based on references.[26]

[b] Determined from the intensity of the Fourier transform infrared peak at 1805 cm^{-1}, which corresponds to the anhydride group of the O-carboxyanhydride.

[c] Determined by gel-permeation chromatography.

Table S6. Redox and photophysical properties of Co complexes. [a]

Entry	$E_{1/2}$ [Co^{III}/Co^{II}] (V vs SCE) [b]	$E_{1/2}$ [Co^{IV}/Co^{III}] (V vs SCE) [b]	Absorption (λabs, nm) [c]	Emission (λem, nm) [d]	$E_{0,0}$ (eV) [e]	$E_{1/2}$[*Co^{III}/Co^{II}] (V vs SCE) [e]	$E_{1/2}$[Co^{III}/*Co^{II}] (V vs SCE) [e]
Co-1	0.746	N/A	397	501	2.48	N/A	-1.734
1 / Co-1	0.688	1.308	391	567	2.19	2.878	N/A
1 / Co-1 / Zn-1 / BnOH -15 °C, *hv*	0.674	N/A	398	500	2.48	N/A	-1.806
Co(HMDS)$_2$	N/A	N/A	319	N/A	N/A	N/A	N/A
Boc-Pro-OH	0.951	N/A	N.D.	N.D.	N/A	N/A	N/A
Z-Phe-OH	0.832	N/A	N.D.	N.D.	N/A	N/A	N/A

[a] Abbreviations: SCE, saturated calomel electrode; $E_{0,0}$, zero–zero excitation energy, which approximates the maximum emission wavelength energy .

[b] Determined from the cyclic voltammetry studies.

[c] Determined from UV/Vis studies, see Fig. 2B.

[d] Determined from fluorescence spectroscopy, see Fig. 2D.

[e] Calculated based on the equations in S2.8.

Discussion:

The estimated $E_{1/2}^{red}$ (*Co^{III}/Co^{II}) value of **1/Co-1** reaction mixture is relatively higher than many reported Ir and Ru photocatalysts. We found that photocatalysts with higher excited state reduction potentials, such as **Ir-1** or Ru(bpz)$_3^{2+}$, could inhibit the polymerization, which suggested that the actual $E_{1/2}^{red}$ (*Co^{III}/Co^{II}) value should be at least over 1V over SCE (see Table 3 reduction potentials comparison of four photocatalysts).

Table S7. Photoredox polymerization of L-1 at -15 °C in the presence of Co and various metal-alkoxide complexes. [a]
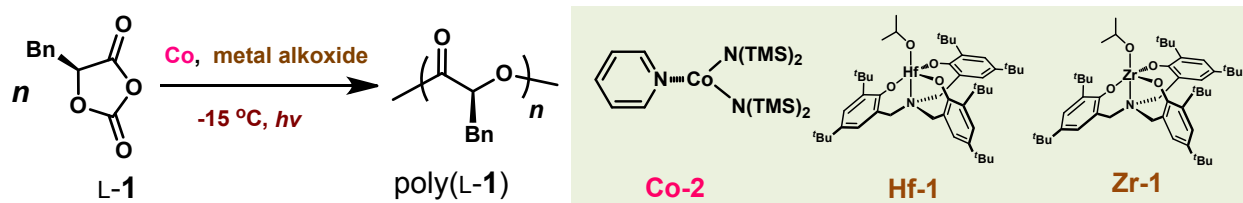
| Entry	Catalyst	FR [b]	Conv. (%) [c]	M_n (kDa) [d]	MW$_{cal}$ (kDa)	Đ [d]
1	**Co-1** / Hf(O^{i}Pr)$_4$	100	0	N.D.	14.8	N.D.
2	**Co-2** / Hf(O^{i}Pr)$_4$	100	100	67.5	14.8	1.01
3	**Co-2** / Hf(O^{i}Pr)$_4$	300	100	68.6	44.4	1.02
4	**Co-2** / Hf(O^{i}Pr)$_4$	400	<10	N.D.	59.2	N.D.
5	(bpy)Ni(COD) / **Ir-1** / Hf(O^{i}Pr)$_4$	50	0	N.D.	7.4	N.D.
6	Hf(O^{i}Pr)$_4$	50	0	N.D.	7.4	N.D.
7	**Co-2** / Y(O^{i}Pr)$_3$	50	0	N.D.	7.4	N.D.
8	**Co-2** / Zr(O^{i}Pr)$_4$	50	0	N.D.	7.4	N.D.
9	**Co-2** / Mg(HMDS)$_2$/BnOH	50	0	N.D.	7.4	N.D.
10	**Co-2** / **Hf-1**	300	100	87.9	44.4	1.05
11	**Co-2** / **Hf-1**	500	100	91.0	74.0	1.02
12	**Co-2** / **Zr-1**	300	50	N.D.	44.4	N.D.

[a] Abbreviations: FR, the feeding ratio of [**1**]/[**Zn-1**]; Conv., monomer conversion; M_n, number-average molecular weight; Đ, molecular weight distribution; COD, cyclooctadiene; MW$_{cal}$, molecular weight calculated from the ratio of the amount of monomer to the catalyst. For all polymerizations, [Co] = [metal alkoxide].

[b] FR is the ratio of the amount of monomer to the amount of metal alkoxide complex.

[c] Determined from the intensity of the Fourier transform infrared peak at 1805 cm^{-1}, which corresponds to the anhydride group of the *O*-carboxyanhydride.

[d] Determined by gel-permeation chromatography.

Table S8. Stereoselective photoredox ring-opening polymerization of racemic monomer 1 mediated by Co/Zn and Co/Hf complexes [a]
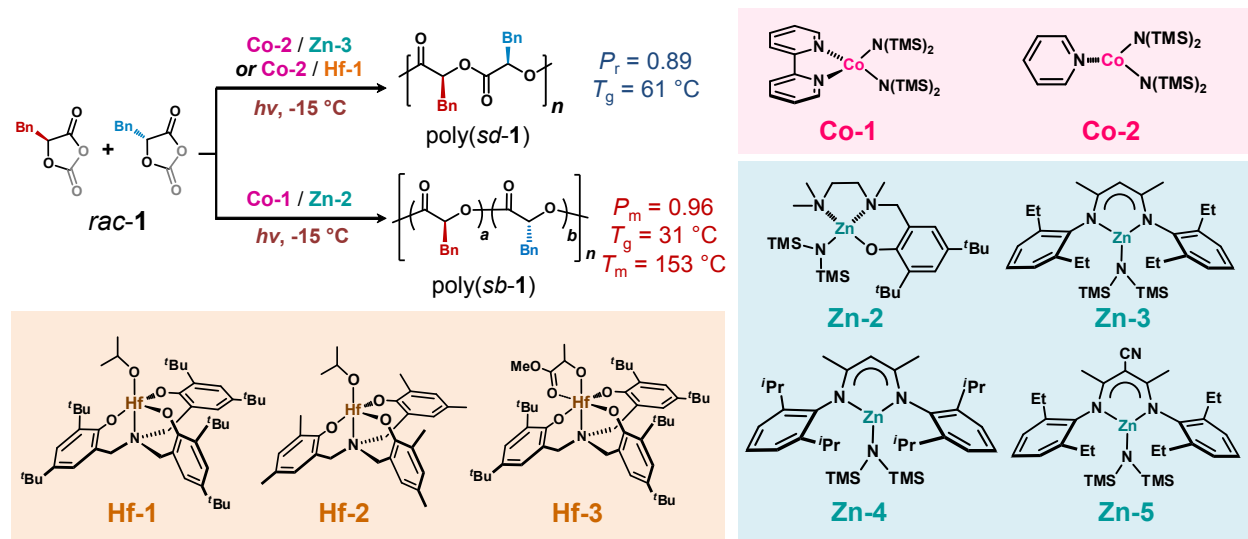
Entry	Co / Zn (Hf) complexes	[L-1]/[D-1]	Time (h)	Conv. (%) [b]	M_n (kDa) [c]	MW$_{cal}$ (kDa)	$Đ$ [c]	P_m / P_r [d]
1	**Co-1 / Zn-2**	150/150	1	100	67.0	44.5	1.05	0.96 / −
2	**Co-2 / Zn-3**	100/100	1	100	57.7	29.7	1.14	− / 0.88
3	**Co-1 / Zn-1**	200/200	2	< 5	N.D.	59.3	N.D.	N.D.
4	**Co-2 / Zn-1**	200/200	2	24	N.D.	59.3	N.D.	N.D.
5	**Co-1 / Zn-3**	100/100	2	100	45.5	29.7	1.28	− / 0.76
6 [e]	**Zn-2**	100/100	12	< 5	N.D.	29.7	N.D.	N.D.
7 [e]	**Zn-3**	100/100	12	31	11.7	29.7	1.13	N.D.
8	**Co-2 / Zn-4**	100/100	2	100	63.2	29.7	1.37	− / 0.84
9	**Co-2 / Zn-5**	100/100	1	100	85.9	29.7	1.03	− / 0.78
10	**Co-2 / Hf-1**	200/200	1	100	105.6	59.3	1.06	− / 0.89
11	**Co-2 / Hf-1**	150/150	1	100	96.6	44.5	1.06	− / 0.89
12	**Co-2 / Hf-1**	100/200	1	100	102.9	44.5	1.03	− / 0.77
13	**Co-2 / Hf-1**	200/100	1	100	102.5	44.5	1.03	− / 0.77
14	**Co-1 / Hf-1**	100/100	1	<5	N.D.	29.7	N.D.	N.D.
15	**Co-2 / Hf-2**	100/100	1	100	49.8	29.7	1.03	− / 0.81
16 [e]	**Hf-1**	25/25	24	16	N.D.	7.5	N.D.	N.D.
17 [e]	**Hf-3**	10/10	96	92	2.6	3.0	1.01	− / 0.65

^{a} Abbreviations: Conv., monomer conversion; M_n, number-average molecular weight; $Đ$, molecular weight distribution; MW_{cal}, molecular weight calculated from the ratio of the amount of monomer to the catalyst; P_m, maximum probability of meso dyad formation; P_r, maximum probability of racemic dyad formation. Polymerization conditions: [Co] = [Zn] = [BnOH] or [Co] = [Hf] at -15 °C.

^{b} Determined from the intensity of the Fourier transform infrared peak at 1805 cm^{-1}, which corresponds to the anhydride group of the O-carboxyanhydride.

^{c} Determined by gel-permeation chromatography.

^{d} Determined by ^{13}C NMR spectroscopy.

^{e} Reaction at room temperature without light irradiation.

Table S9. Stereoselective photoredox ring-opening polymerization of racemic *O*-carboxyanhydrides mediated by Co/Zn and Co/Hf complexes [a]

Entry	Co / Zn (Hf) complexes	OCA	FR	Time (h)	Conv. (%) [b]	M_n (kDa) [c]	MW$_{cal}$ (kDa)	Đ [c]	P_m / P_r [d]
1	**Co-1 / Zn-2**	*rac*-2	100	1	100	20.0	17.9	1.03	0.81 / −
2	**Co-2 / Zn-3**	*rac*-2	200	1	100	26.1	35.7	1.05	0.64 / −
3	**Co-1 / Hf-1**	*rac*-2	100	1	100	26.4	17.9	1.05	0.63 / −
4	**Co-1 / Zn-2**	*rac*-4	200	1	100	16.3	14.5	1.09	0.90 / −
5	**Co-2 / Zn-3**	*rac*-4	200	1	100	17.6	14.5	1.07	0.71 / −
6	**Co-2 / Hf-1**	*rac*-4	400	1	100	32.8	28.9	1.04	0.74 / −
7 [e]	**Hf-1**	*rac*-4	200	2	100	50.0	14.4	1.11	− / 0.82
8	**Co-1 / Zn-2**	*rac*-3	200	1	100	46.5	44.1	1.03	0.94 / −
9	**Co-2 / Zn-3**	*rac*-3	200	1	100	39.3	44.1	1.09	− / 0.63
10	**Co-2 / Hf-1**	*rac*-3	200	1	100	38.0	44.1	1.07	− / 0.78
11	**Co-1 / Zn-2**	*rac*-5	100	2	86	8.9	13.5	1.05	0.77 / −
12	**Co-2 / Zn-3**	*rac*-5	100	2	100	8.4	13.5	1.08	− / 0.82
13	**Co-2 / Hf-1**	*rac*-5	100	1	100	27.7	13.5	1.19	0.97 / −
14	**Co-2 / Hf-4**	*rac*-5	100	3	93	14.2	13.5	1.07	− / 0.91

[a] Abbreviations: OCA, *O*-carboxyanhydride; FR, the feeding ratio of monomer to catalyst; Conv., monomer conversion; M_n, number-average molecular weight; Đ, molecular weight distribution; MW$_{cal}$, molecular weight calculated from the ratio of the amount of monomer to the catalyst; P_m, maximum probability of meso dyad formation; P_r, maximum probability of racemic dyad formation. Polymerization conditions: [Co] = [Zn] = [BnOH] or [Co] = [Hf]; [L-OCA]/[D-OCA] = 1/1 at -15 °C.

[b] Determined from the intensity of the Fourier transform infrared peak at 1805 cm^{-1}, which corresponds to the anhydride group of the *O*-carboxyanhydride.

[c] Determined by gel-permeation chromatography.

[d] Determined by ^{13}C NMR spectroscopy.

[e] Reaction at room temperature without light irradiation.

Table S10. Phase transition temperatures of stereoregular polyesters prepared by Co-assisted photoredox ring-opening polymerization of *O*-carboxyanhydrides [a]

Entry	polymer	P_m / P_r [b]	M_n (kDa) [c]	$Đ$ [c]	T_g / T_m (°C) [d]
1	poly(L-**1**)	1 / −	187.6	1.07	51 / −
2	poly(*sb*-**1**)	0.96 / −	67.0	1.05	31 / 153
3	poly(*sd*-**1**)	− / 0.89	105.6	1.06	61 / −
4	poly(L-**2**)	1 / −	79.6	1.03	8 / −
5	poly(*sb*-**2**)	0.81 / −	20.0	1.03	8 / −
6	poly(L-**3**)	1 / −	122.8	1.08	8 / −
7	poly(*sb*-**3**)	0.94 / −	46.5	1.03	4 / −
8	poly(*sd*-**3**)	− / 0.78	38.0	1.07	6 / −
9	poly(L-**4**)	1 / −	33.2	1.02	− / 173
10	poly(*sb*-**4**)	0.90 / −	16.3	1.09	50 / 146
11	poly(L-**5**)	1 / −	55.2	1.07	91 / 213
12	poly(*sb*-**5**)	0.77 / −	8.9	1.05	85 / −
13	poly(*sb*-**5**)	0.97 / −	27.7	1.19	97 / −
14	poly(*sd*-**5**)	− / 0.82	8.4	1.08	76 / −
15	poly(*sd*-**5**)	− / 0.91	14.2	1.07	74 / 145
16	poly(*sc*-**5**) [e]	1 / −	55.2	1.07	86 / 180

[a] Abbreviations: M_n, number-average molecular weight; $Đ$, molecular weight distribution; P_m, maximum probability of meso dyad formation; P_r, maximum probability of racemic dyad formation; T_g, glass transition temperature; T_m, melting temperature; *sb*, stereoblock; *sd*, syndiotactic; *sc*, stereocomplex.

[b] Determined by ^{13}C NMR spectroscopy.

[c] Determined by gel-permeation chromatography.

[d] Determined by differential scanning calorimetry.

[e] Prepared by 1/1 mixing of poly(L-**5**) and poly(D-**5**) with similar MWs.

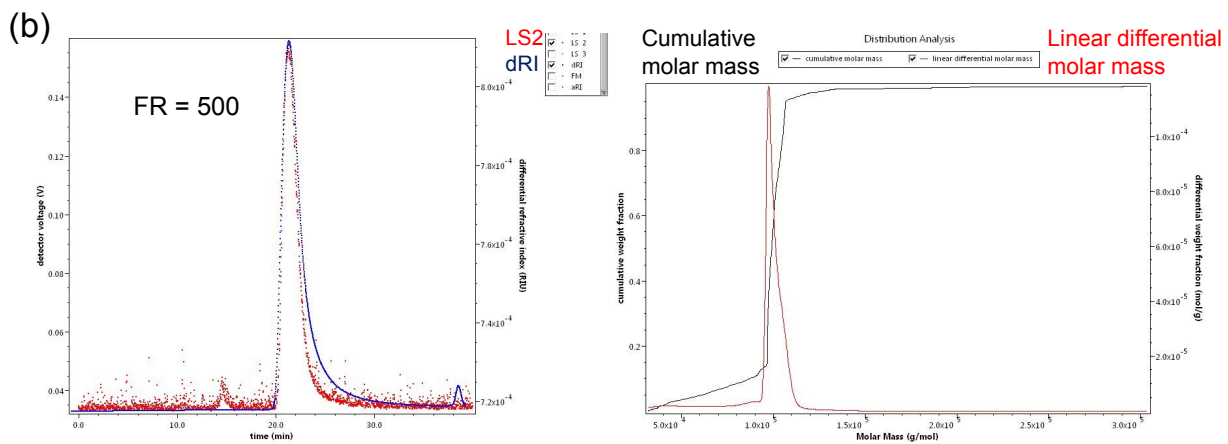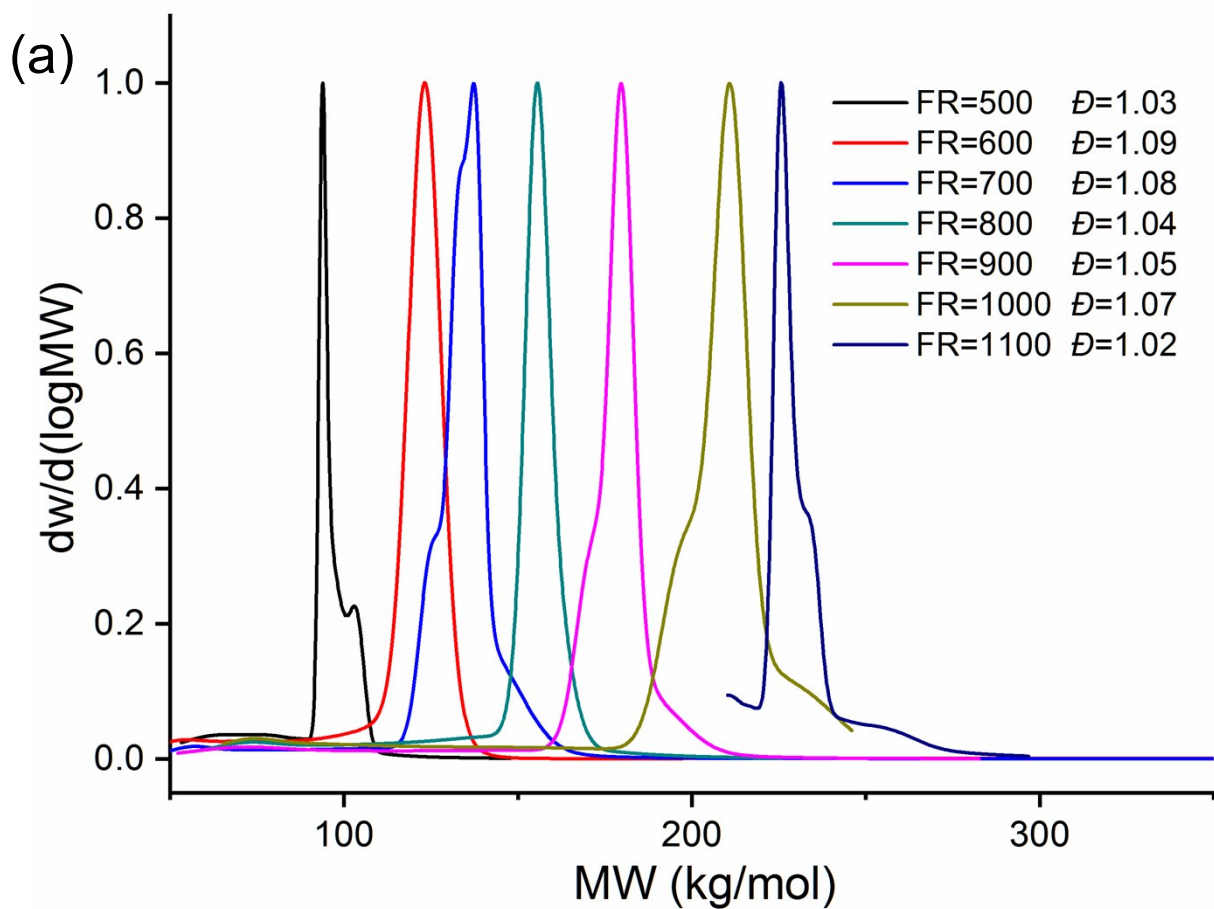**Table S11. Multiple runs of Co/Zn-mediated polymerization of L-1, measured by gel-permeation chromatography** [a]

Entry	FR	Temp. (°C)	Time (h)	Conv. (%) [b]	M_n (kDa) [c]	MW_{cal} (kDa)	$Đ$ [c]
1	1000	-15	3	100	188.6	148.1	1.06
2	1000	-15	3	100	189.1	148.1	1.05
3	1000	-15	3	100	187.5	148.1	1.08

[a] Abbreviations: FR, the feeding ratio of [OCA]/[Zn]; Conv., monomer conversion; Temp., temperature; M_n, number-average molecular weight; MW_{cal}, molecular weight calculated from the ratio of the amount of monomer to the amount of catalyst; $Đ$, molecular weight distribution. For all polymerization reactions, [**Co-1**] = [**Zn-1**] = [BnOH].

[b] Determined from the intensity of the Fourier transform infrared peak at 1805 cm^{-1}, which corresponds to the anhydride group of the OCA.

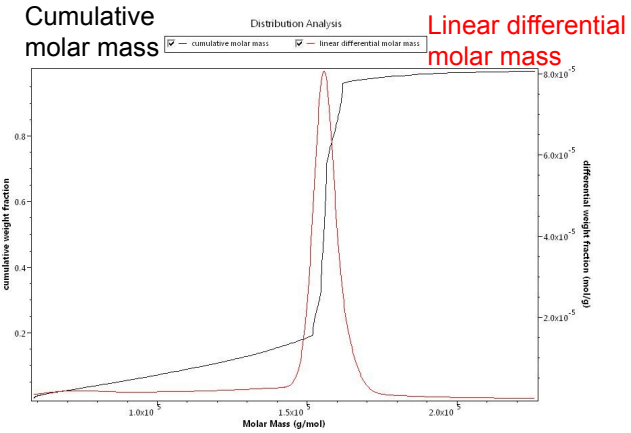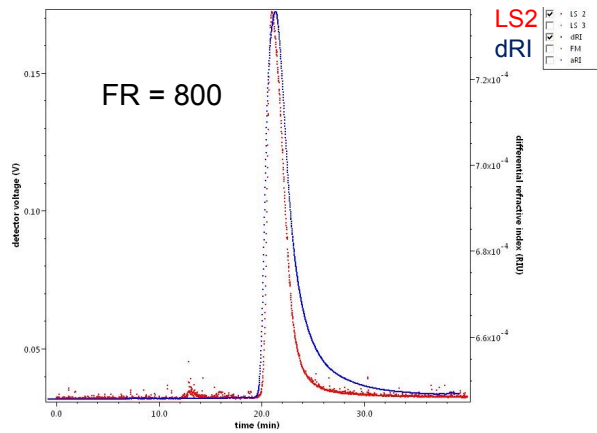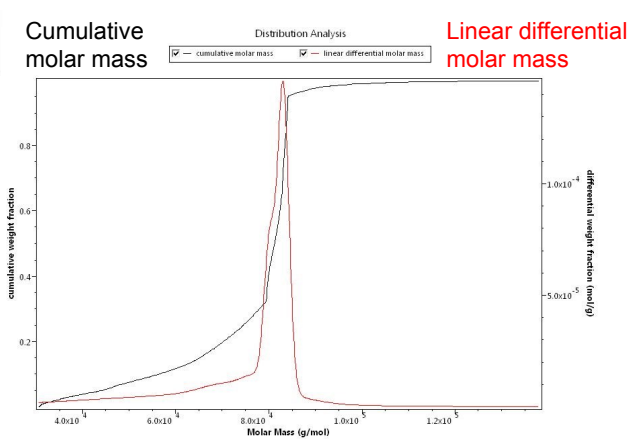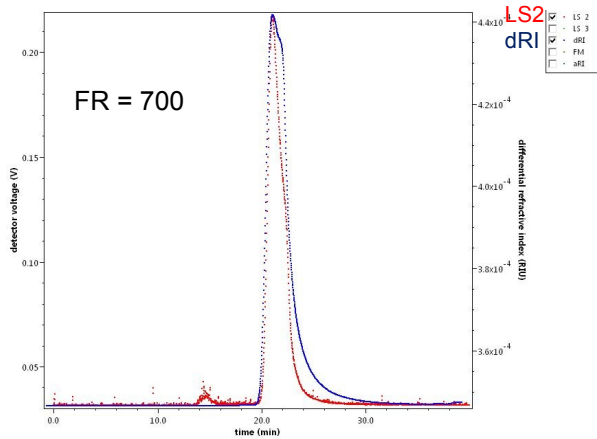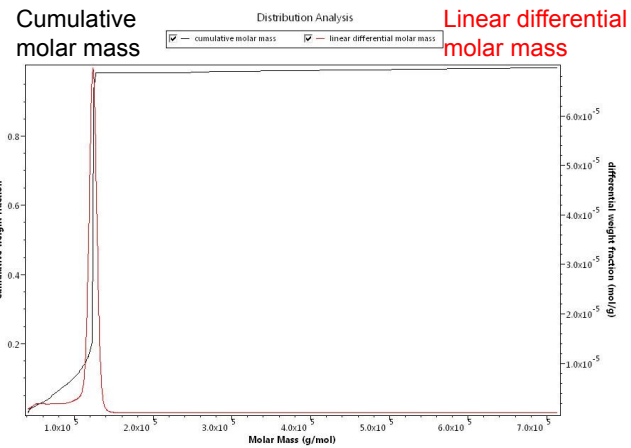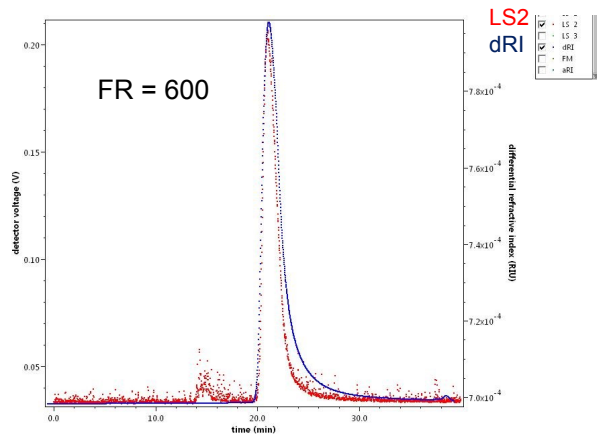[c] Determined by gel-permeation chromatography.
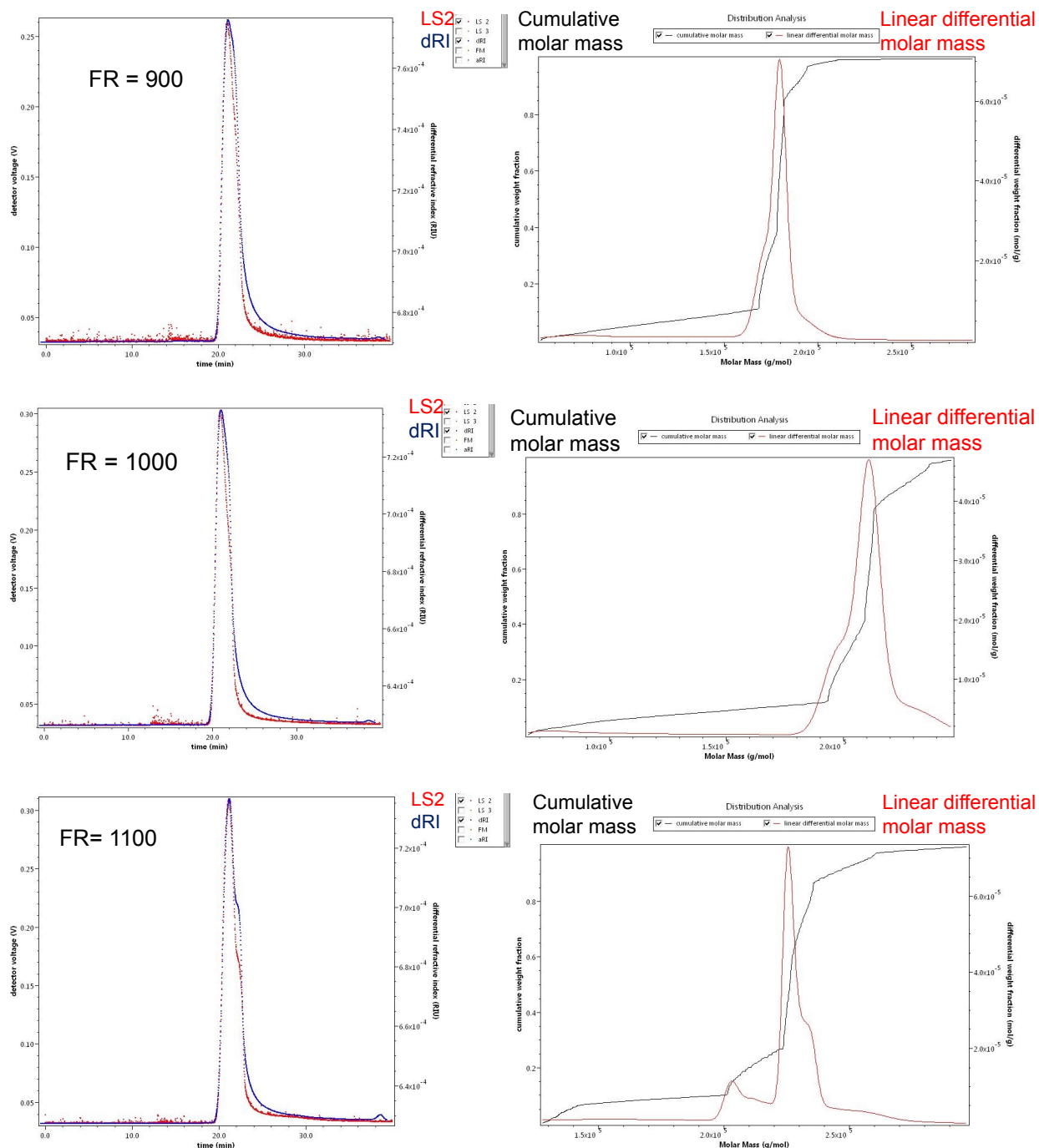
S6. Supplementary Figures
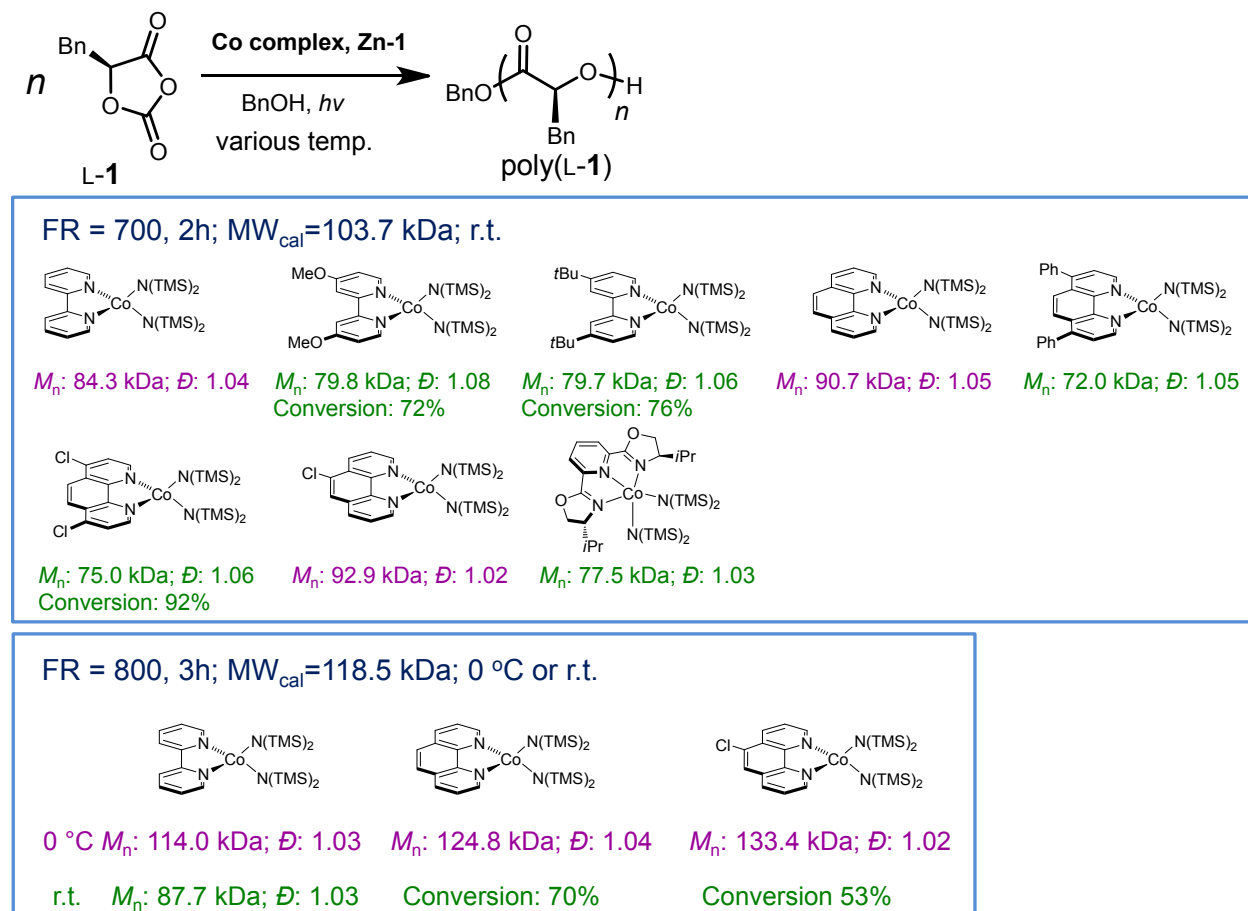
Figure S1. Screening of Co complexes and Co(HMDS)$_2$ ligands for photoredox ring-opening polymerization of L-1. The photoredox polymerization reaction was performed at [L-1]/[**Zn-1**]/[Co]/[BnOH] ratios of 700/1/1/1 and 800/1/1/1 at different temperature (room temperature (r.t.) or 0 °C) with light irradiation. The molecular weight (M_n) and molecular weight distribution ($Đ$) data in purple indicated the well-controlled polymerization reactions. The data in green indicated the results of less controlled polymerization reactions (incomplete monomer conversions or lower than expected MWs).

(a)

FR=500 Đ=1.03
FR=600 Đ=1.09
FR=700 Đ=1.08
FR=800 Đ=1.04
FR=900 Đ=1.05
FR=1000 Đ=1.07
FR=1100 Đ=1.02

(b)

FR = 500

LS2
dRI

Cumulative molar mass

Linear differential molar mass

FR = 600

Cumulative molar mass

Linear differential molar mass

FR = 700

Cumulative molar mass

Linear differential molar mass

FR = 800

Cumulative molar mass

Linear differential molar mass

(see next page)

Figure S2. (a) GPC overlays of poly(L-**1**) at different feeding ratios (FR = [L-**1**]/[**Zn-1**]) as shown in Fig. 1A (blue line). Note that the y axis is the raw data of dw/dlogMW, which is the normalized distribution of molecular weights (MWs) at each time slice, and is used for the MW distribution calculation in GPC. (b) The GPC raw data, including signals in the light scattering (LS) and refractive index (DI) detectors versus time (left panel), and their corresponding dw/dlogMW versus MWs plots (right panel), which are stacked in (a). The data clearly indicate the unimodal narrow MW distribution of the obtained polymers.
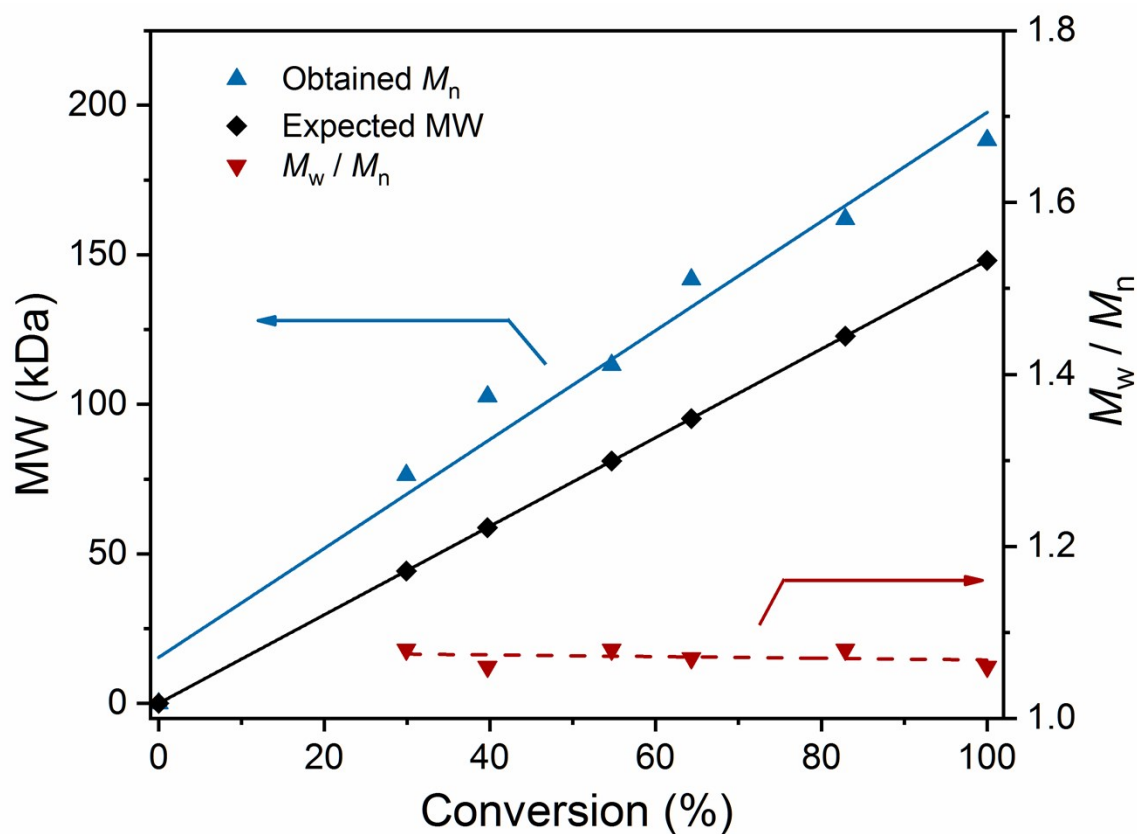
Figure S3. Linear correlation between the monomer conversion and polymer molecular weights (MWs). The photoredox ROP was performed at the ratio of [L-**1**]/[**Co-1**]/[**Zn-1**]/[BnOH] of 1000/1/1/1 at -15 °C with light irradiation. The MWs of the obtained polymers showed linear correlation with the monomer conversions, with narrow molecular weight distributions ($Đ = M_w/M_n$). In general, the MWs of the obtained polymers are slightly higher than the expected MWs at -15 °C with light irradiation, which are observed in the photoredox polymerization at different monomer feeding ratios as shown in Figure 1a.
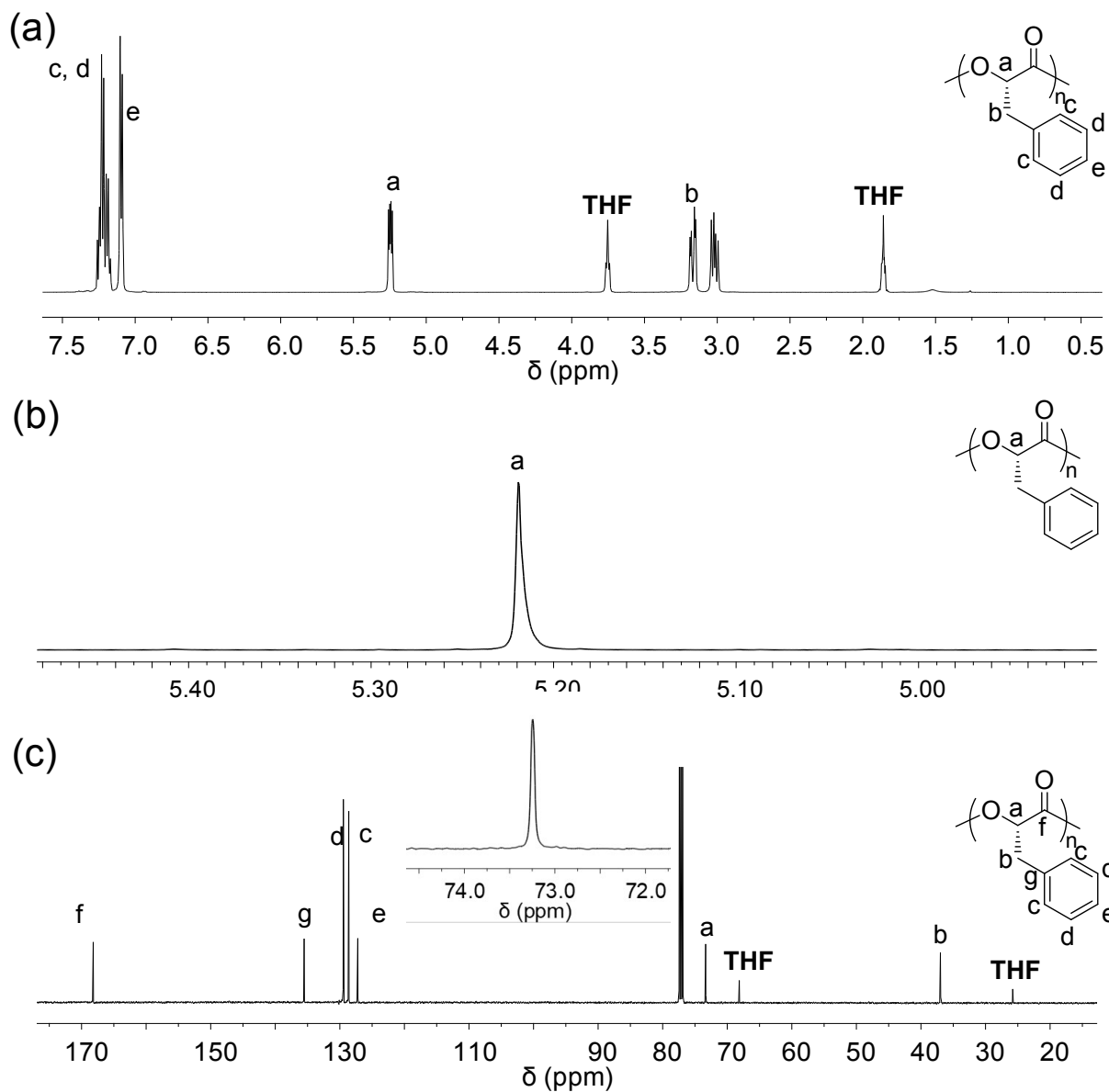
Figure S4. NMR spectra of poly(L-**1**) in CDCl$_3$ (M_n = 215.2 kDa; FR = 1000; 500 MHz, CDCl$_3$). (a) ^{1}H NMR spectrum; (b) Homodecoupling ^{1}H NMR spectrum; (c) ^{13}C NMR spectrum.
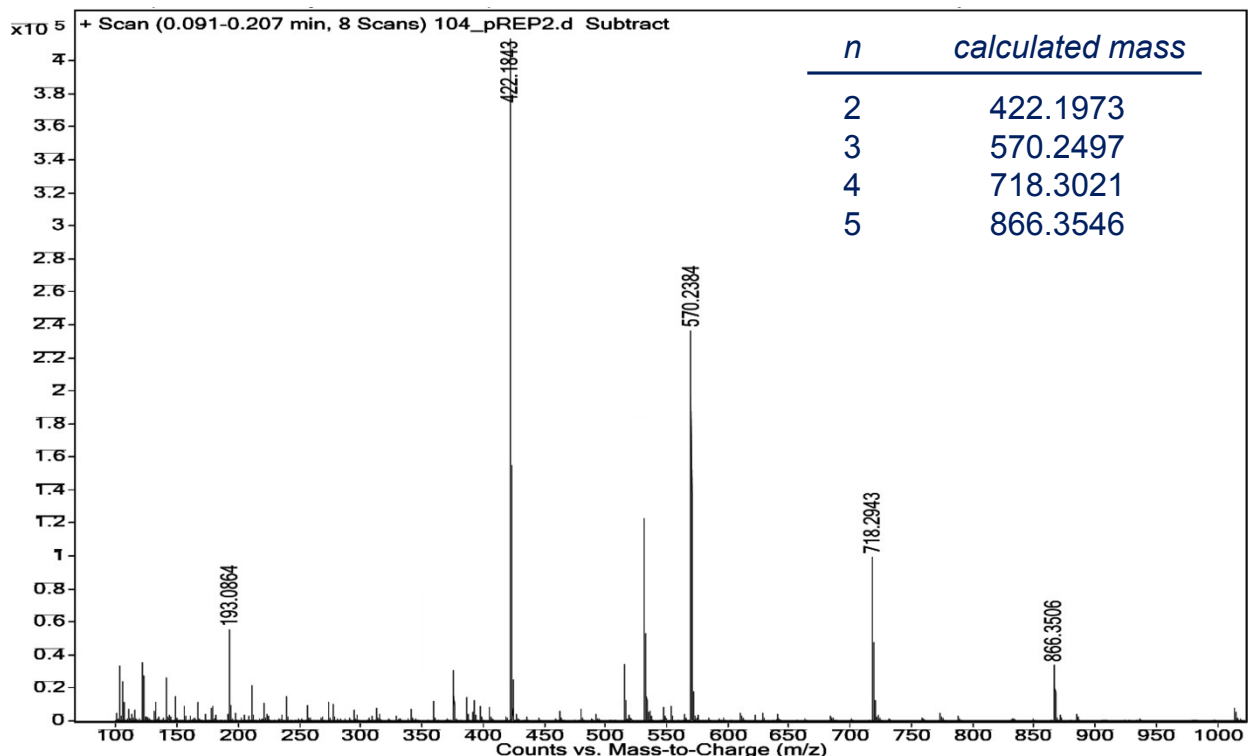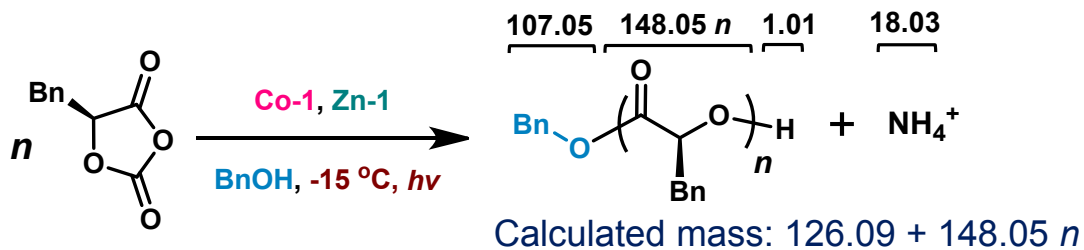
Figure S5. Alcohol participated in the initiation and was incorporated at the chain-end. (a) ESI-MS spectrum of oligo(L-**1**)$_{2-5}$ initiated by BnOH ([**1**]/[**Co-1**]/[**Zn-1**]/[BnOH] = 1/1/1/1) at -15 °C with light irradiation.

Discussion:

High resolution ESI-MS results:

n = 2 $C_{25}H_{28}NO_5$ calculated: 422.1973   found: 422.1843

n = 3 $C_{34}H36NO_7$ calculated: 570.2497   found: 570.2384

n = 4 $C_{43}H44NO_9$ calculated: 718.3021   found: 718.2943

n = 5 $C_{52}H_{52}NO_{11}$ calculated: 866.3546   found: 866.3506
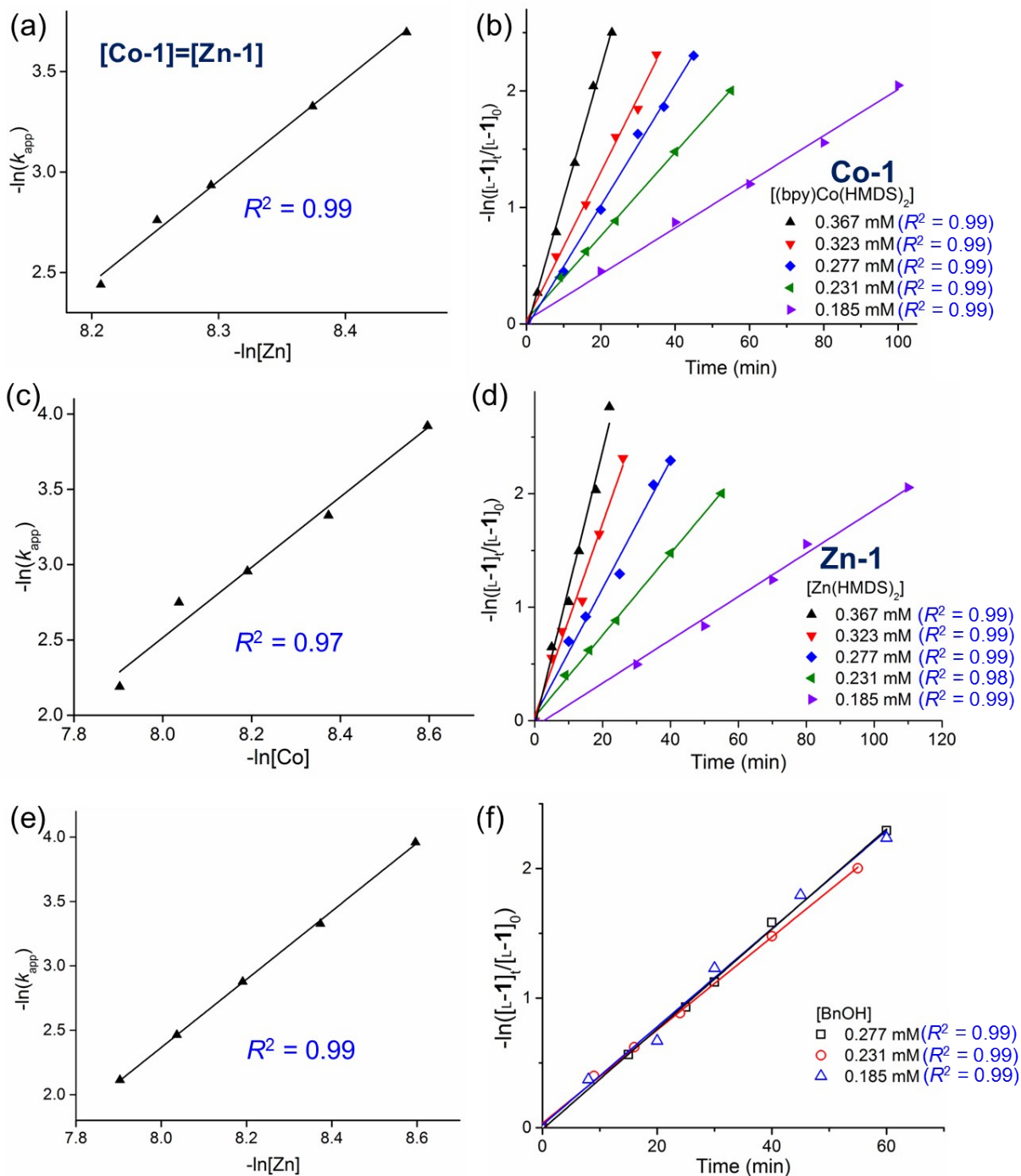
Figure S6. Kinetic plots of the photoredox polymerization of L-1 mediated by Co-1/Zn-1/BnOH at -15 °C. $[L\text{-}1]$ = 150 mM in all studies. (a) plots the kinetic rates data in Fig. 1B. (a, c, e) Plot of $-\ln(k_{app})$ versus $-\ln[\text{catalyst}]$ for ROP of L-1, the slope of which suggests the reaction order. (b, d, f) only the noted catalyst's concentration was changed, and the rest is fixed at 0.231 mM in THF.

Discussion:

The reaction orders with respect to **Co-1**, and **Zn-1** were 2.33 ± 0.20 and 2.64 ± 0.03. For Fig. 1B ([**Co-1**] = [**Zn-1**] = [BnOH], Co and Zn complexes at the same concentration), the polymerization reaction order is 5.06 ± 0.21. The value is close to the sum of the individual reaction order of **Co-1** and **Zn-1**, suggesting that there is no complex formed between each (also see Fig. S25). Therefore the reaction kinetics can be described by the following equation:

$$-d[\text{L-}\mathbf{1}]/dt = k_p [\mathbf{Co\text{-}1}]^{2.33}[\text{Zn-1}]^{2.64}[\text{L-}\mathbf{1}]^1$$

where k_p is the rate constant of chain propagation.
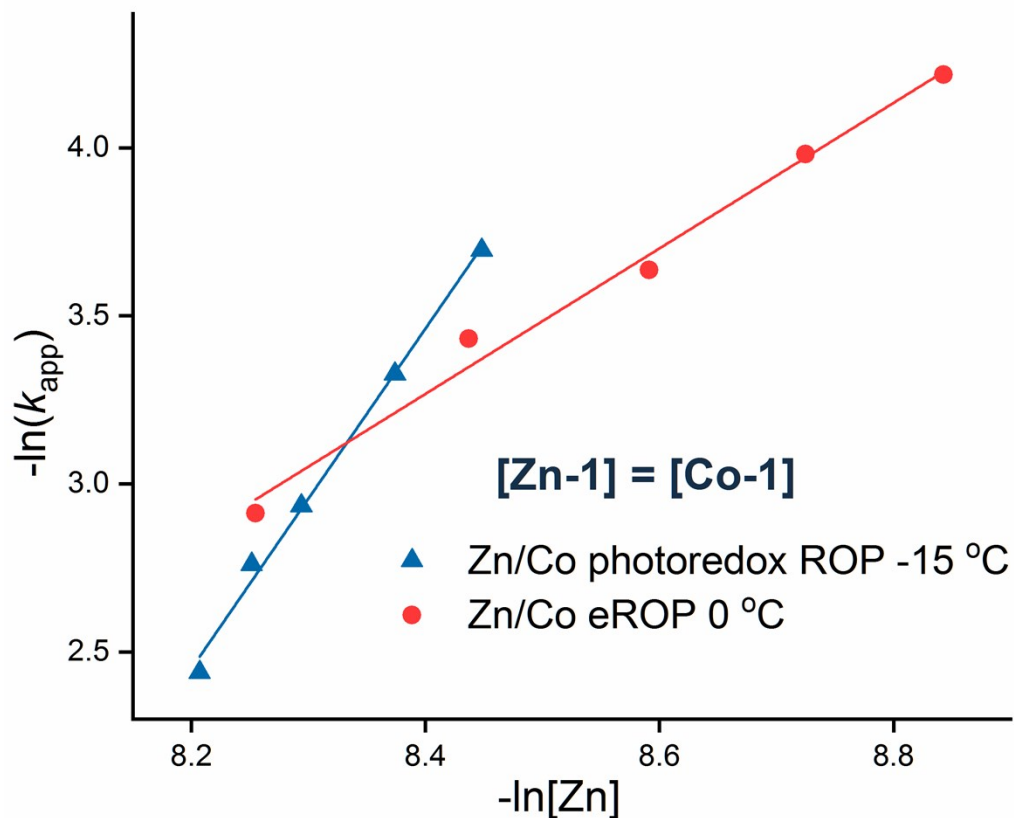
Figure S7. Comparison of kinetic plots of the photoredox ROP and eROP of L-1 mediated by Co-1/Zn-1/BnOH. Based on the figure, eROP had higher polymerization rates at higher feeding ratios. Note that the observed kinetic laws in eROP:[17]

$$-d[\text{L-}\mathbf{1}]/dt = k_p\,[\mathbf{Co\text{-}1}]^{0.90}[\mathbf{Zn\text{-}1}]^{1.10}[\text{L-}\mathbf{1}]^1$$

which indicated less aggregation of metal complexes in the eROP reaction setup, and possibly different reaction temperatures.
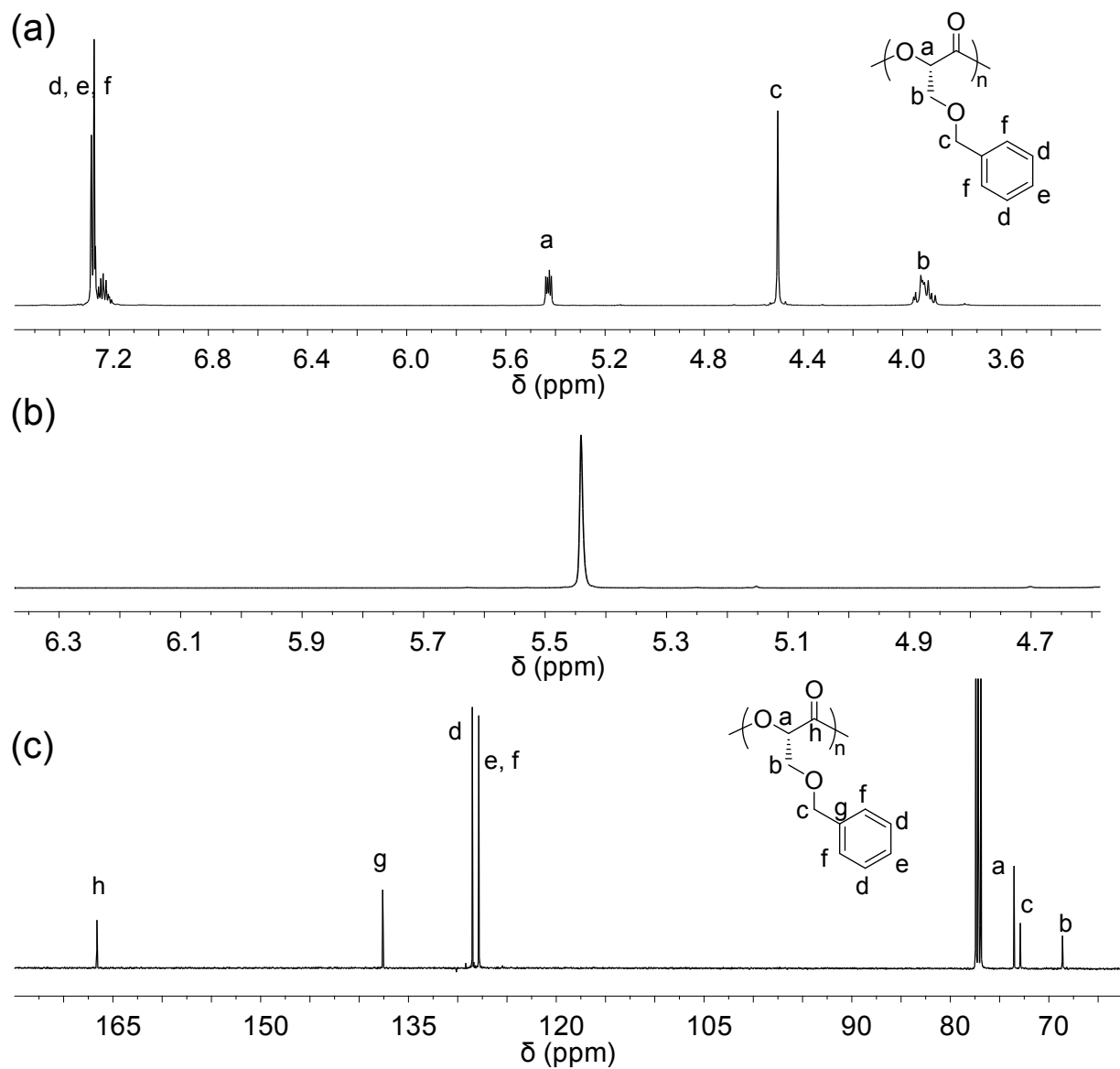
Figure S8. NMR spectra of poly(L-**2**) in CDCl$_3$ (Table S3, entry 1; 500 MHz, CDCl$_3$). (a) ^{1}H NMR spectrum; (b) Homodecoupling ^{1}H NMR spectrum; (c) ^{13}C NMR spectrum.
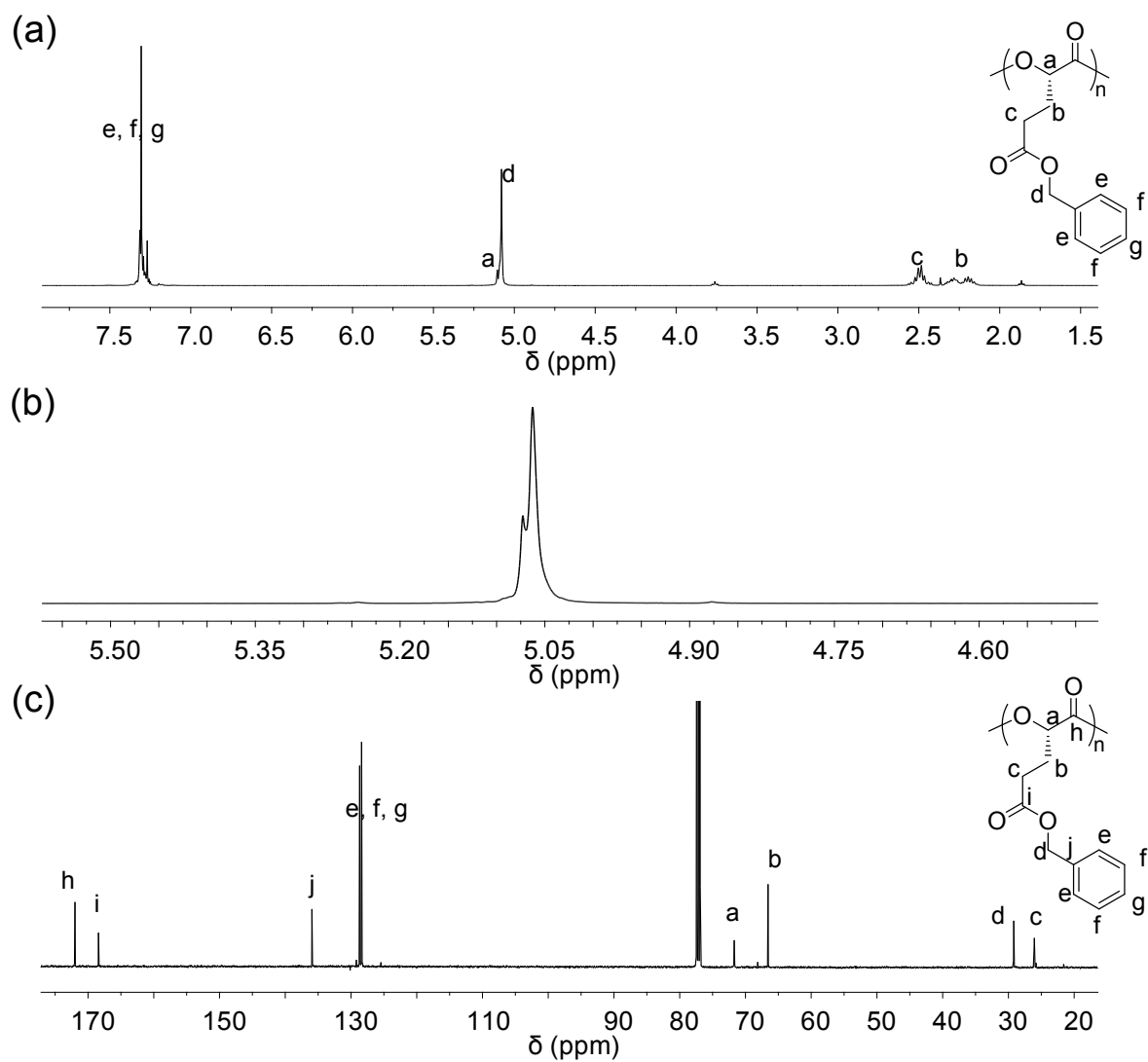
Figure S9. NMR spectra of poly(L-**3**) in CDCl$_3$ (Table S3, entry 5; 500 MHz, CDCl$_3$). (a) ^{1}H NMR spectrum; (b) Homodecoupling ^{1}H NMR spectrum; (c) ^{13}C NMR spectrum.
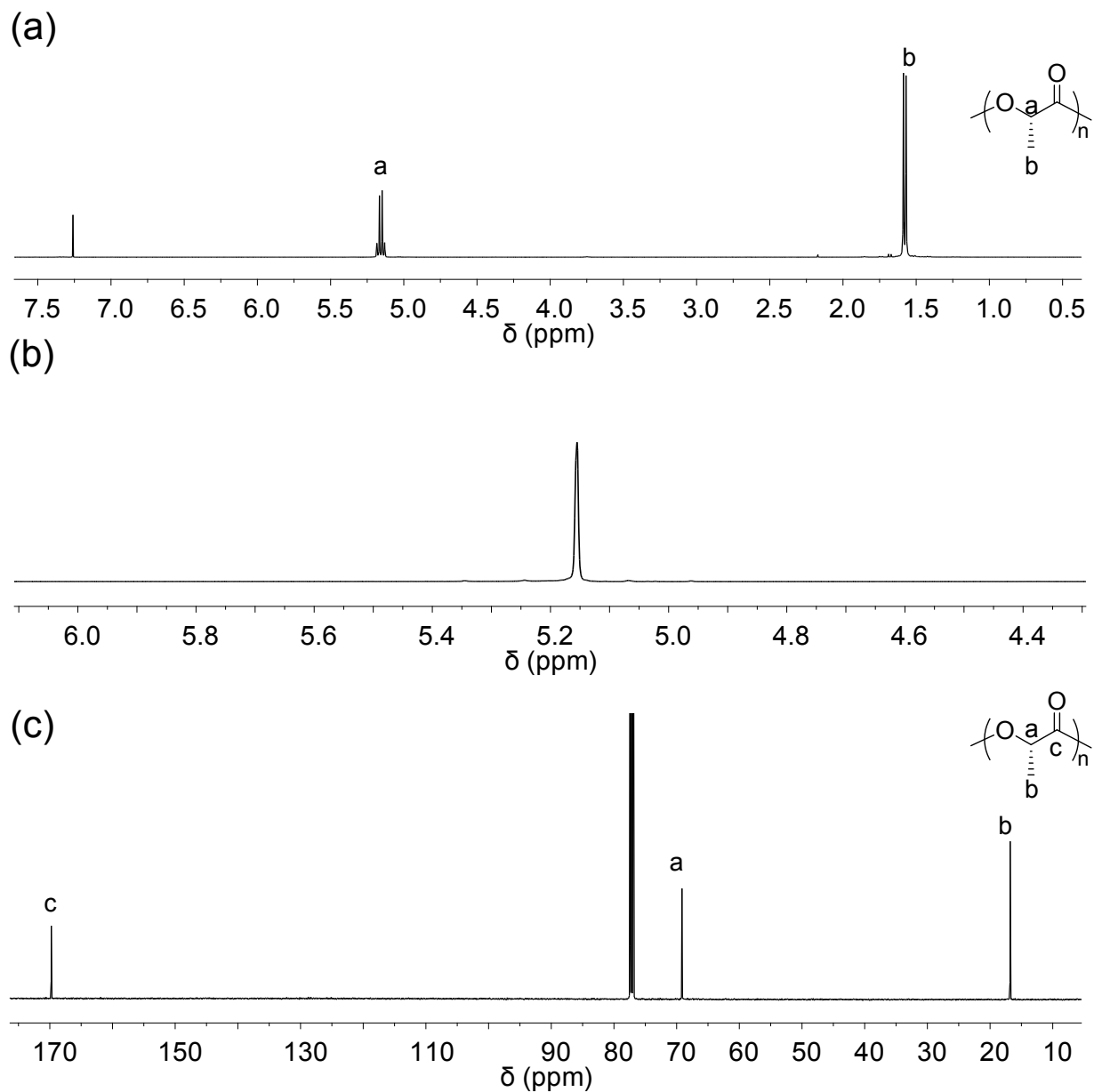
Figure S10. NMR spectra of poly(L-**4**) in CDCl$_3$ (Table S3, entry 9; 500 MHz, CDCl$_3$). (a) ^{1}H NMR spectrum; (b) Homodecoupling ^{1}H NMR spectrum; (c) ^{13}C NMR spectrum.
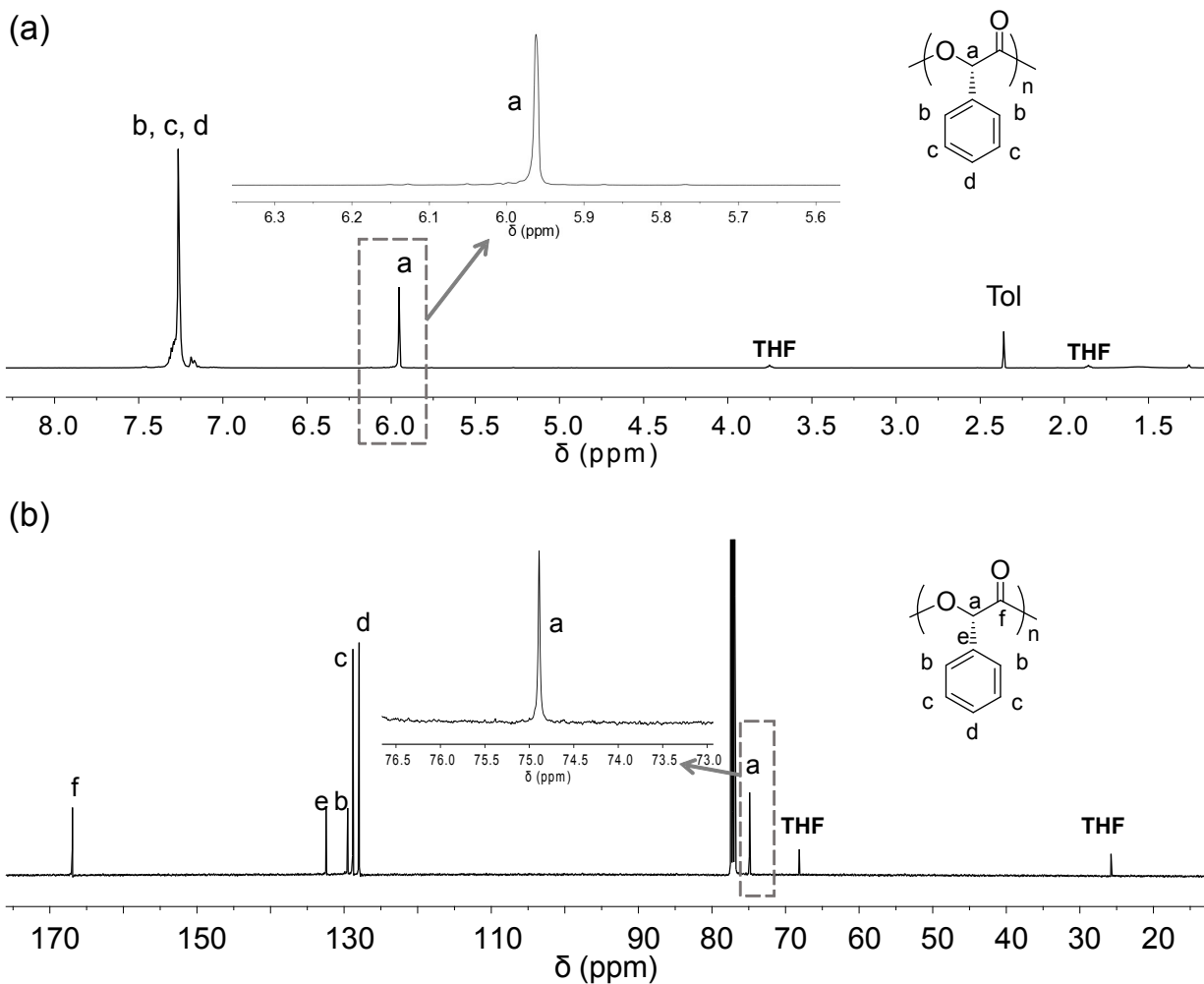
Figure S11. NMR spectra of poly(L-**5**) in CDCl$_3$ (Table S3, entry 13; 500 MHz, CDCl$_3$). (a) ^{1}H NMR spectrum; (b) ^{13}C NMR spectrum.
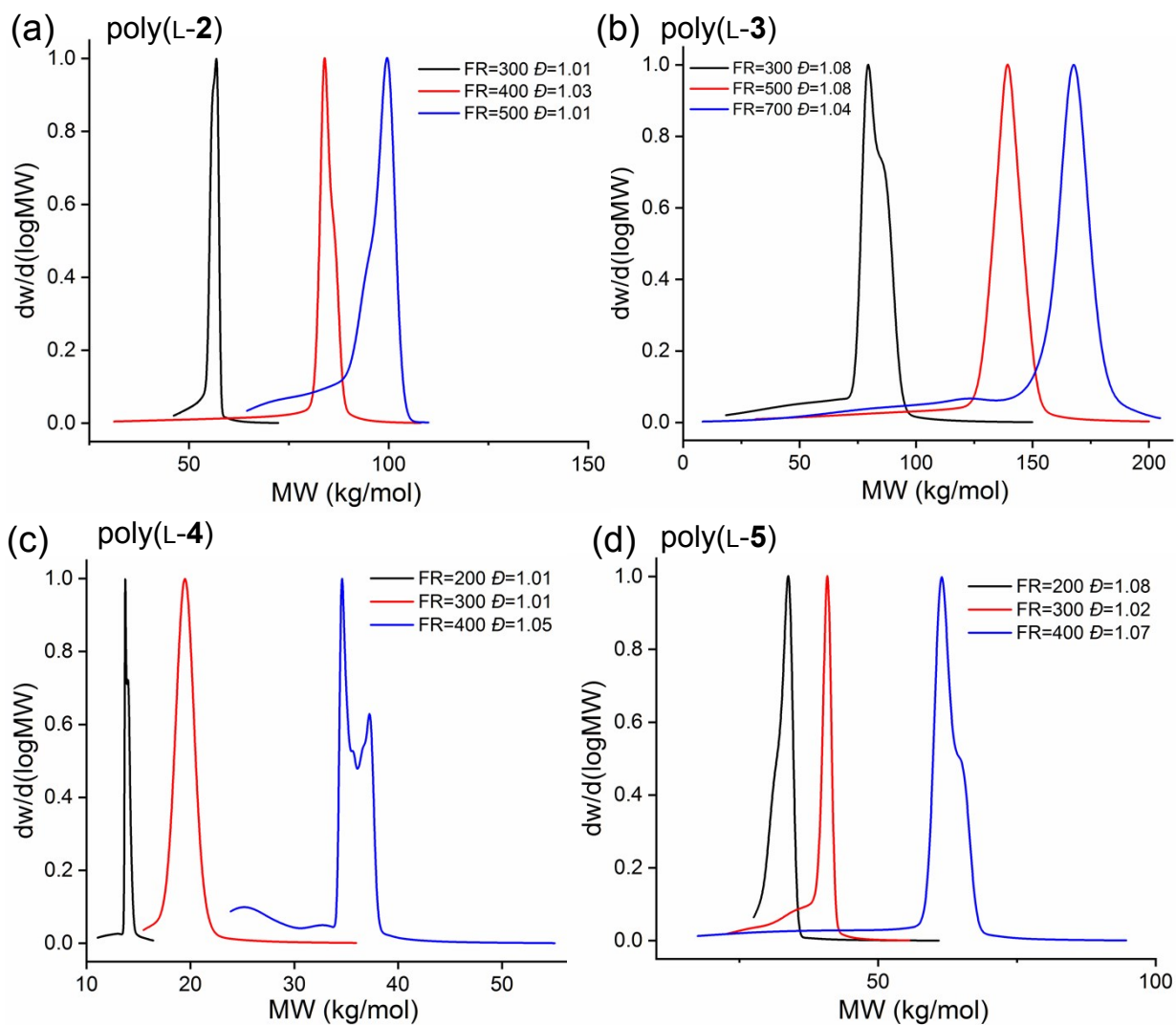
Figure S12. GPC overlays of polymerization of OCA monomers L-**2**, L-**3**, L-**4**, L-**5** via Co/Zn photoredox ROP. Note that the y axis is the raw data of dw/dlogMW, which is the normalized distribution of molecular weights (MWs) at each time slice, and is used for the MW distribution calculation in GPC. Detailed polymerization data in Table S3.
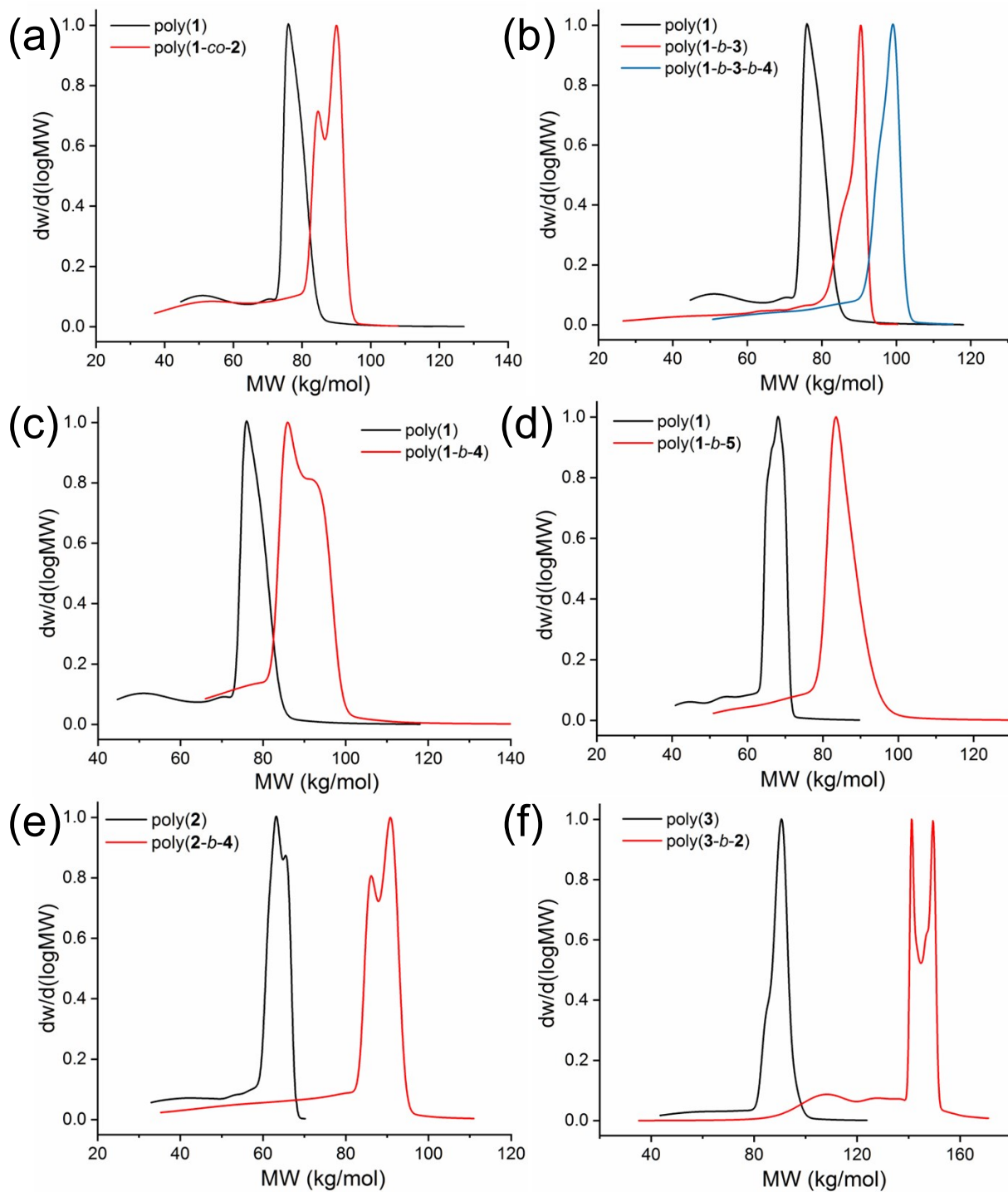
(see next page)
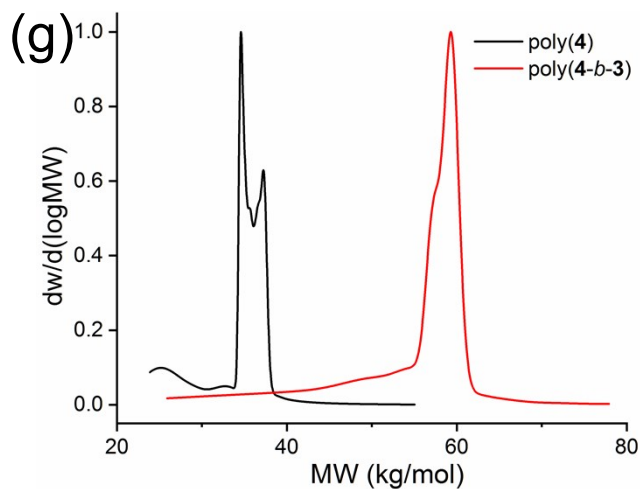
Figure S13. GPC overlays of copolymerization of OCA monomers via Co/Zn photoredox ROP, before and after the addition of second blocks. Note that the y axis is the raw data of dw/dlogMW, which is the normalized distribution of molecular weights (MWs) at each time slice, and is used for the MW distribution calculation in GPC. Polymerization data of copolymers in Table S4: (a) entry 1; (b) entries 2 and 8; (c) entry 3; (d) entry 4; (e) entry 5; (f) entry 6; (g) entry 7.

(a)

(b)

(see next page)

(c)
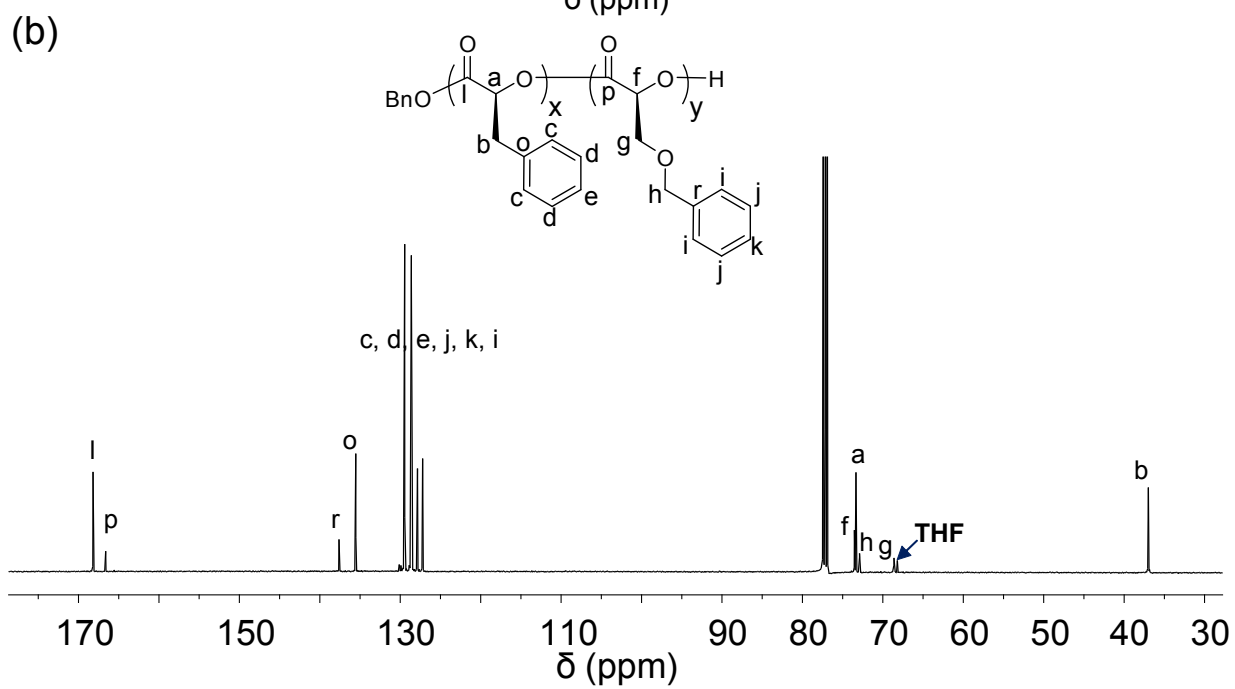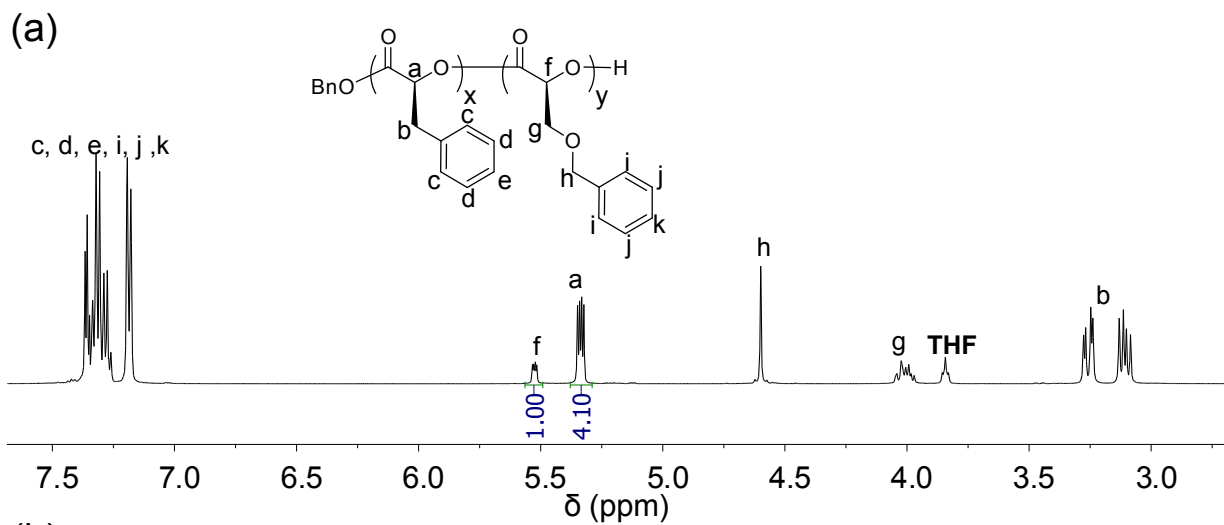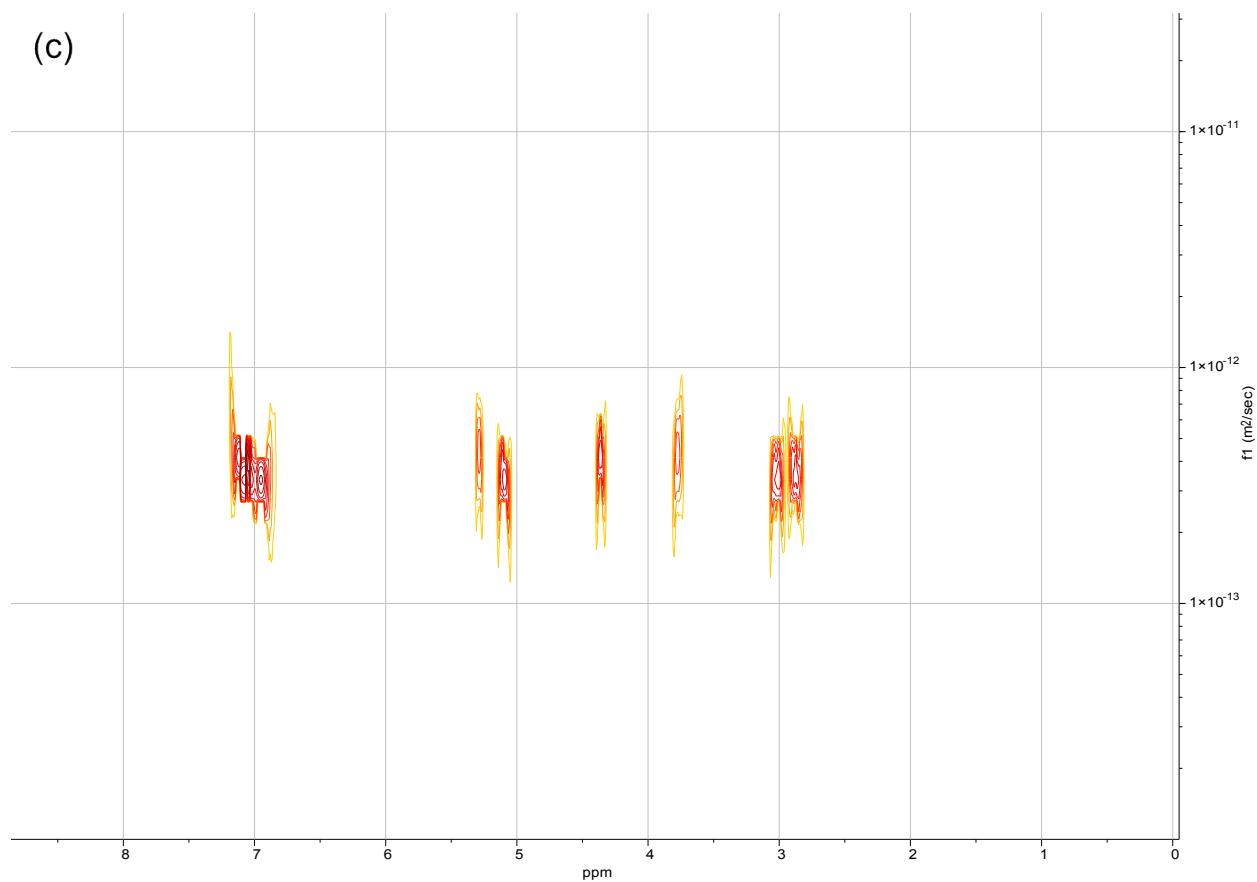
Figure S14. NMR spectra of poly(L-**1**-*b*-L-**2)** in CDCl$_3$ (Table S4, entry 1; 500 MHz, CDCl$_3$). (a) ^{1}H NMR spectrum; (b) ^{13}C NMR spectrum; (c) DOSY-NMR of the copolymer.

.

(a)

c, d, e, j, k, l

i

a

f

THF

b

THF

h

g

3.90
3.00

7.5 7.0 6.5 6.0 5.5 5.0 4.5 4.0 3.5 3.0 2.5 2.0 1.5 1.0

δ (ppm)

(b)

c, d, e, j, k, l

q,o

r

p

s

a

f

i

b

h g THF

THF

170 150 130 110 90 80 70 60 50 40 30 20

δ (ppm)
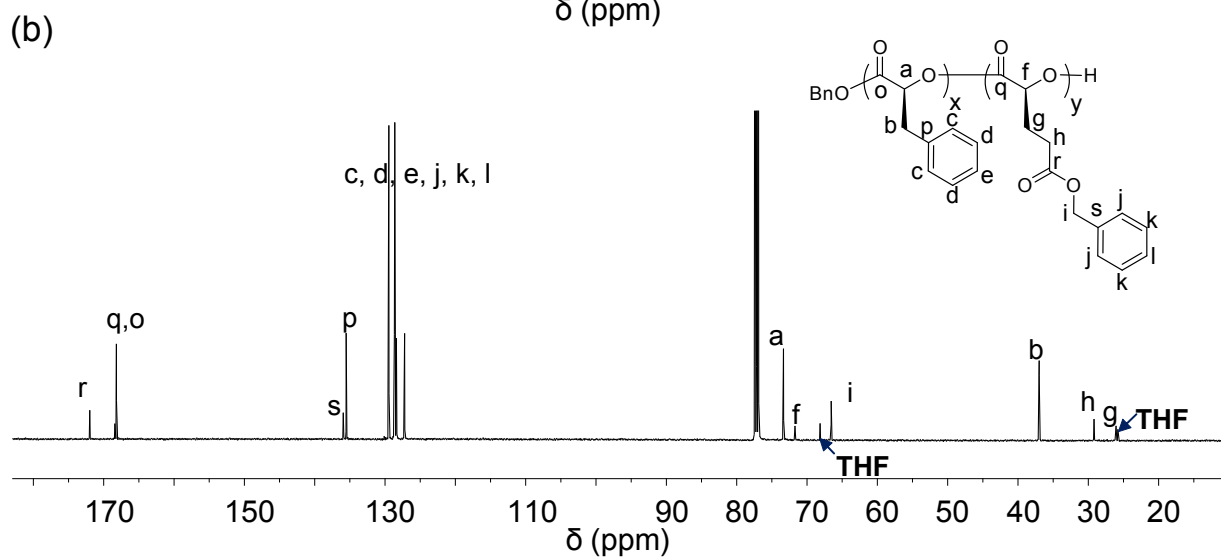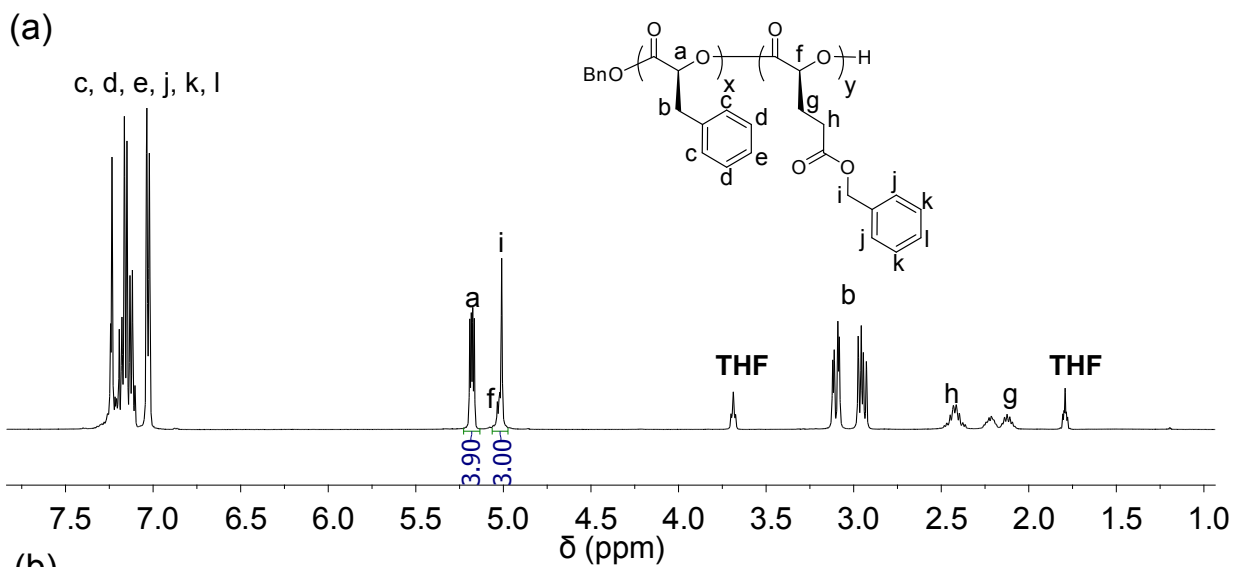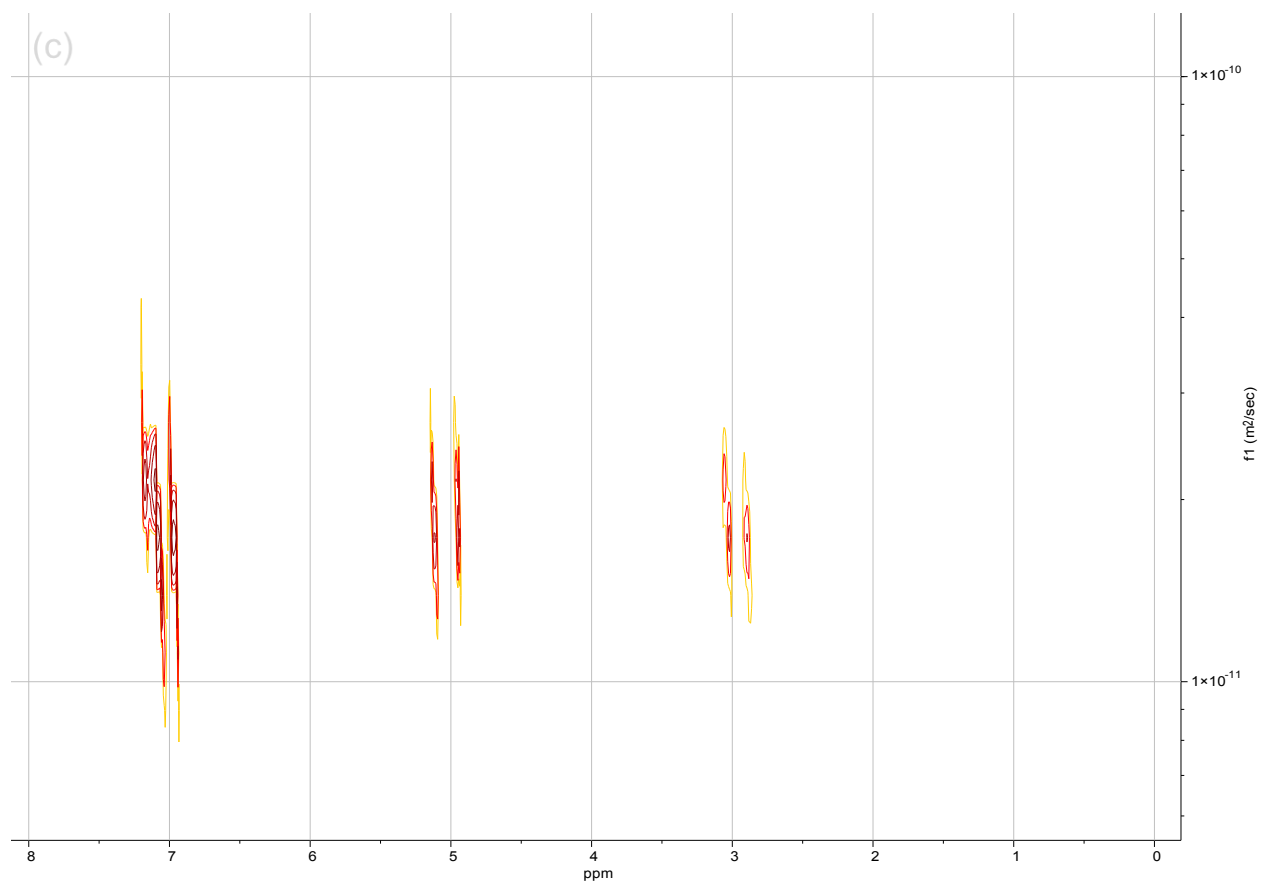
(see next page)

Figure S15. NMR spectra of poly(L-**1**-*b*-L-**3**) in CDCl$_3$ (Table S4, entry 2; 500 MHz, CDCl$_3$). (a) ^{1}H NMR spectrum; (b) ^{13}C NMR spectrum; (c) DOSY-NMR of the copolymer.

(a)

(b)
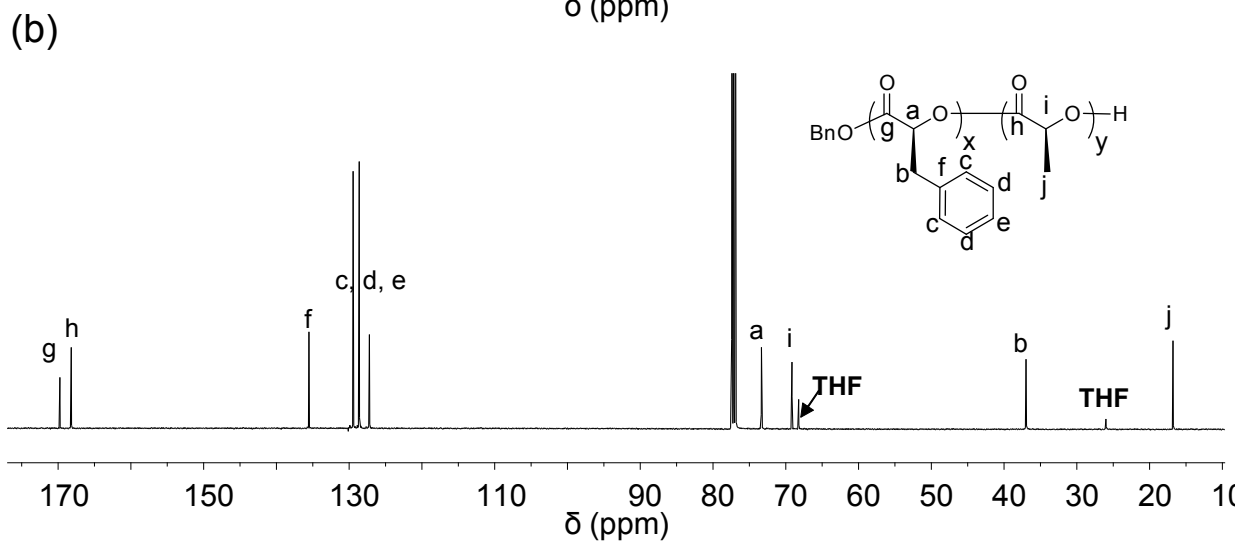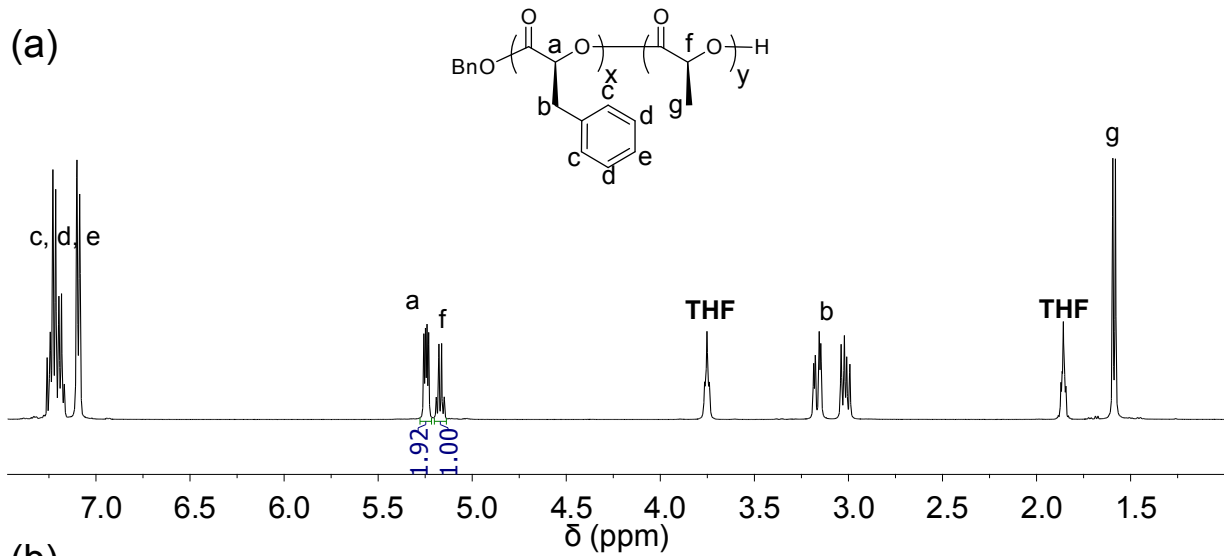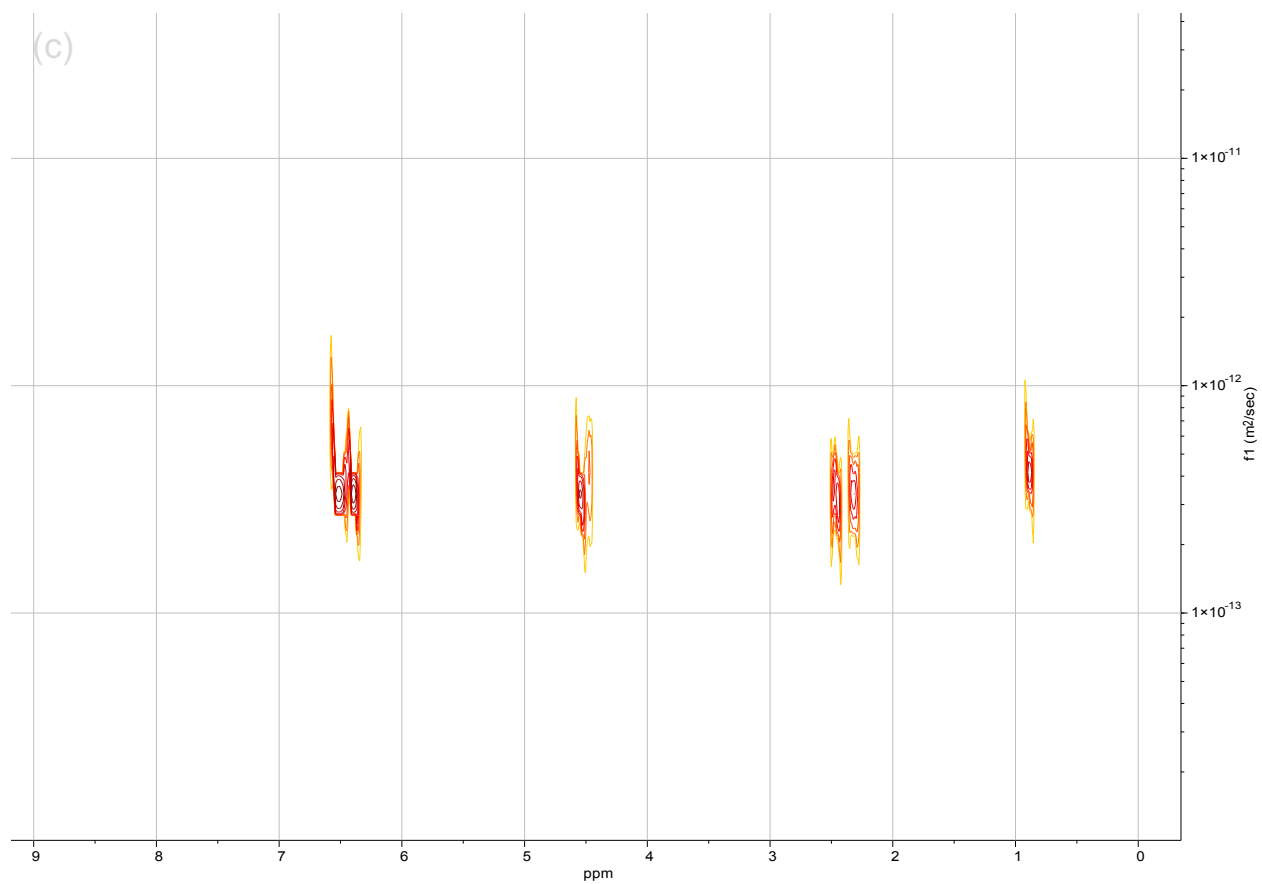
(see next page)

Figure S16. NMR spectra of poly(L-**1**-*b*-L-**4**) in CDCl$_3$ (Table S4, entry 3; 500 MHz, CDCl$_3$). (a) ^{1}H NMR spectrum; (b) ^{13}C NMR spectrum; (c) DOSY-NMR of the copolymer.

(a)

c, d, e, g, h, i

f

a

THF

b

THF

0.67

4.00

7.5   7.0   6.5   6.0   5.5   5.0   4.5   4.0   3.5   3.0   2.5   2.0

δ (ppm)

(b)

c, d, e

p

j

g, h, i

q

k

a

THF

f

b

THF

170   150   130   110   90   80   70   60   50   40   30   20

δ (ppm)
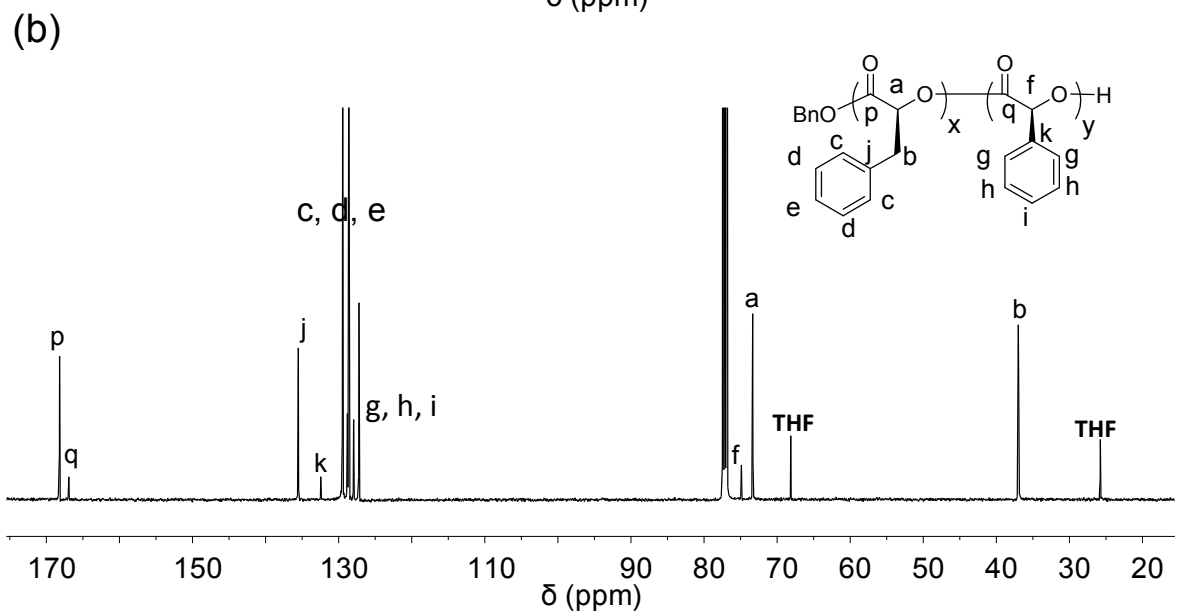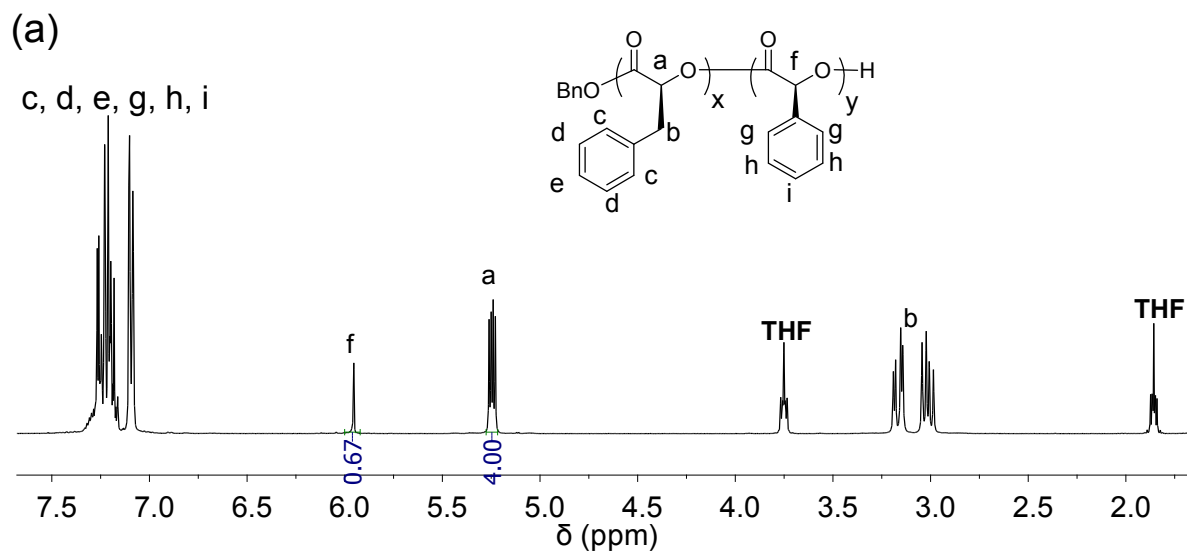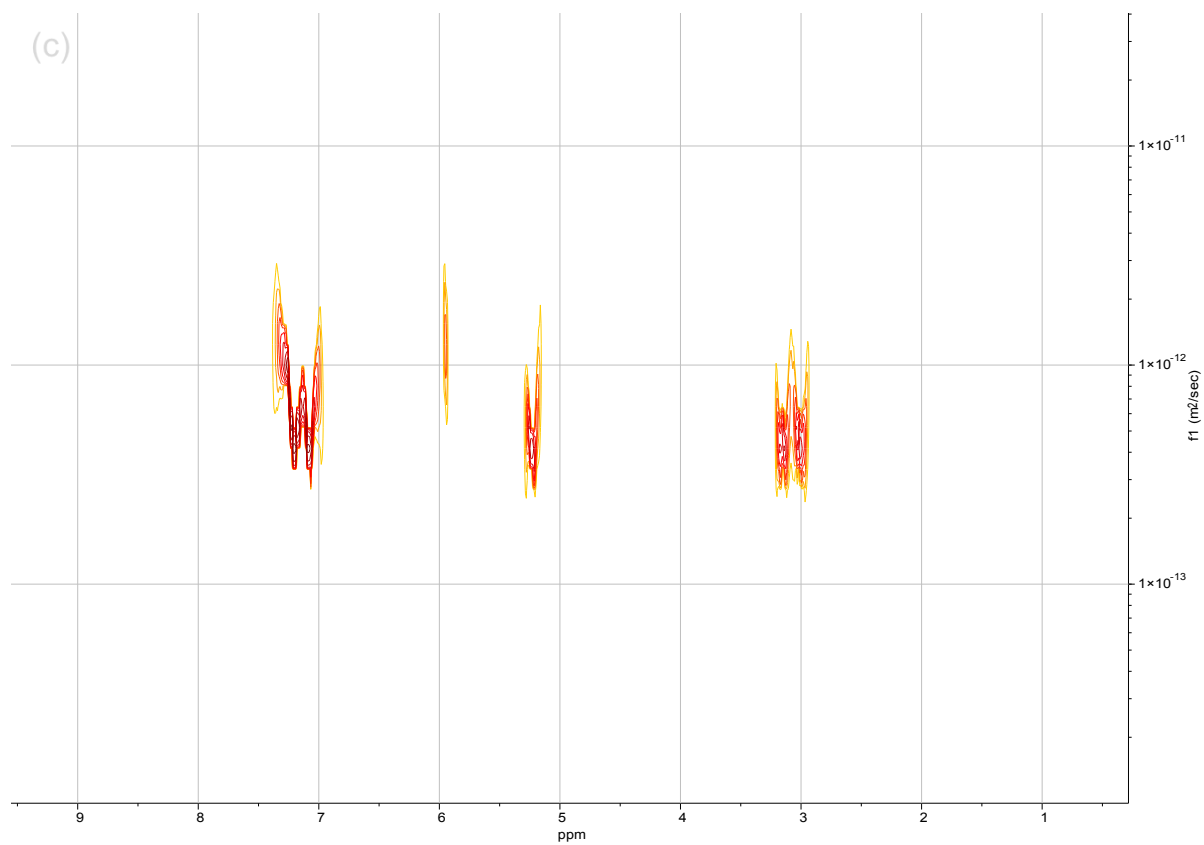
(see next page)

Figure S17. NMR spectra of poly(L-**1**-*b*-L-**5**) in CDCl₃ (Table S4, entry 4; 500 MHz, CDCl₃). (a) ¹H NMR spectrum; (b) ¹³C NMR spectrum; (c) DOSY-NMR of the copolymer.

(a)

(b)
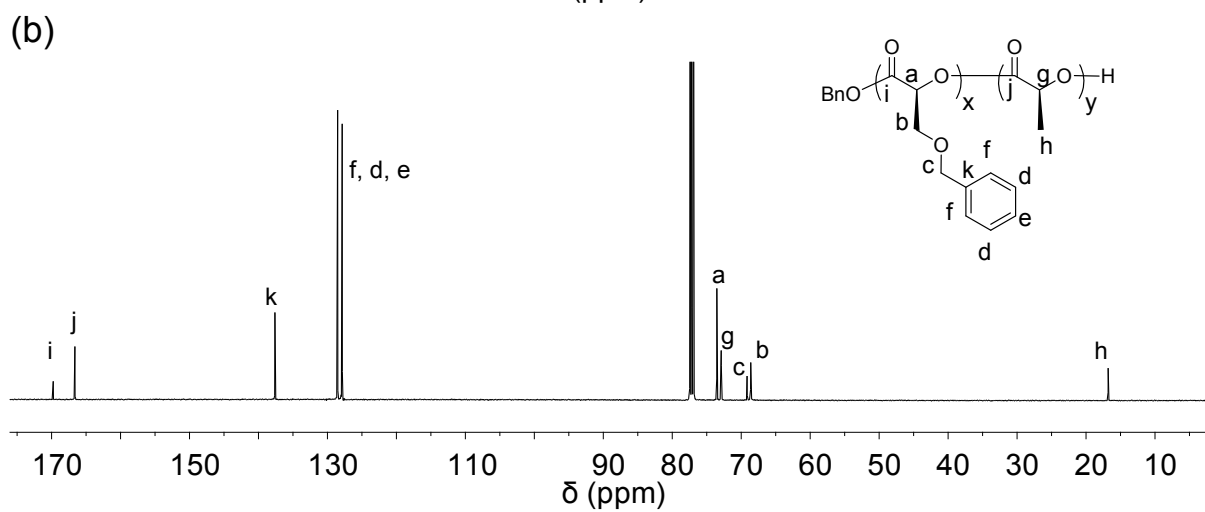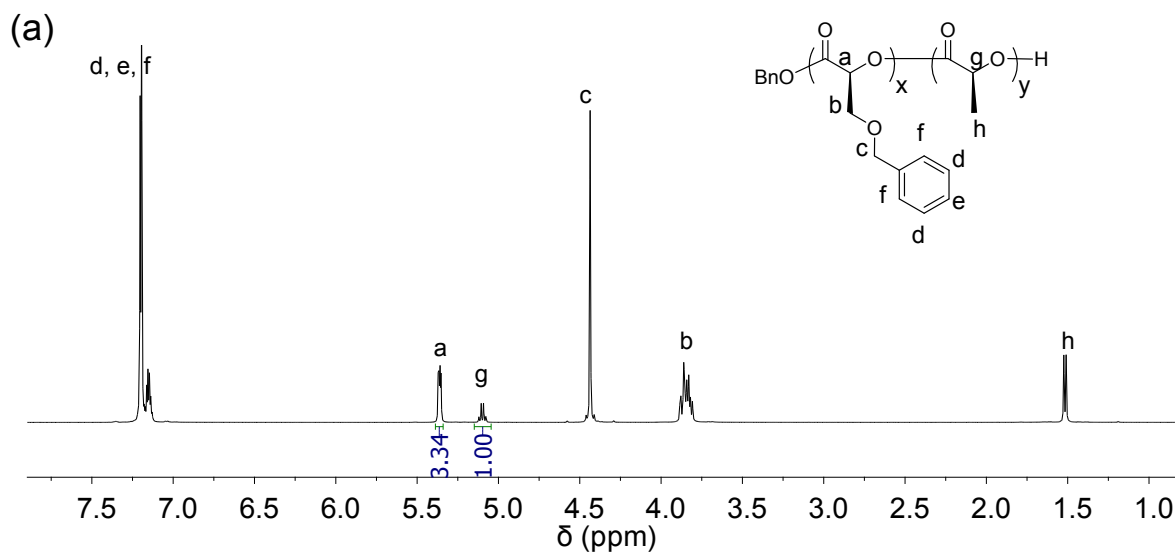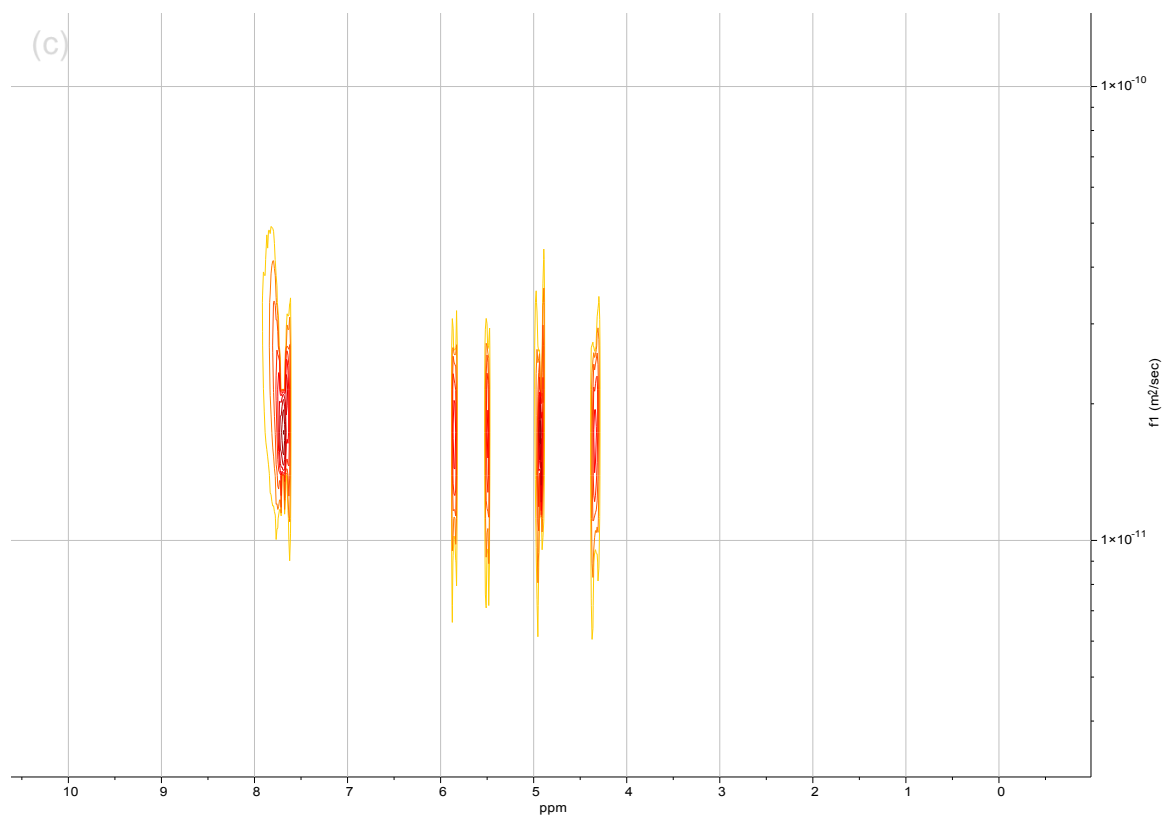
(see next page)

Figure S18. NMR spectra of poly(L-**2**-*b*-L-**4**) in CDCl₃ (Table S4, entry 5; 500 MHz, CDCl₃). (a) ¹H NMR spectrum; (b) ¹³C NMR spectrum; (c) DOSY-NMR of the copolymer.

(a)

(b)
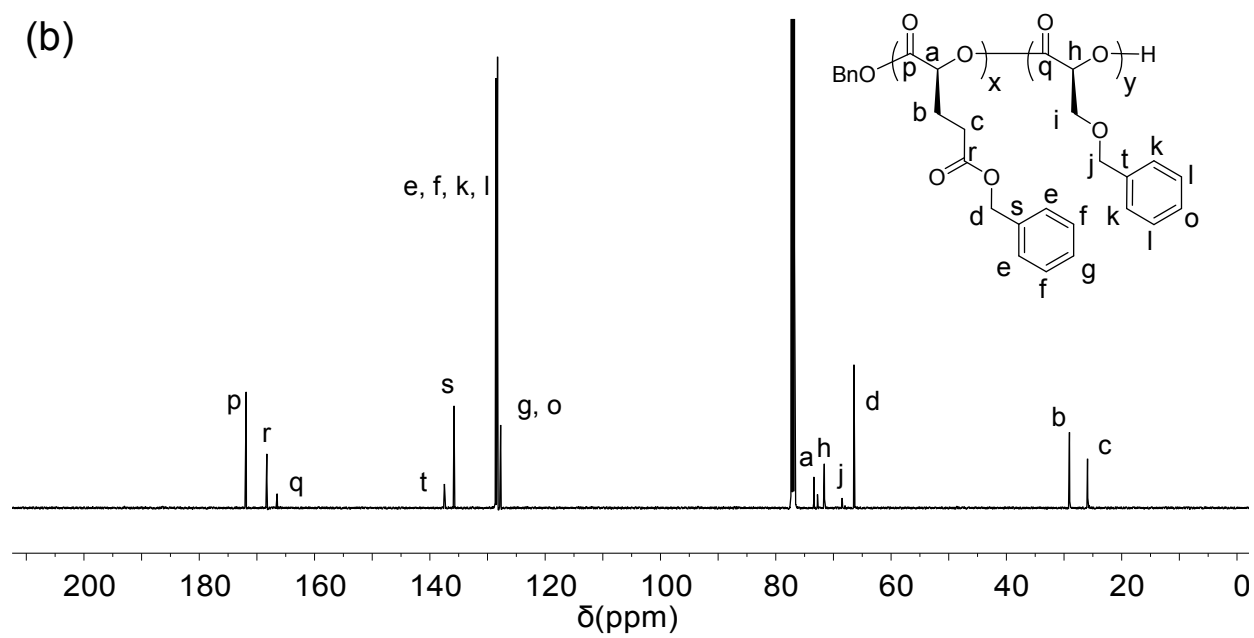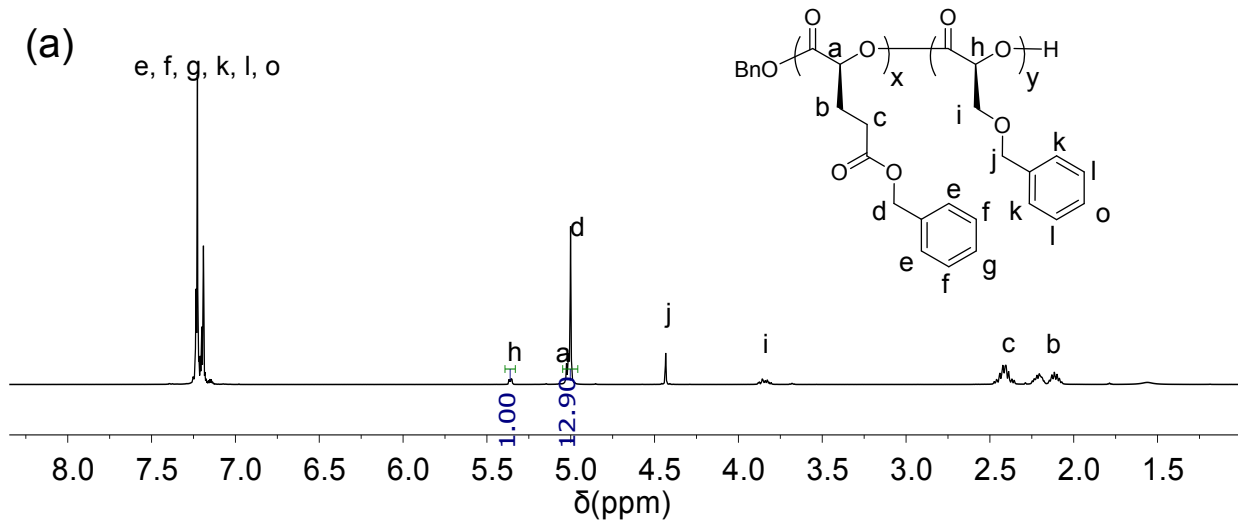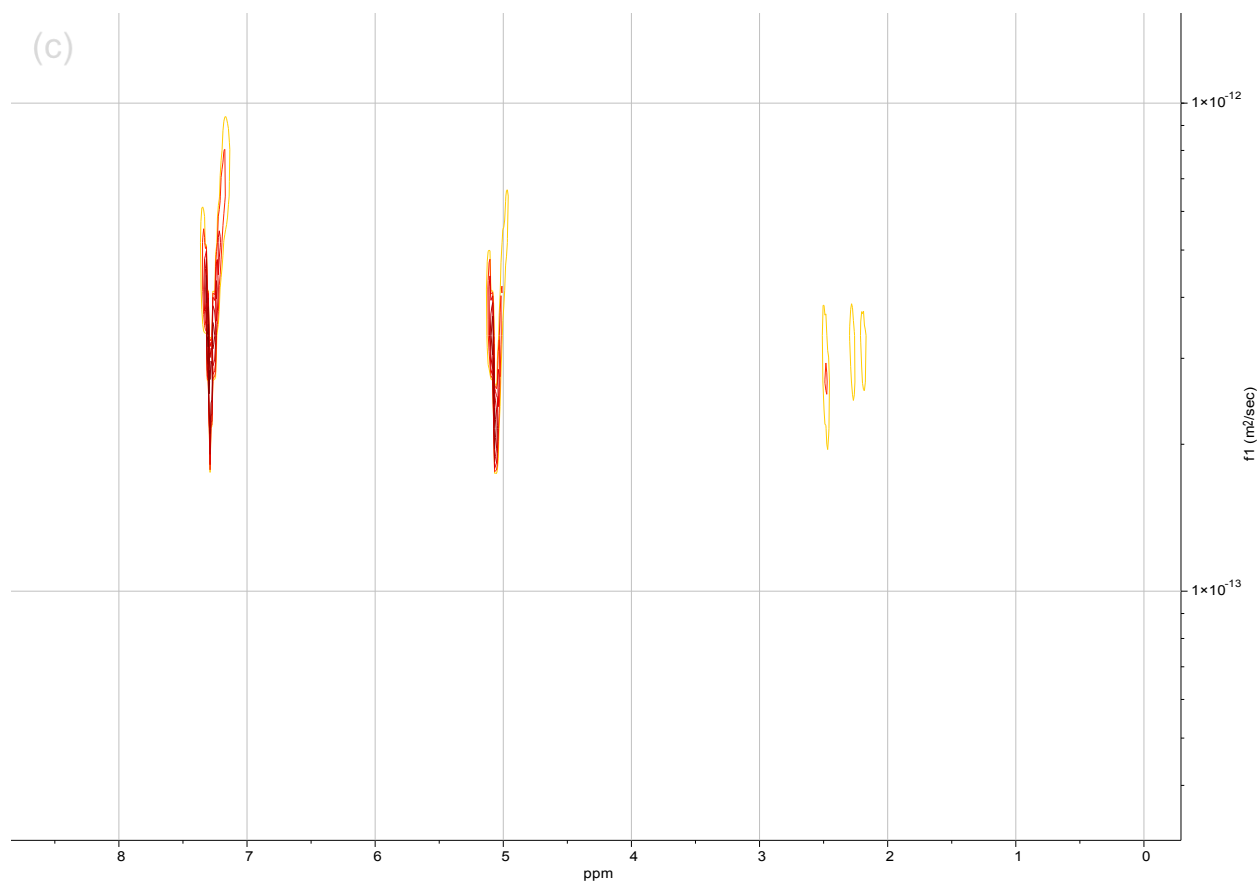
(see next page)

Figure S19. NMR spectra of poly(L-**3**-*b*-L-**2**) in CDCl₃ (Table S4, entry 6; 500 MHz, CDCl₃). (a) ¹H NMR spectrum; (b) ¹³C NMR spectrum; (c) DOSY-NMR of the copolymer.

(a)

(b)

(see next page)

(c)
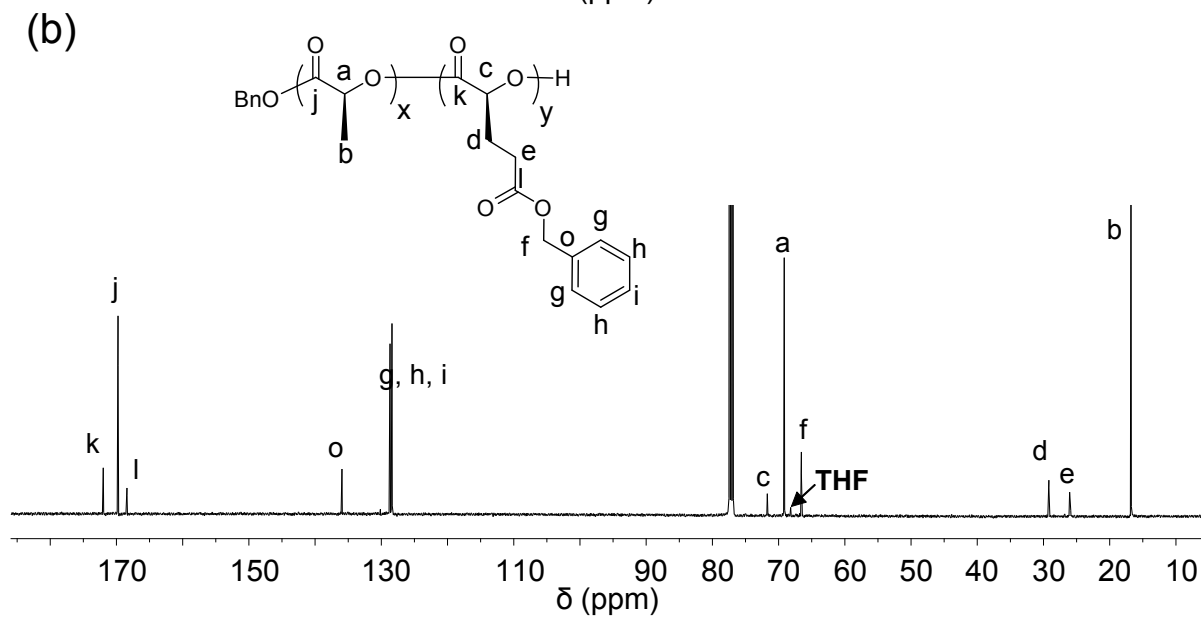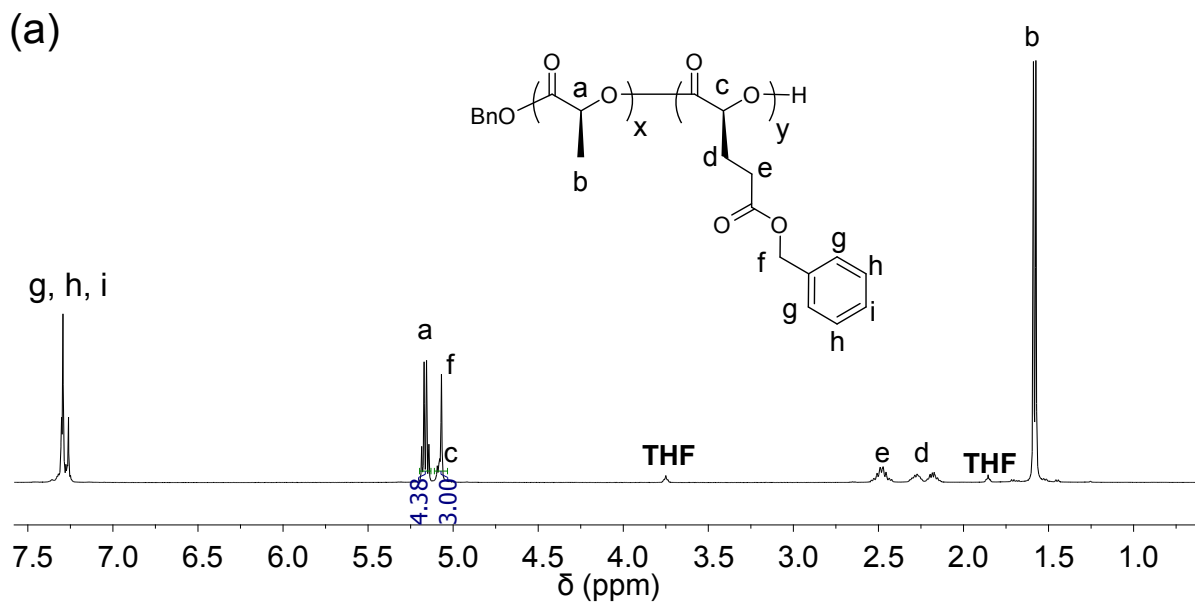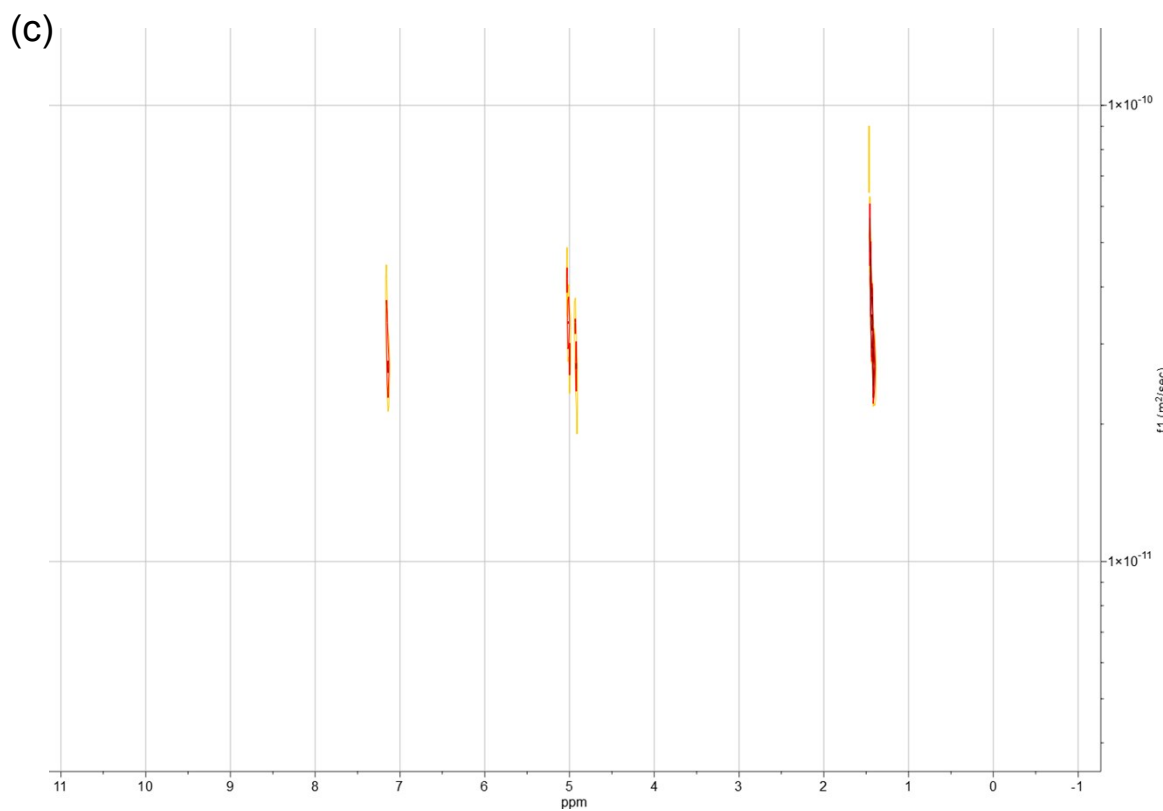
Figure S20. NMR spectra of poly(L-**4**-*b*-L-**3**) in CDCl$_3$ (Table S4, entry 7; 500 MHz, CDCl$_3$). (a) ^{1}H NMR spectrum; (b) ^{13}C NMR spectrum; (c) DOSY-NMR of the copolymer.

(a) c, d, e, j, k, l

(b) c, d, e, j, k, l

(see next page)

(c)
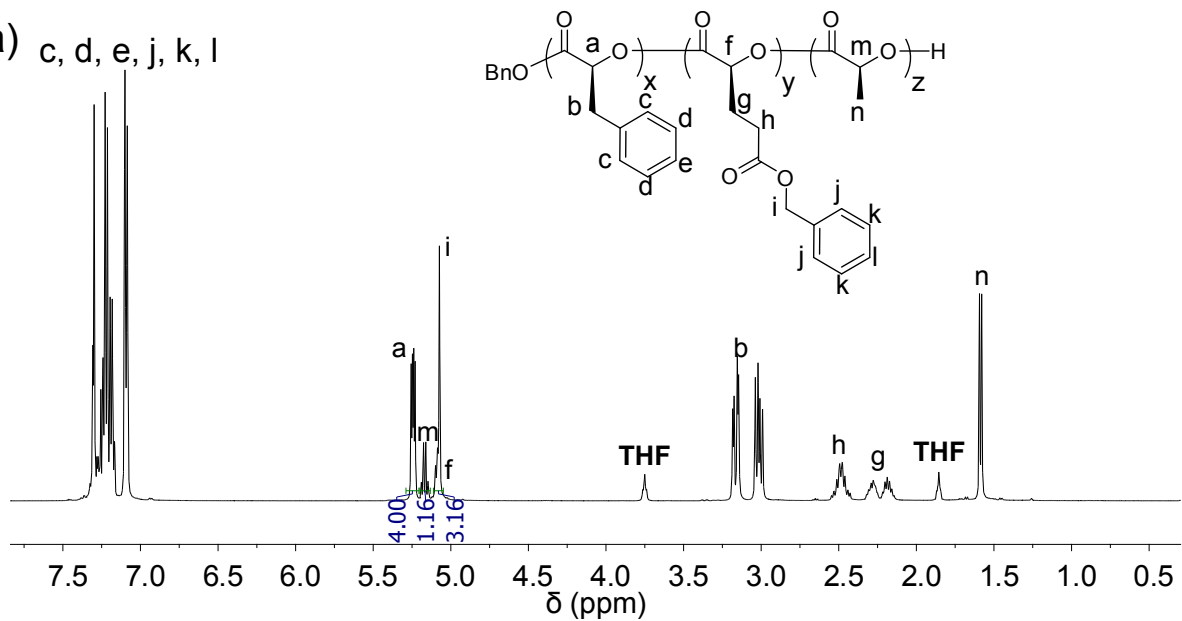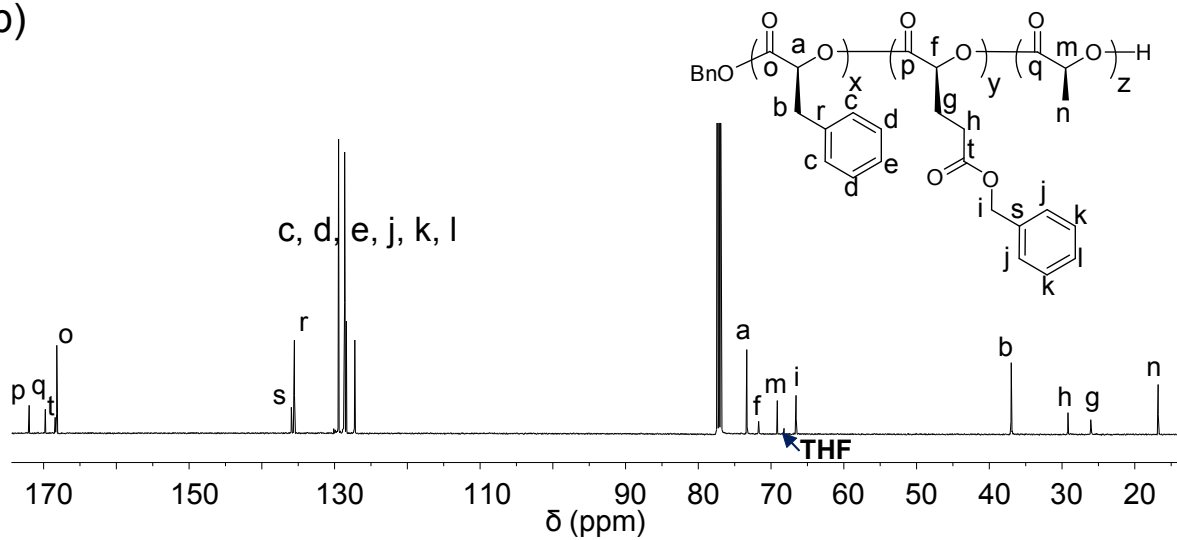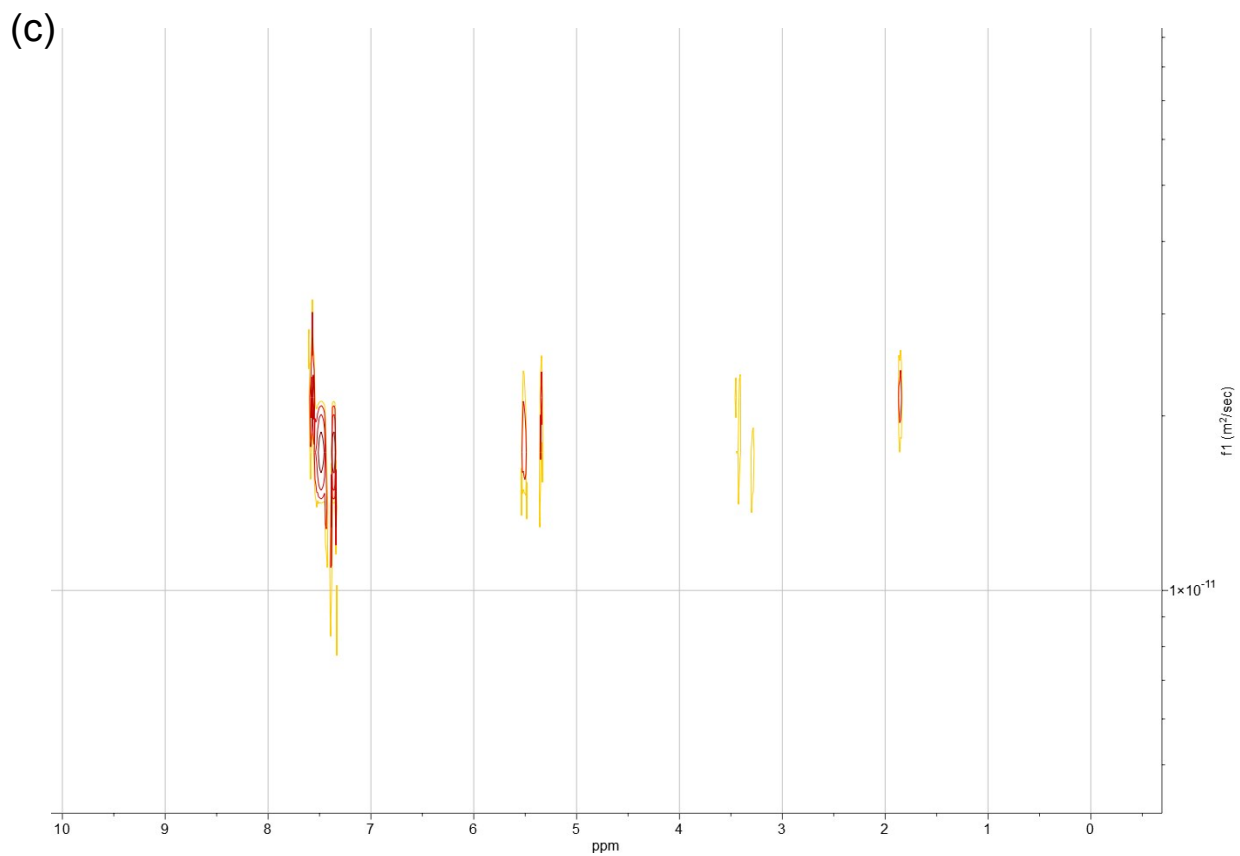
Figure S21. NMR spectra of poly(L-**1**-*b*-L-**3**-*b*-L-**4**) in CDCl$_3$ (Table S4, entry 8; 500 MHz, CDCl$_3$). (a) ^{1}H NMR spectrum; (b) ^{13}C NMR spectrum; (c) DOSY-NMR of the copolymer.
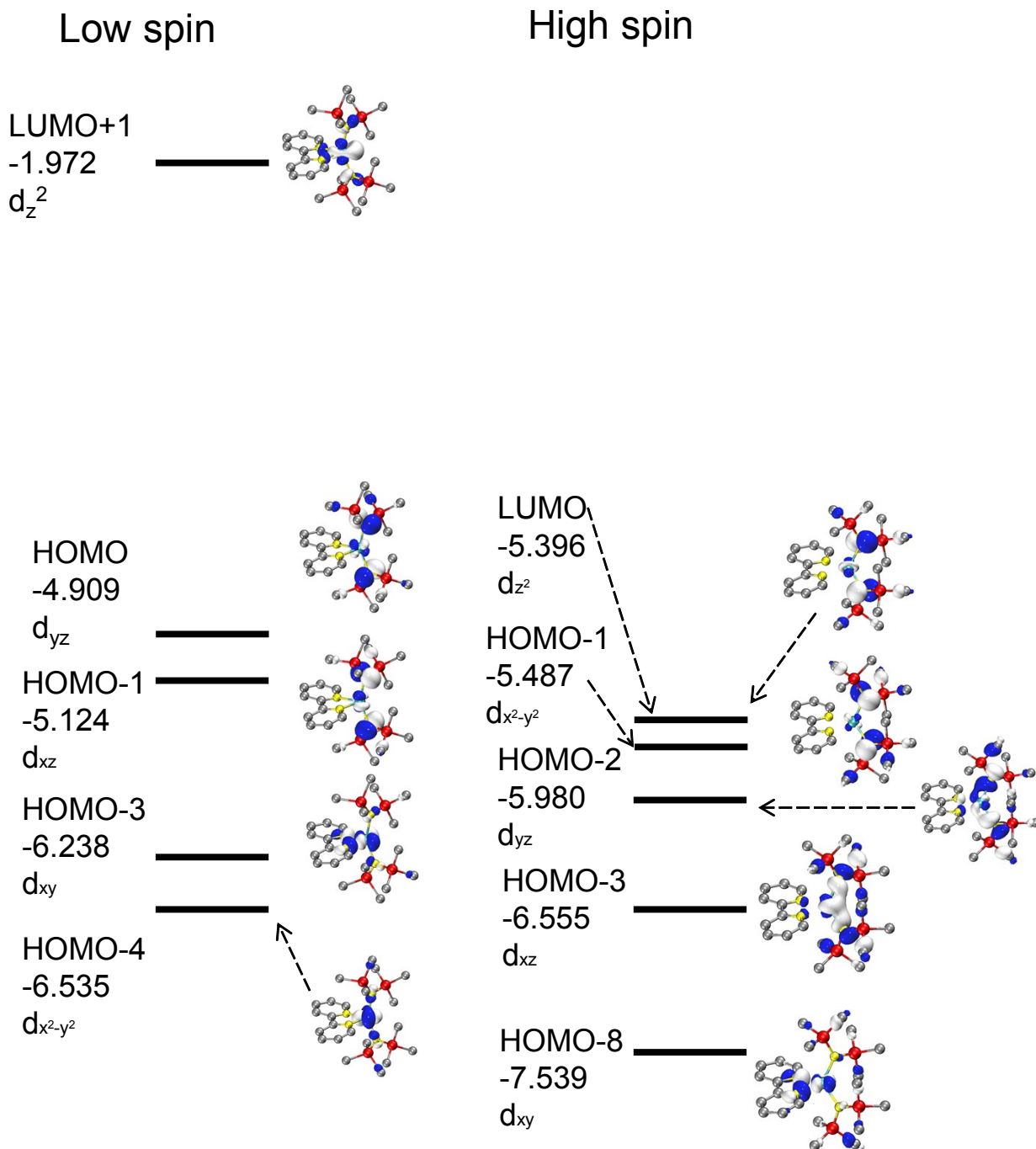
Figure S22. Frontier molecular orbitals and energy diagrams (eV) of **Co-1** complex from DFT calculations. Left: low spin **Co-1**. Right: high spin **Co-1**. HOMO: highest occupied molecular orbital. LUMO: lowest unoccupied molecular orbital.
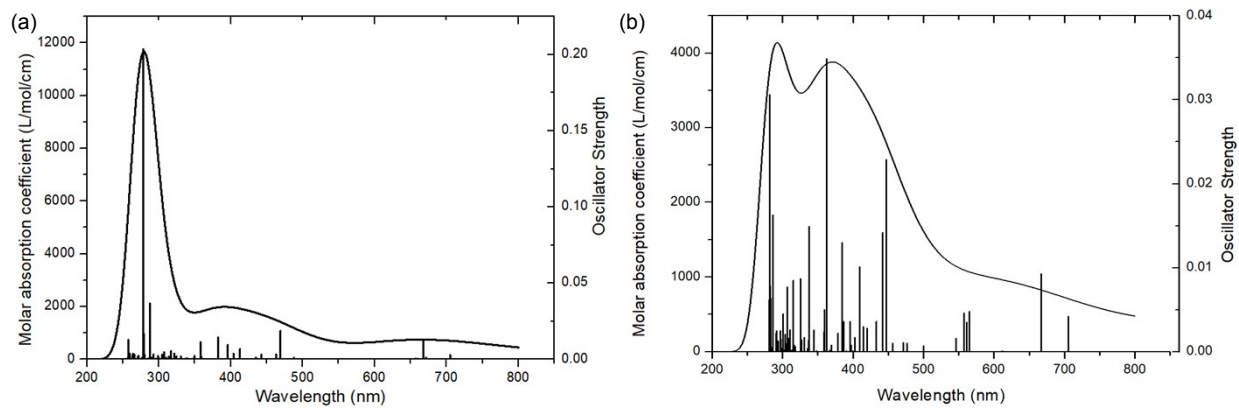
Figure S23. Time-dependent density functional theory (TD-DFT) computed absorption spectrum, and population analysis of (a) Co-1, and (b) Co-1/L-1. Detailed computations results in section S7.

Low spin   High spin

                                            LUMO+5
                                            -1.331
                                            d_{z^2} ▬▬▬▬

                                            SOMO3
                                            -1.879
                                            d_{xy} ▬▬▬▬

                                            SOMO2   ▬▬▬▬
                                            -2.216
                                            $d_{x^2-y^2}$ ▬▬▬▬

       SOMO   ▬▬▬▬   SOMO1
       -3.358   -2.644
       d_{yz}

       HOMO   ▬▬▬▬   HOMO   ▬▬▬▬
       -5.201   -5.676

       HOMO-1   HOMO-1   ▬▬▬▬
       -6.488   -5.918
       $d_{x^2-y^2}$ d_{yz}

       HOMO-2   ▬▬▬▬
       -6.600   ▬▬▬▬
       d_{z^2} HOMO-4   ▬▬▬▬
                                            -7.004
 HOMO-9 d_{xz}
 -7.357 ····▶   ▬▬▬▬
 d_{xy} ▬▬▬▬
       HOMO-11
       -7.559
       d_{xz}
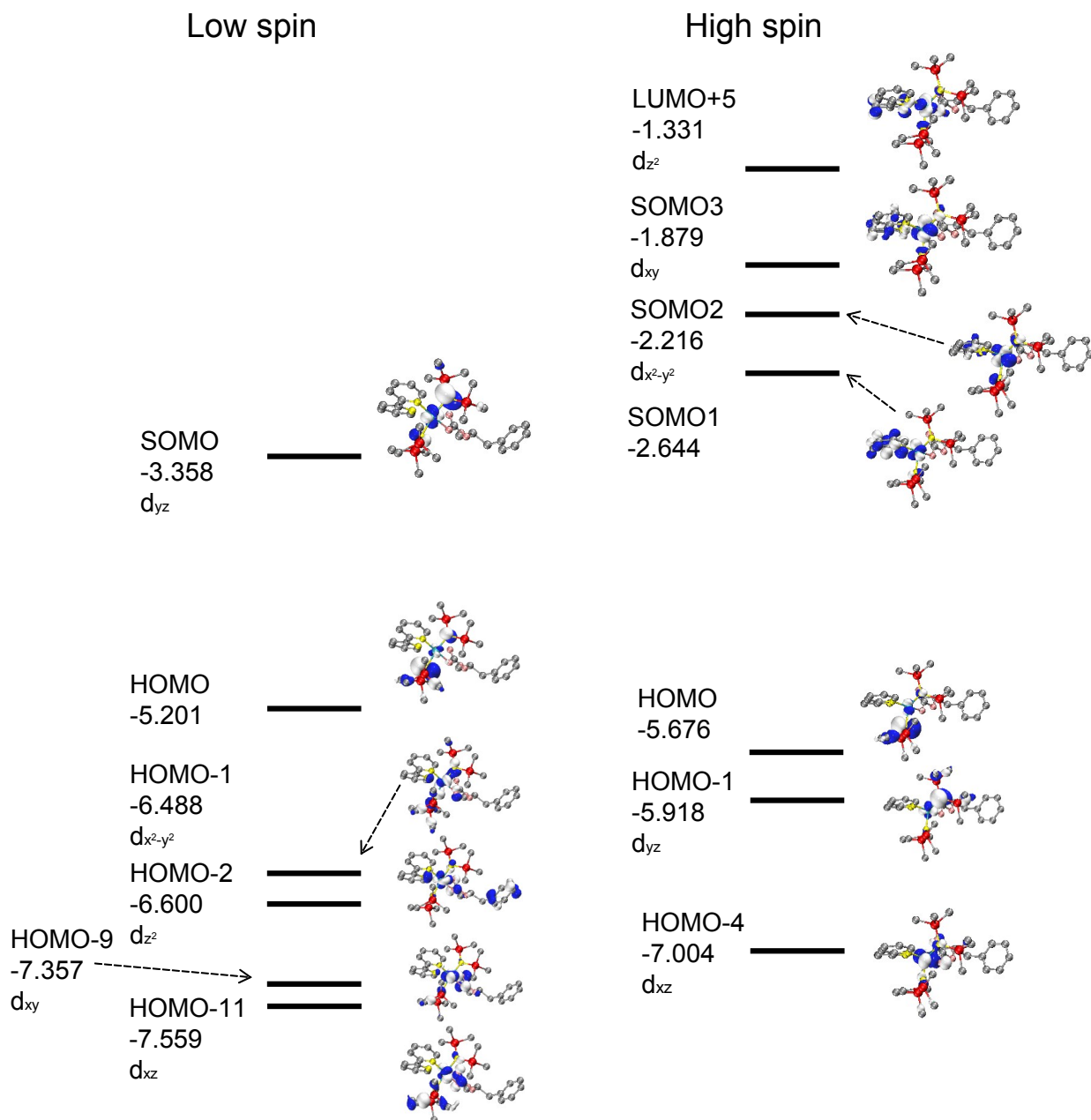
Figure S24. Frontier molecular orbitals and energy diagrams (eV) of L-**1**/**Co-1** complex from DFT calculations. Left: low spin complex. Right: high spin complex. SOMO: singly occupied molecular orbital. HOMO: highest occupied molecular orbital. LUMO: lowest unoccupied molecular orbital.
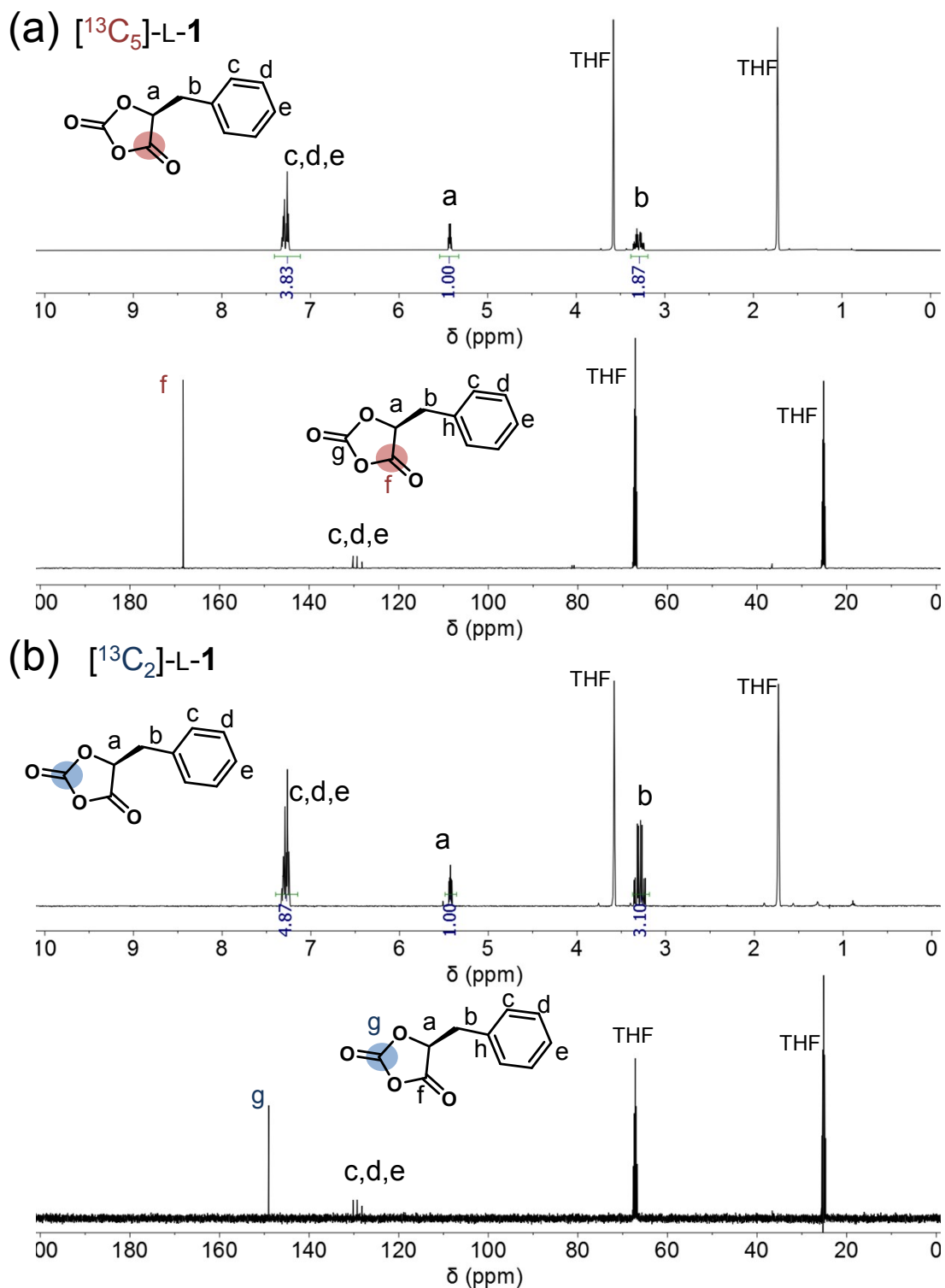
Figure S25. ^1H and ^{13}C NMR spectra of ^{13}C-labeled monomers (a) $[^{13}C_5]$-L-**1**, and (b) $[^{13}C_2]$-L-**1.** ^{13}C atoms are highlighted by color circles in chemical structures (500 MHz, THF-d_8).
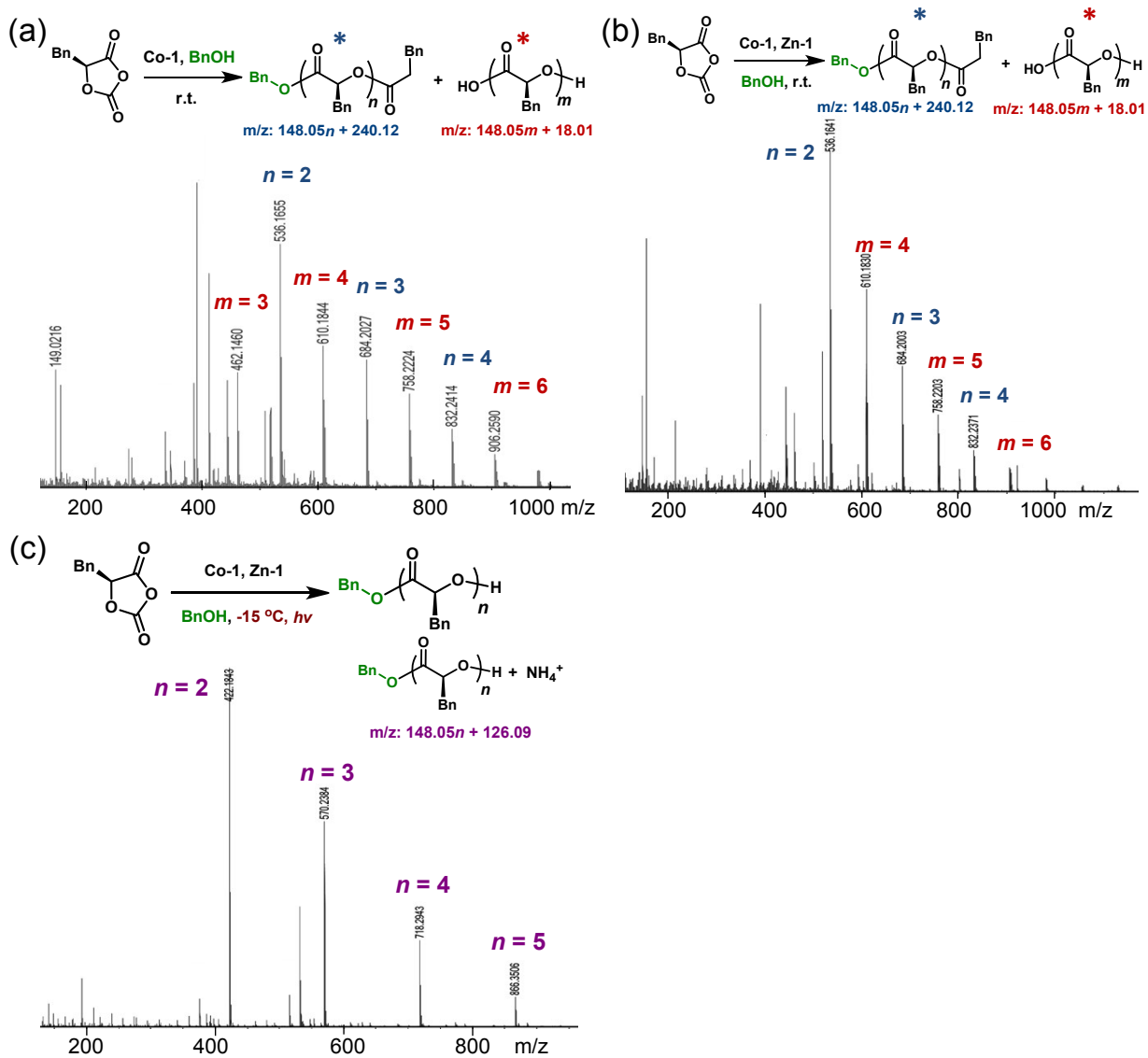
Figure S26. Effect of reaction temperature on the side reactions in Co/Zn-mediated photoredox polymerization of L-1. ESI-MS spectra were obtained at different reaction temperatures. [L-**1**]/[**Co-1**]/[**Zn-1**]/[BnOH] = 1/1/1/1. (a) and (b) indicate side reactions in Co/Zn photoredox ROP at room temperature; whereas (c) suggests no side reactions at −15 °C.

a1) **1/Co-1** r.t.

20180322AZ2-131-1LPheOCA-1Co_bpy-r.t.-no hv-1hr

2206.515 1994.865

1601.845 131.072

1760.198 1524.688

1251.566 964.894

1181.078 1099.610

v(COO): 1760 (ester) cm^{-1}

a2) **1/Co-1/Zn-1**/BnOH r.t.

1944.114 16.969

1855.737 18.623

1677.145 648.538

1603.748 235.698

1758.099 547.325

1496.247 241.434

1442.436 134.776
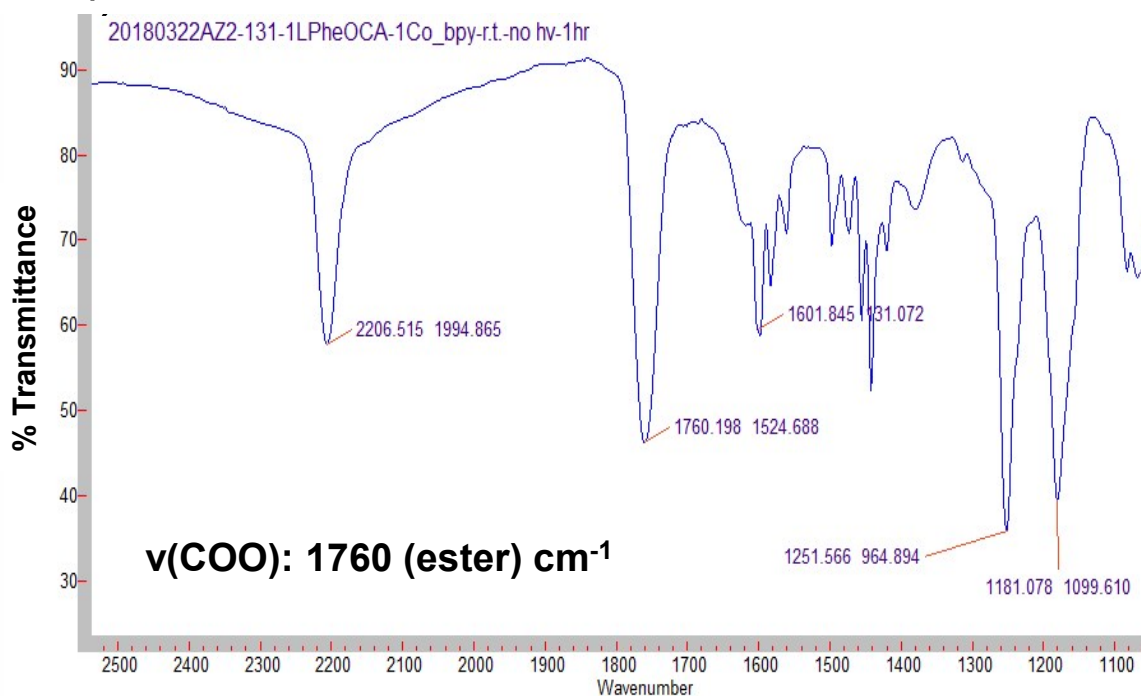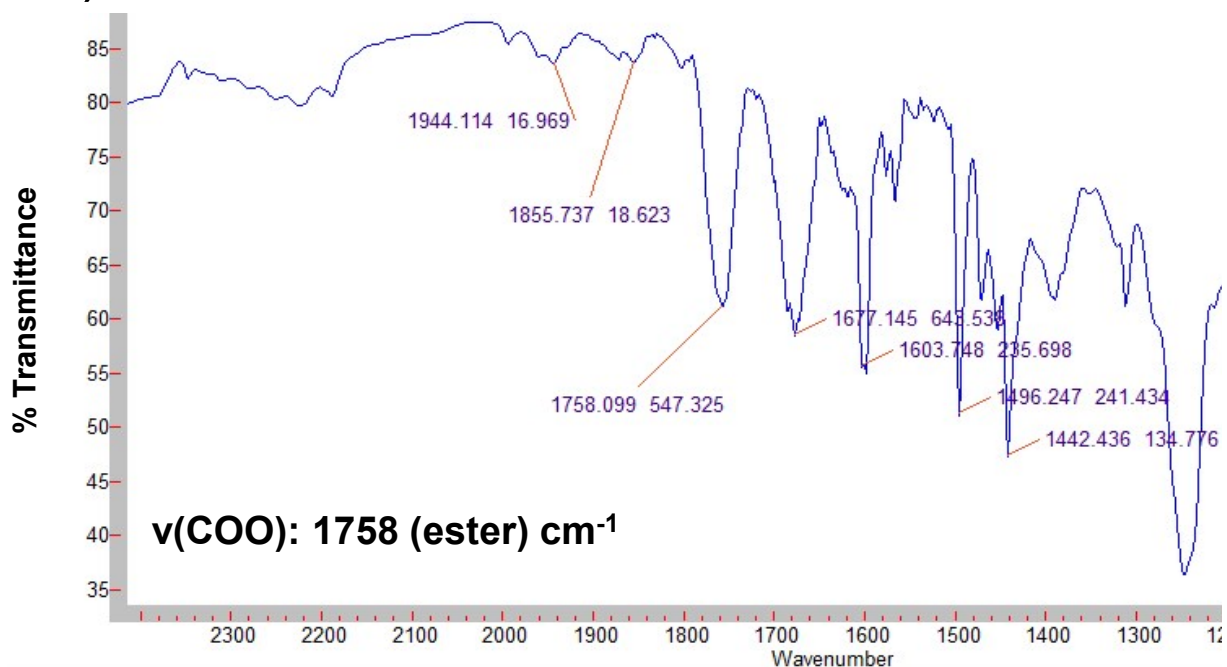
v(COO): 1758 (ester) cm^{-1}

(see next page)

a3) **1**/**Co-1**/**Zn-1**/BnOH 0 °C, *hv*

% Transmittance

v(COO): 1746 (ester) cm⁻¹

a4) **1**/**Co-1**/**Zn-1**/BnOH -15 °C, *hv*

% Transmittance

v(COO): 1751 (ester) cm⁻¹

(see next page)

b1) **1/Co-1** + (PPh$_3$)$_3$RhCl r.t.

% Transmittance

v(COO): 1763 (ester) cm^{-1}

b2) **1/Co-1/Zn-1**/BnOH + (PPh$_3$)$_3$RhCl r.t.

% Transmittance

v(COO): 1753 (ester) cm^{-1}

(see next page)

b3) **1/Co-1/Zn-1**/BnOH + (PPh$_3$)$_3$RhCl 0 °C, *hv*

v(COO): 1763 (ester) cm^{-1}
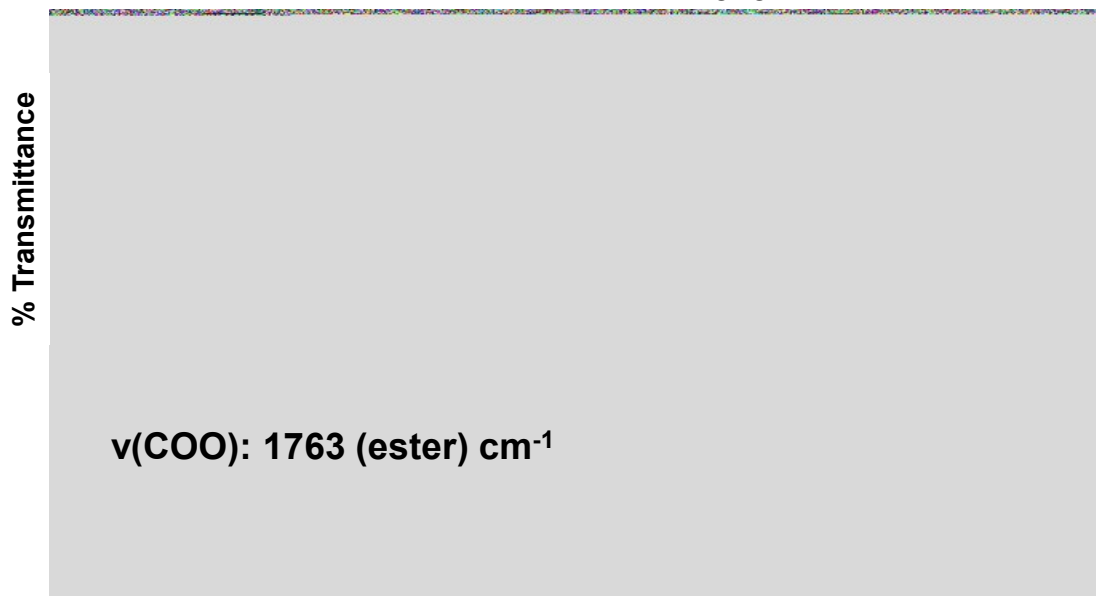
b4) **1/Co-1/Zn-1**/BnOH + (PPh$_3$)$_3$RhCl -15 °C, *hv*

v(COO): 1750 (ester) cm^{-1}

Figure S27. FTIR spectra of the ring-opening reactions of **1** at various reaction conditions. The spectra indicated the absence of a Co-carbonyl intermediate (~1973 cm^{-1}) was observed in the spectrum of L-**1/Co-1** at a ratio of 1/1 at different conditions, even in the presence of (PPh$_3$)$_3$RhCl as a CO scavenger.[27] The results suggested that Co-induced decarbonylation was essentially inefficient in this room temperature reaction, different from similar reactions mediated by a Ni(0) complex.[22]
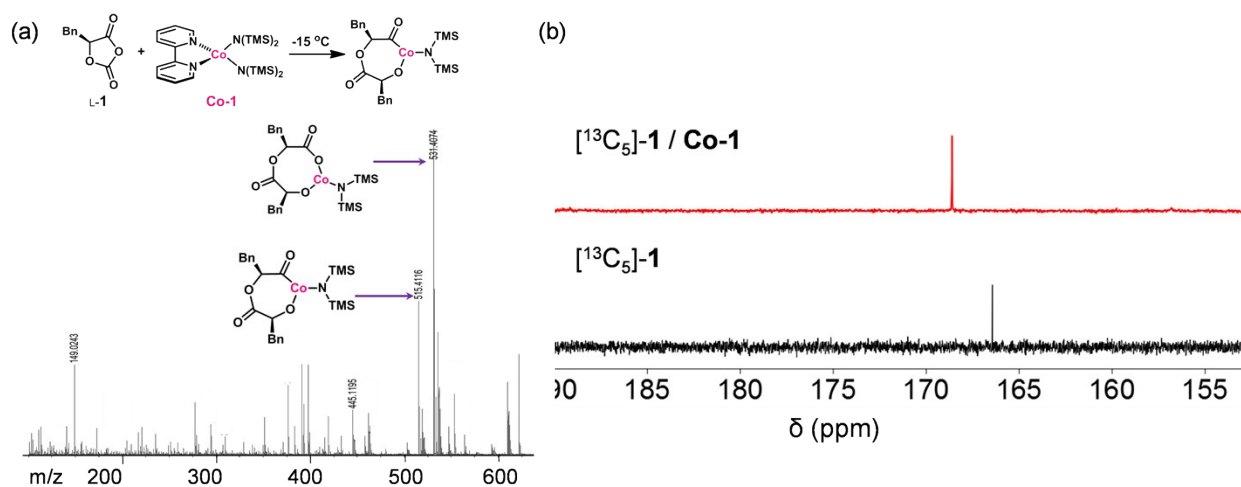
Figure S28. (a) ESI-MS spectrum of the mixture of L-**1**/**Co-1** (1/1). (b) ^{13}C NMR spectra overlay of the mixture of $[^{13}C_5]$-**1** / **Co-1** (1/1), and $[^{13}C_5]$-**1** (500 MHz, THF-d$_8$).

Discussion:

We did not find peaks corresponding to lactones or hydroxyl acids. The peak of 531.4 (m/z) in (a) may be due to the oxidation in the ESI-MS operation that cannot completely maintain anhydrous conditions.
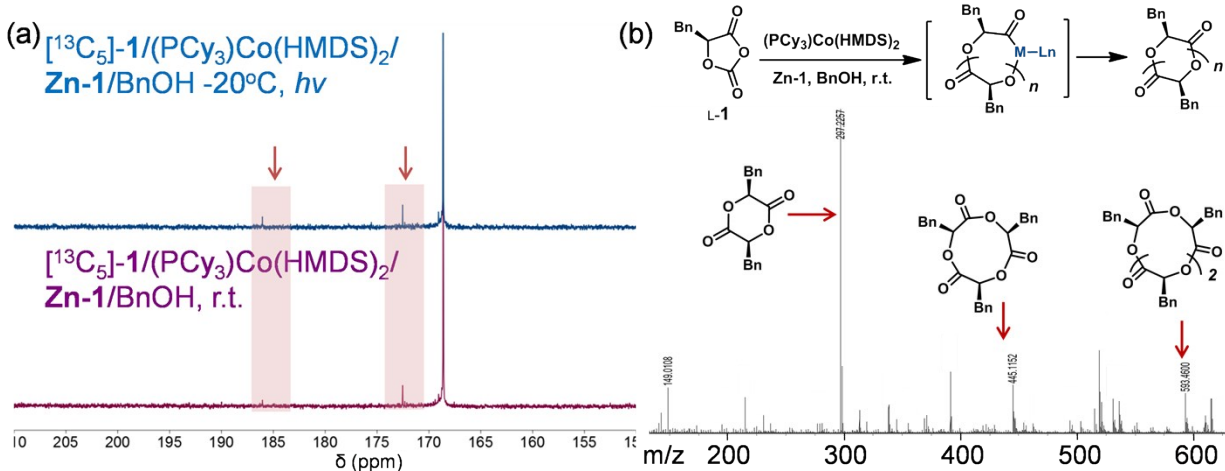
Figure S29. (a) ^{13}C NMR spectra overlay of the mixture of $[^{13}C_5]$-**1** / (PCy$_3$)Co(HMDS)$_2$ / **Zn-1** / BnOH (1/1/1/1) at room temperature or at -20 °C with light (500 MHz, THF-d$_8$). The highlighted red area indicated the existence of carbonyls possibly assigned as lactones and ketones. (b) ESI-MS spectrum of the mixture of L-**1** / (PCy$_3$)Co(HMDS)$_2$ / **Zn-1** / BnOH (1/1/1/1) at room temperature, which presented lactone peaks.

Discussion:

We also used (PCy$_3$)Co(HMDS)$_2$ aiming to capture (PCy$_3$)Co(CO) complex in ^{31}P NMR spectrum. However, no (PCy$_3$)Co(CO) peaks were observed in ^{31}P NMR studies. Given the observation of hydroxyl acids as the side products, we probed the possibility that these hydroxyl acids were hydrolyzed from lactones, which could be formed via the Co-mediated decarboxylation. No lactone peaks were found in the ESI-MS and NMR spectra of the mixture of L-**1/Co-1** (Fig. S28). However, peaks assigned as six- and nine-membered lactones were found in ESI-MS of the mixture of L-**1**/(PCy$_3$)Co(N(SiMe$_3$)$_2$)/**Zn-1**/BnOH (1/1/1/1) at room temperature, but no peaks corresponding to hydroxyl acids were observed. The presence of lactone was also confirmed by the presence of carbonyl carbon peak at 172 ppm in the ^{13}C NMR spectrum of L-$[^{13}C_5]$-**1**/(PCy$_3$)Co(N(SiMe$_3$)$_2$)/**Zn-1**/BnOH at room temperature (Fig. S29), excluding the possibility that hydroxyl acids were generated by hydrolysis of lactones in ESI-MS experimental conditions.
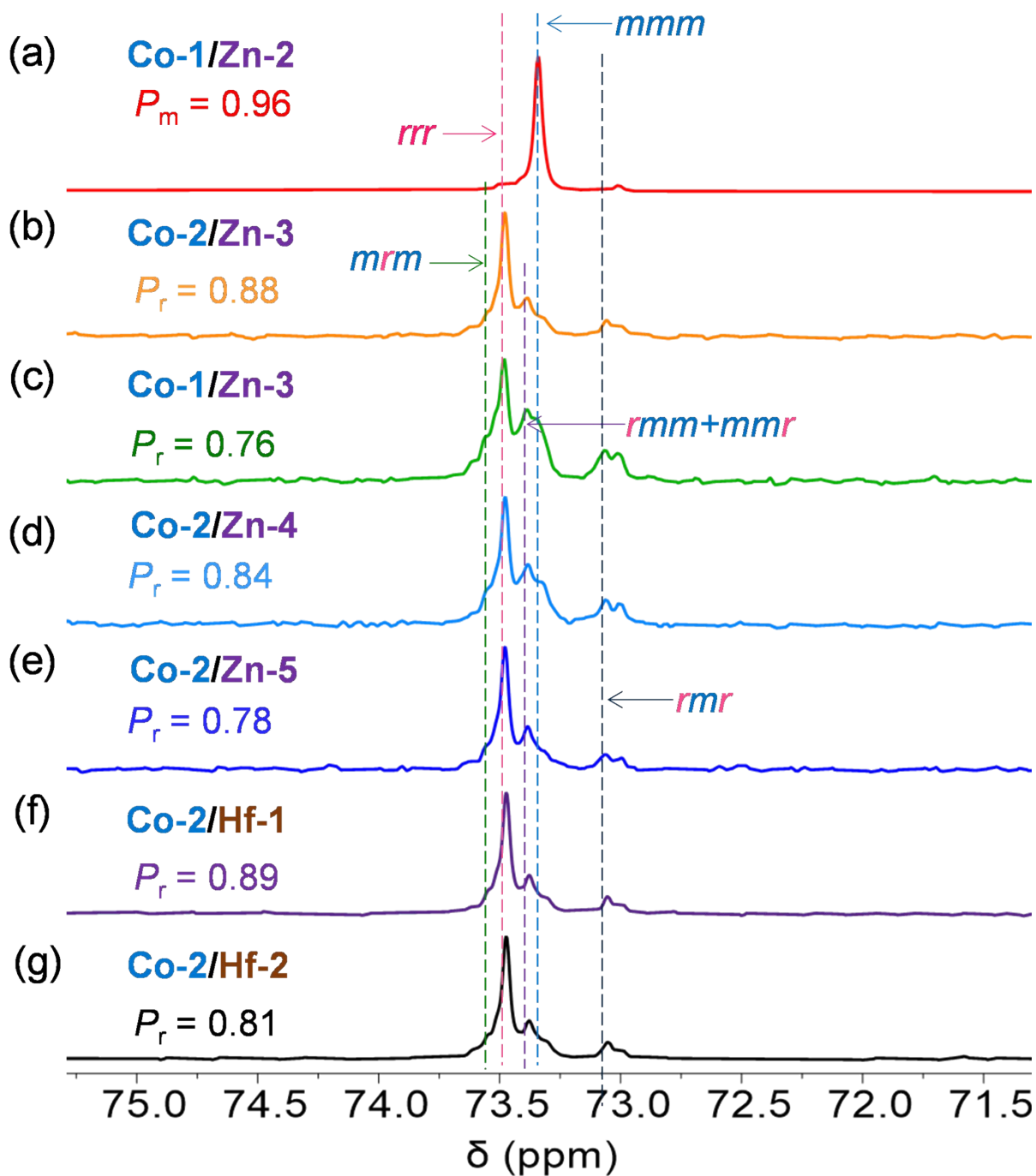
Figure S30. ^{13}C NMR spectra overlay of the methine region of poly(*rac*-**1**) presented in Table S8. (a) entry 1; (b) entry 2; (c) entry 5; (d) entry 8; (e) entry 9; (f) entry 10; (g) entry 15.

(a)

Conversion %

Co-2/Zn-3

▼ L-**1**, FR = 400
▲ D-**1**, FR = 400
◆ L-**1**/D-**1** = 200/200

Time (min)

(b)

Conversion %

Co-2/Hf-1

▼ L-**1**, FR = 400
▲ D-**1**, FR = 400
◆ L-**1**/D-**1** = 200/200

Time (min)

(c)

Conversion %

Co-2/Hf-1

▼ L-**4**, FR = 400
▲ D-**4**, FR = 400
◆ L-**4**/D-**4** = 200/200

Time (min)
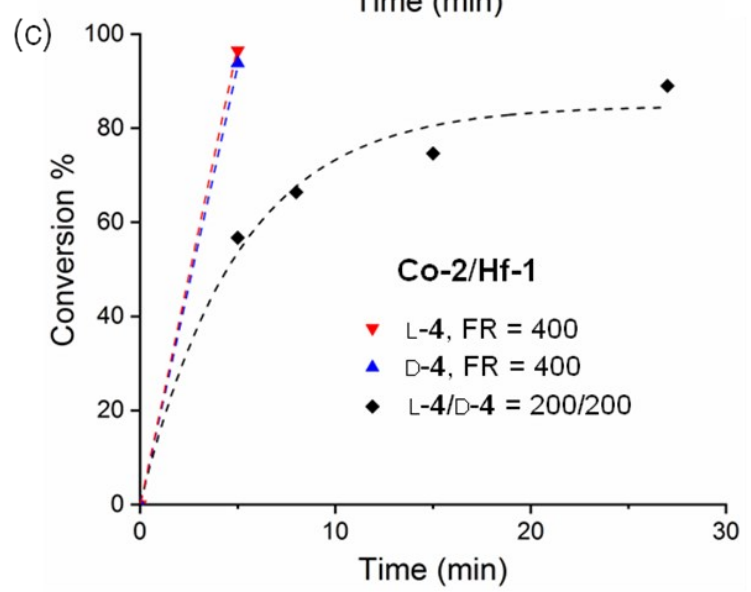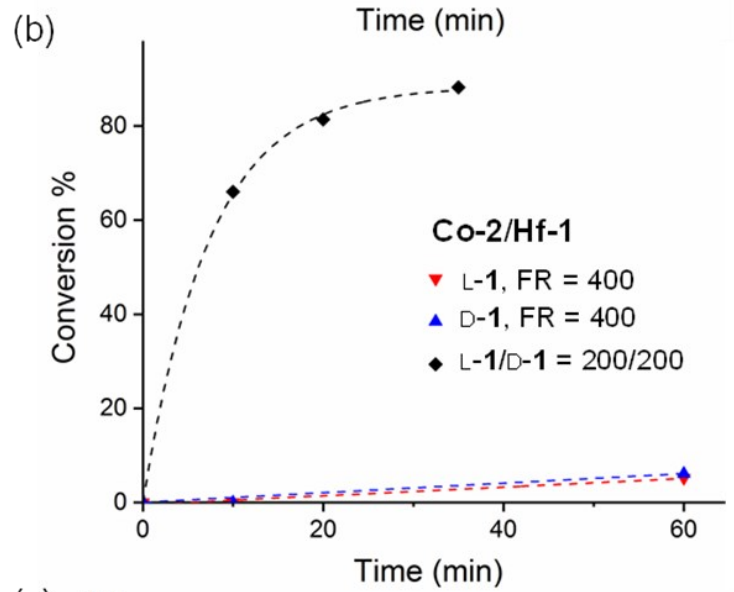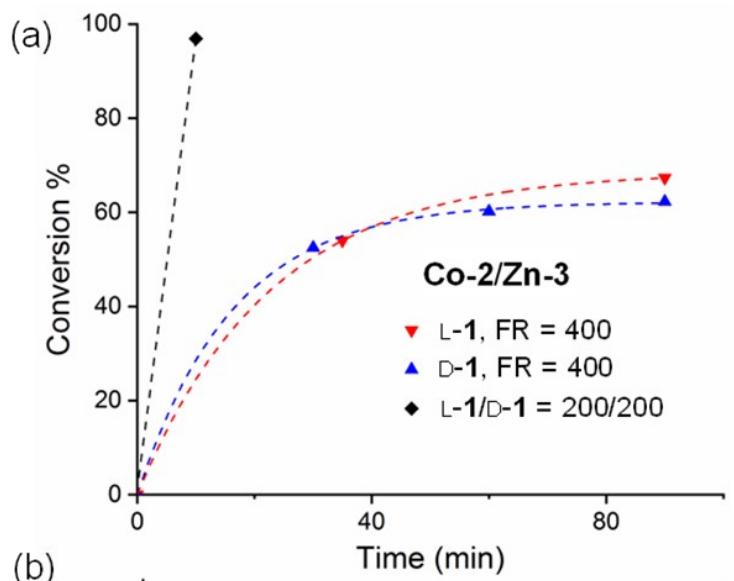
Figure S31. Plots of monomer conversion in polymerization reactions of (a) L-**1** ([L-**1**]/[**Zn-3**]/[**Co-2**]/[BnOH] = 400/1/1/1), D-**1** ([D-**1**]/[**Zn-3**]/[**Co-2**]/[BnOH] = 400/1/1/1), and *rac*-**1** ([L-**1**]/[D-**1**]/[**Zn-3**]/[**Co-2**]/[BnOH] = 200/200/1/1/1; [**1**] = 260.4 mM); (b) L-**1** ([L-**1**]/[**Hf-1**]/[**Co-2**] = 400/1/1), D-**1** ([D-**1**]/[**Hf-1**]/[**Co-2**] = 400/1/1), and *rac*-**1** ([L-**1**]/[D-**1**]/[**Hf-1**]/[**Co-2**] = 200/200/1/1; [**1**] = 130.2 mM); (c) L-**4** ([L-**4**]/[**Hf-1**]/[**Co-2**] = 400/1/1), D-**4** ([D-**4**]/[**Hf-1**]/[**Co-2**] = 400/1/1), and *rac*-**4** ([L-**4**]/[D-**4**]/[**Hf-1**]/[**Co-2**] = 200/200/1/1; [**4**] = 172.4 mM). FR, the feeding ratio of monomer to catalyst.
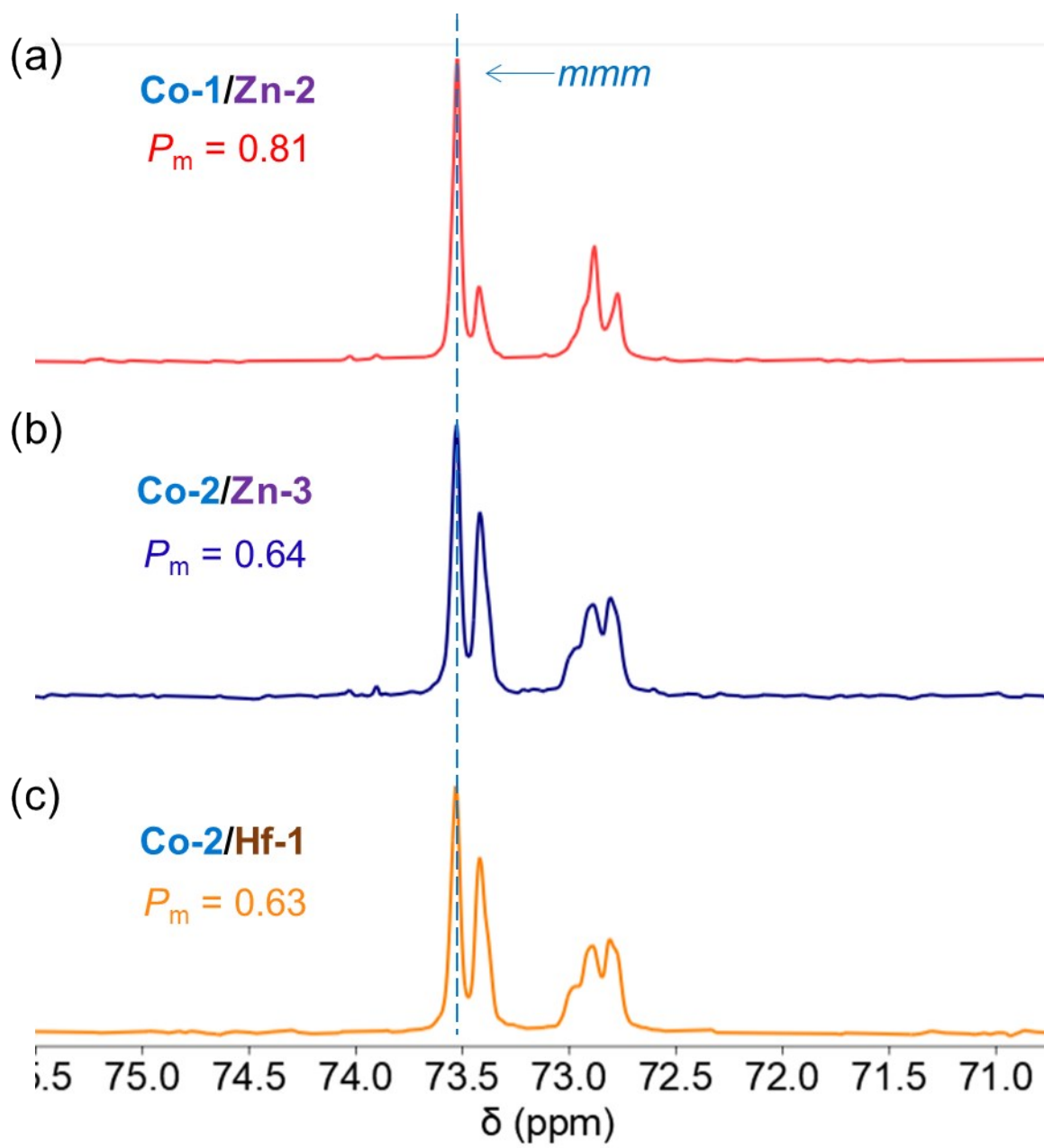
Figure S32. ^{13}C NMR spectra overlay of the methine region of poly(*rac*-**2**) in Table S9. (a) entry 1; (b) entry 2; (c) entry 3.
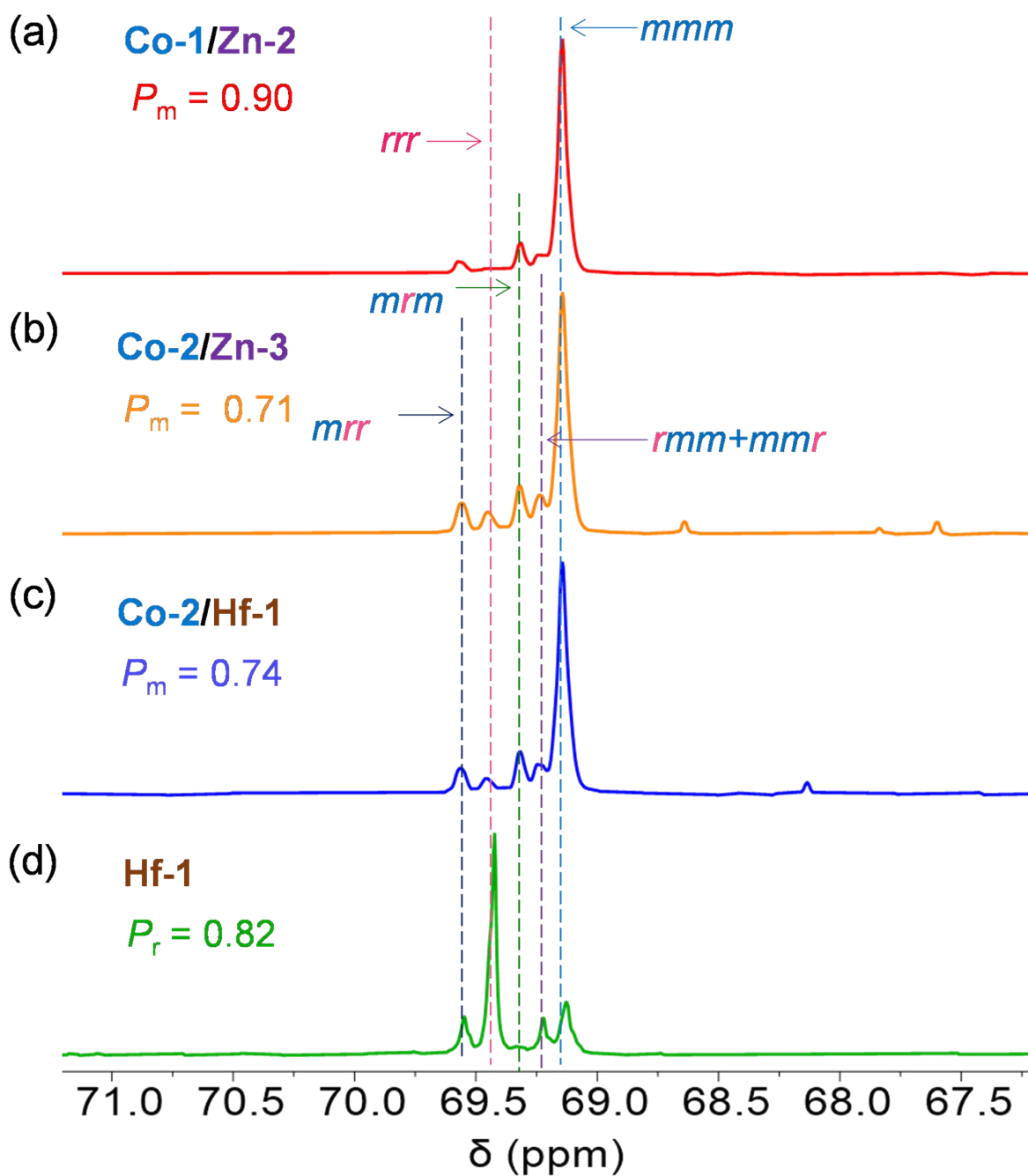
Figure S33. ^{13}C NMR spectra overlay of the methine region of poly(*rac*-**4**) in Table S9. (a) entry 4; (b) entry 5; (c) entry 6; (d) entry 7.
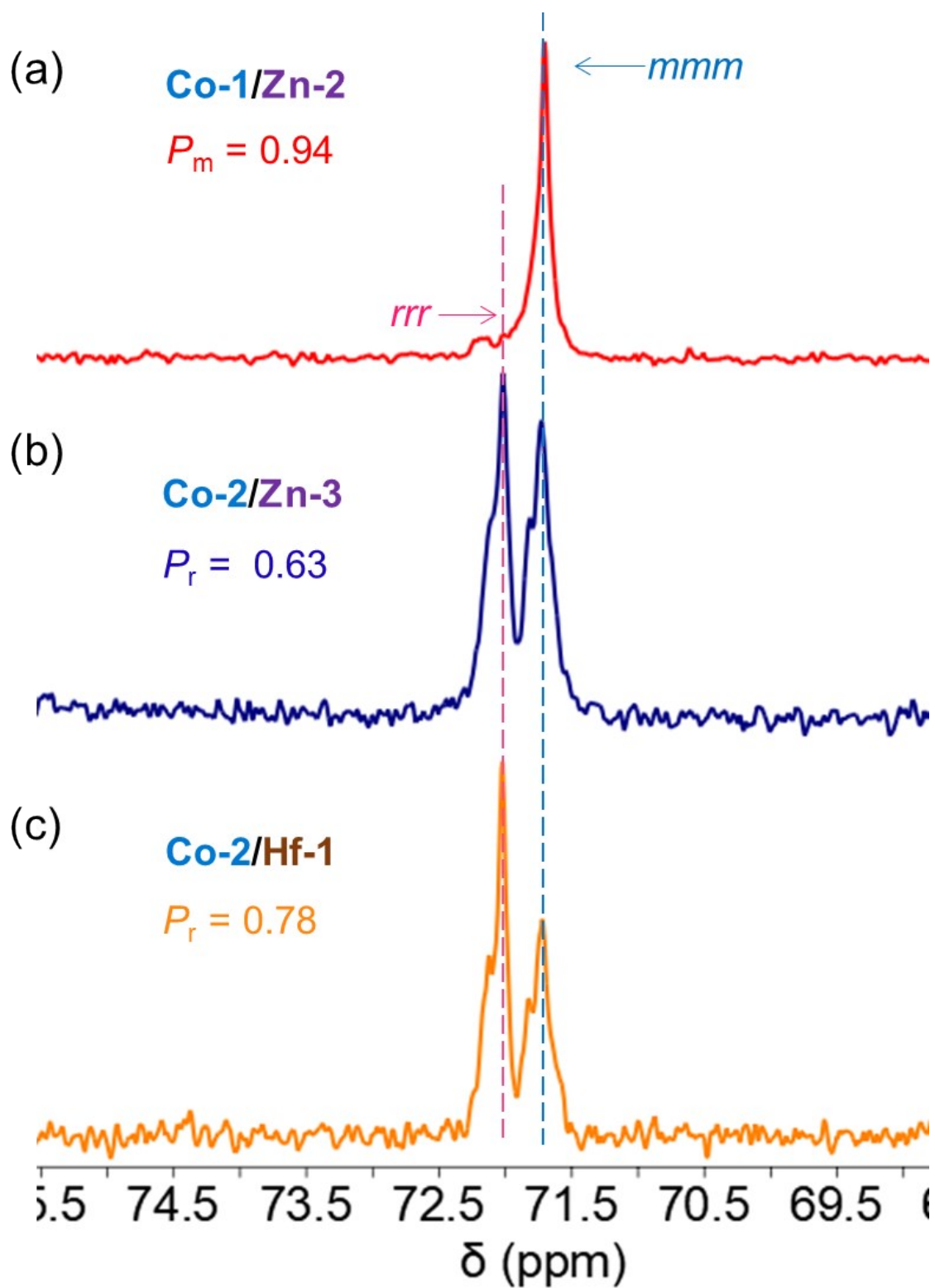
Figure S34. ^{13}C NMR spectra overlay of the methine region of poly(*rac*-**3**) in Table S9. (a) entry 8; (b) entry 9; (c) entry 10.
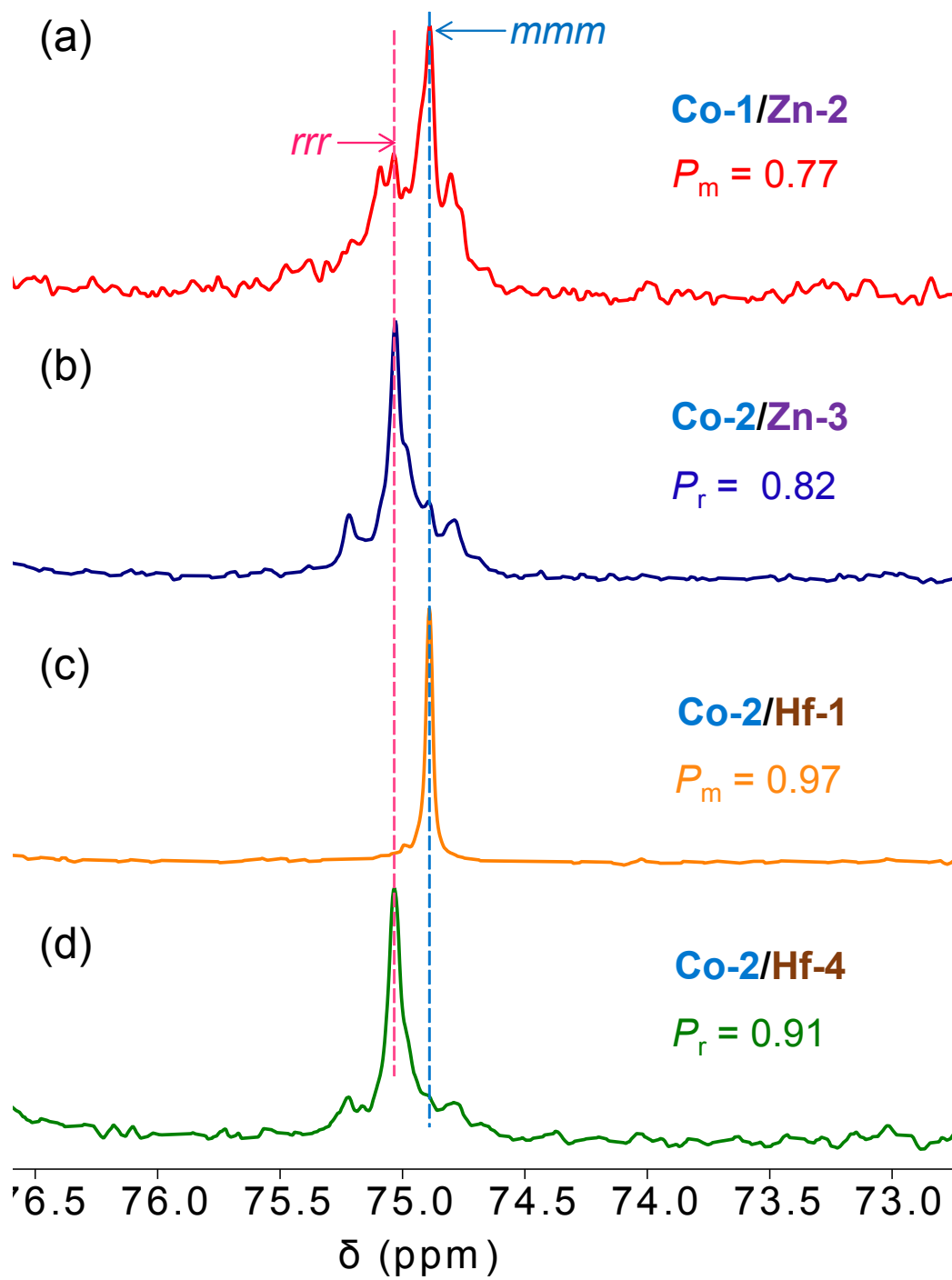
Figure S35. ^{13}C NMR spectra overlay of the methine region of poly(*rac*-**5**) in Table S9. (a) entry 11; (b) entry 12; (c) entry 13; (d) entry 14.
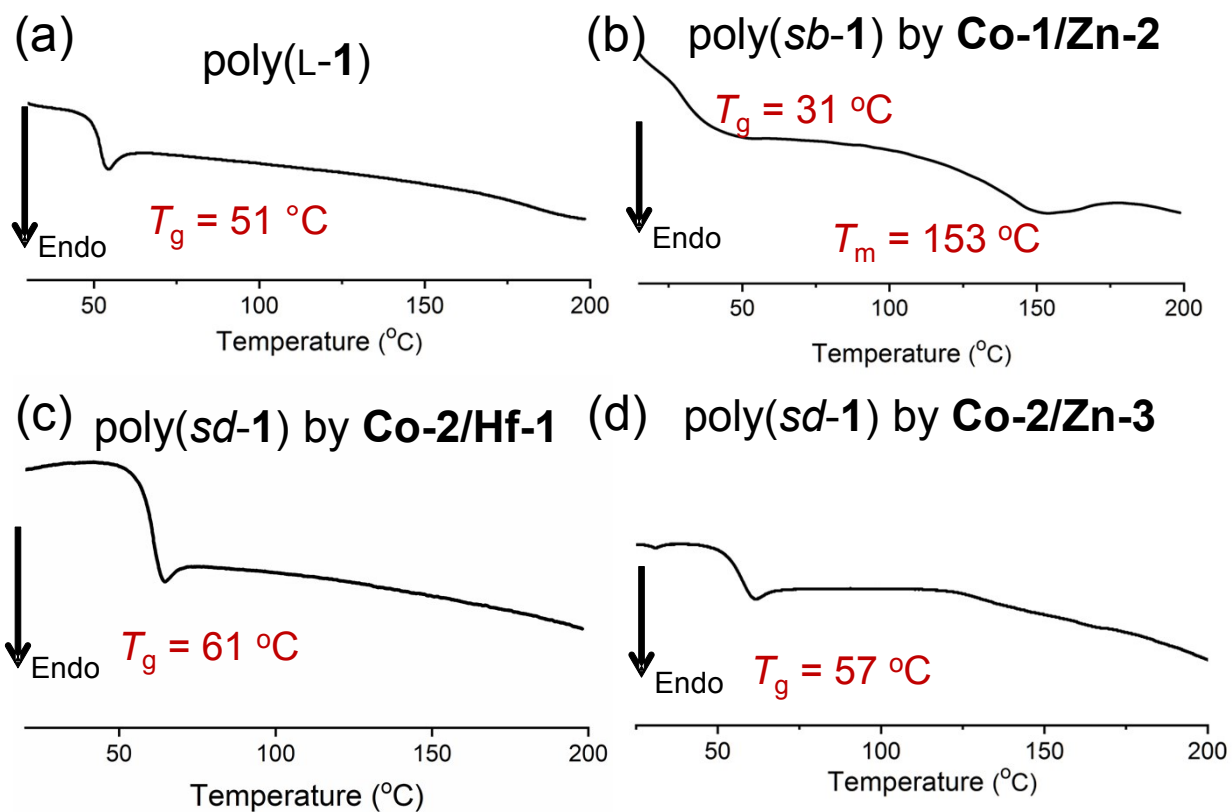
Figure S36. DSC thermograms of poly(*rac*-**1**) with various microstructures.

(a) poly(L-**2**)

Endo $T_g = 8\ ^oC$

0   50   100   150

Temperature (^oC)

(b) poly(*sb*-**2**) by **Co-1/Zn-2**

$T_g = 8\ ^oC$

Endo

0   50   100   150   200

Temperature (^oC)
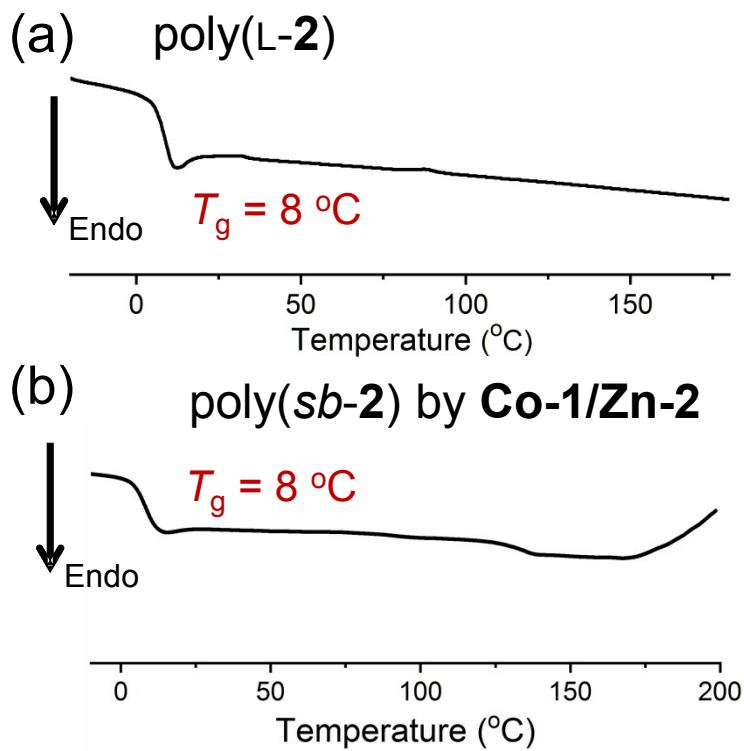
Figure S37. DSC thermograms of poly(*rac*-**2**) with various microstructures.

(a) poly(L-**3**)

T_g = 8 °C

Endo

0   50   100   150
Temperature (°C)

(b)

poly(*sb*-**3**) by **Co-1/Zn-2**

T_g = 4 °C

Endo

0   50   100   150
Temperature (°C)

(c)

poly(*sd*-**3**) by **Co-2/Hf-1**

T_g = 6 °C

Endo

0   50   100   150
Temperature (°C)
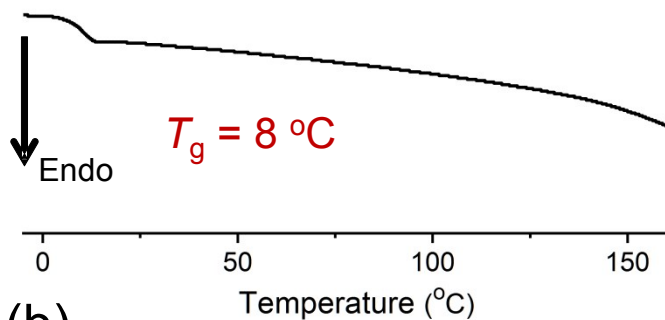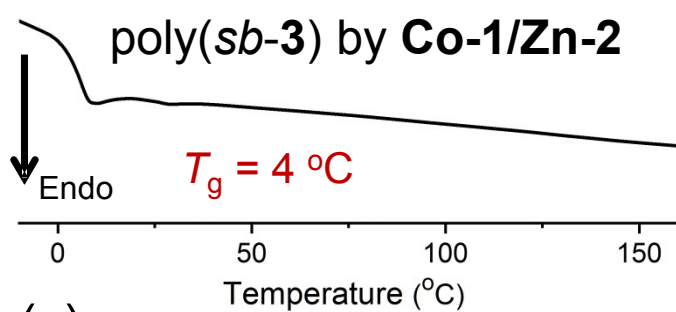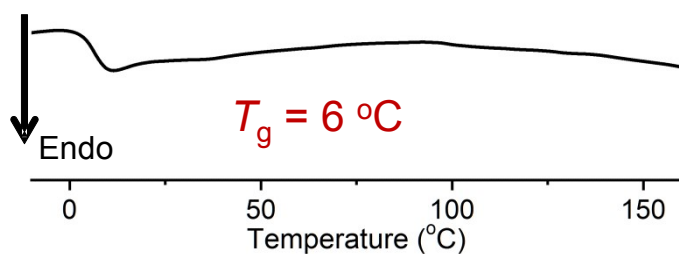
Figure S38. DSC thermograms of poly(*rac*-**3**) with various microstructures.

(a) poly(L-**4**)

T_m = 173 °C

Endo

Temperature (°C)

50   100   150   200

(b) poly(*sb*-**4**) by **Co-1/Zn-2**

T_g = 50 °C

Endo

T_m = 146 °C

Temperature (°C)

50   100   150   200
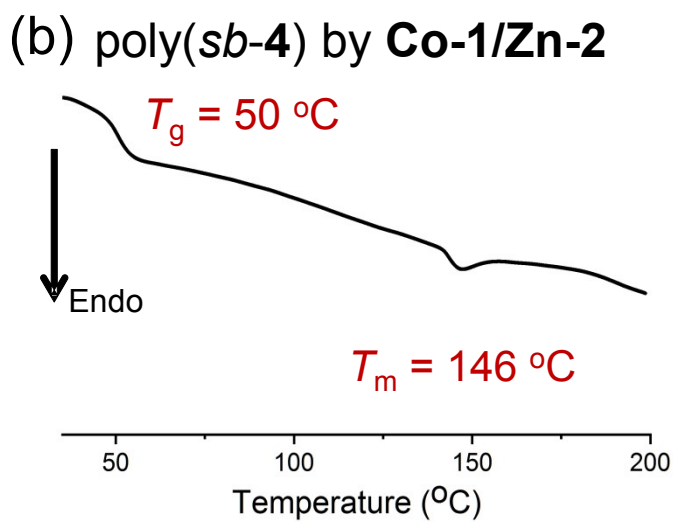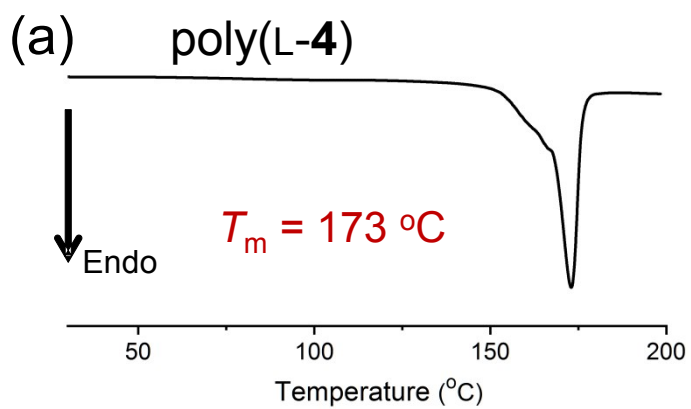
Figure S39. DSC thermograms of poly(*rac*-**4**) with various microstructures.
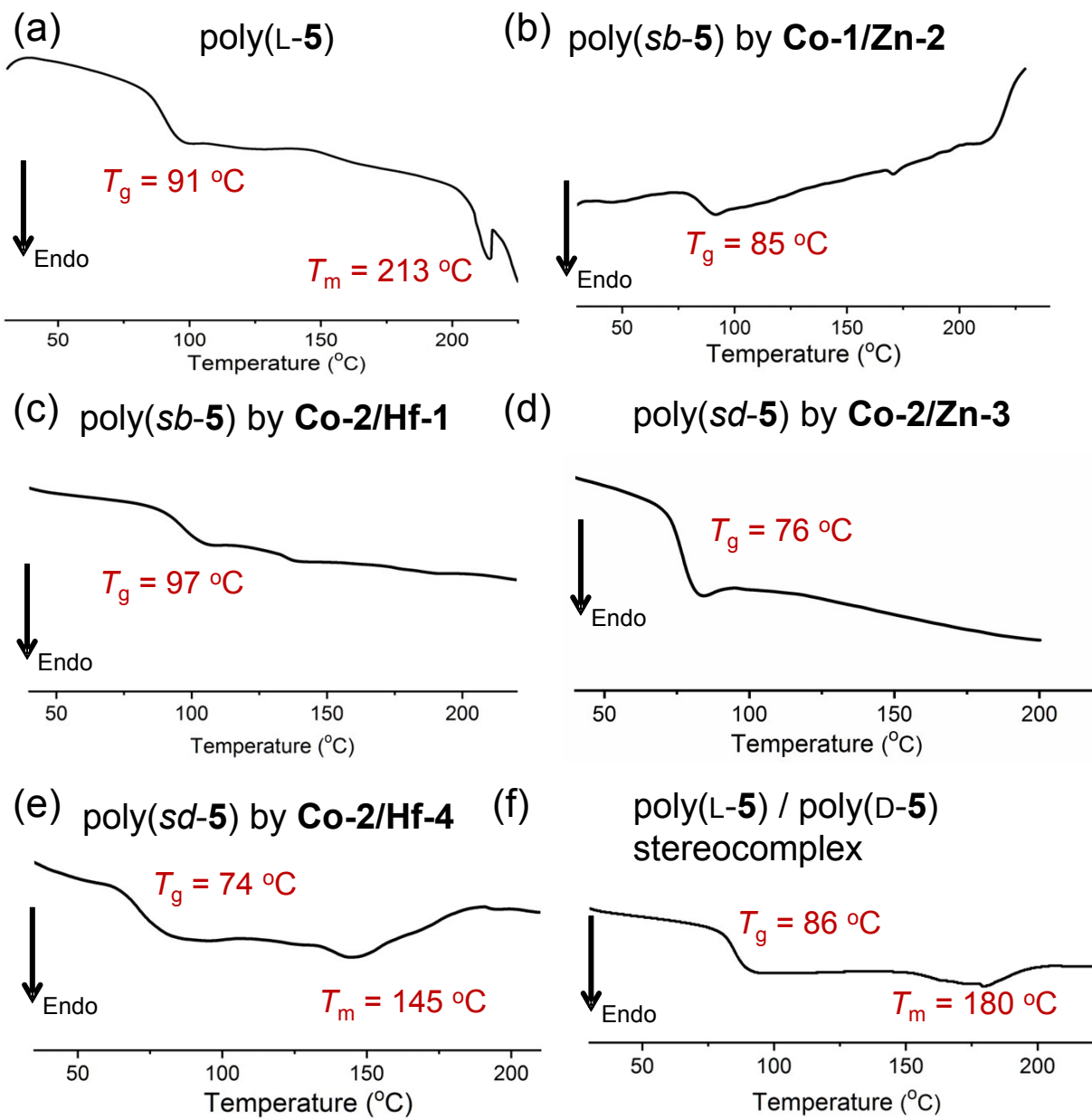
Figure S40. DSC thermograms of poly(*rac*-**5**) with various microstructures.
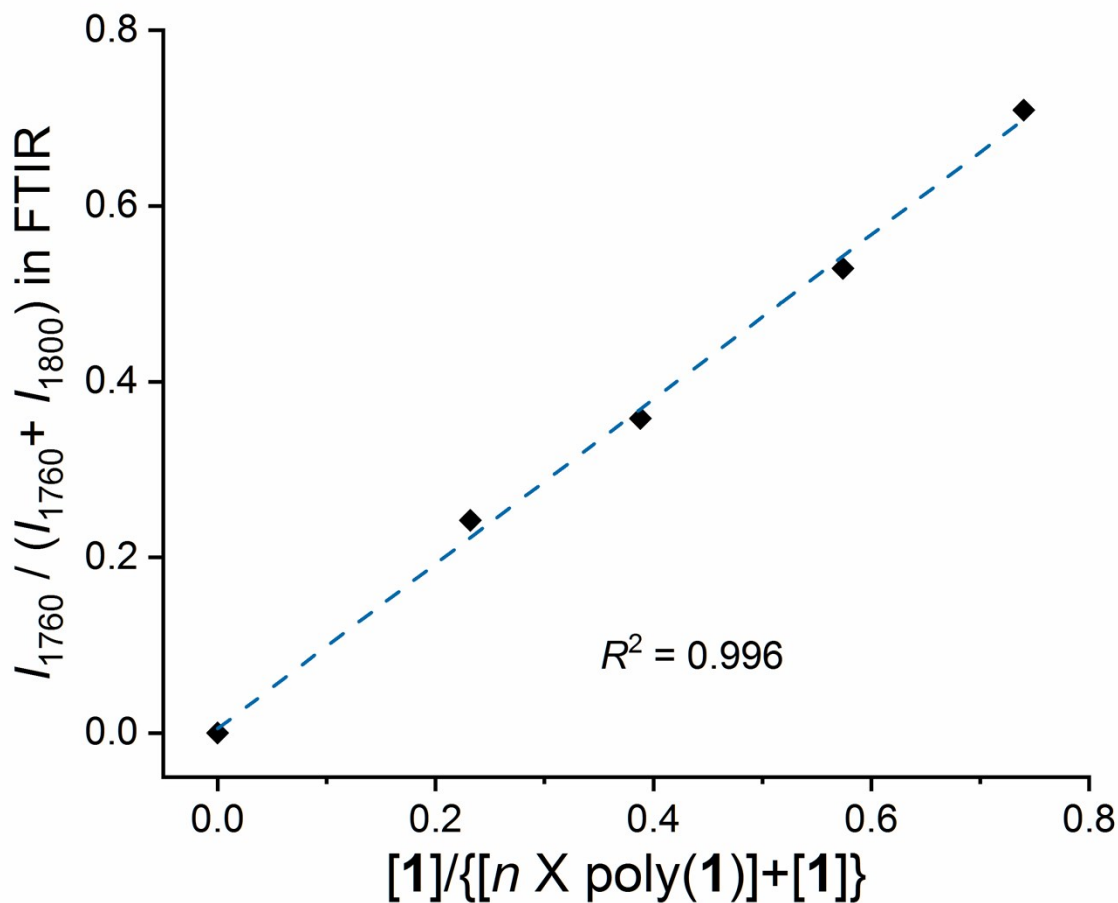
Figure S41. The measured monomer molar ratios in monomer/polymer mixtures by Fourier-transform infrared spectra (FTIR) versus known monomer concentration in the mixture. The OCA monomer **1** was mixed with poly(**1**) with known molecular weight and concentrations at predetermined ratios (numbers in x axis). The mixture was measured by FTIR to determine the monomer concentrations in the mixtures (values in y axis). Note that the monomer anhydride peaks (~ 1800 cm^{-1}) are separated from the esters peaks (~ 1760 cm^{-1}), and the anhydride peaks intensity gradually decrease through the polymerization process.

S7. Computation results

Co-1:

Low spin

Energy: -2387.13484063

C	3.34856100	-2.13298700	0.16740700
C	1.79299700	-4.55347900	1.00201700
C	1.23399600	-3.31673700	-1.70778400
C	1.90501700	0.96001000	2.55178300
C	0.67373200	0.30828200	-2.54249500
C	-0.67373200	-0.30828200	-2.54249500
C	-1.95093100	-3.76821800	1.35225400
C	-1.90501700	-0.96001000	2.55178300
C	2.47265000	0.99654400	-1.25359100
C	1.30135400	0.76768100	-3.70710500
C	-2.47265000	-0.99654400	-1.25359100
C	-1.30135400	-0.76768100	-3.70710500
C	-1.23399600	3.31673700	-1.70778400
C	-3.34856100	2.13298700	0.16740700
C	0.00000000	3.03021600	3.60050400
C	2.56098000	1.35164400	-3.61948800
C	3.16138800	1.47039900	-2.36692900
C	-3.16138800	-1.47039900	-2.36692900
C	-2.56098000	-1.35164400	-3.61948800
C	0.00000000	-3.03021600	3.60050400
C	1.95093100	3.76821800	1.35225400
C	-1.79299700	4.55347900	1.00201700
Co	0.00000000	0.00000000	0.27549300
H	2.70765500	1.38285800	3.17214900
H	0.77584200	3.15337000	4.36798700
H	3.05875000	1.71683700	-4.51277200
H	4.13981200	1.92289100	-2.24555600

H	2.89757100	1.07329200	-0.26017400
H	0.80257100	0.69326100	-4.66631900
H	-2.89757100	-1.07329200	-0.26017400
H	-4.13981200	-1.92289100	-2.24555600
H	-3.05875000	-1.71683700	-4.51277200
H	-0.80257100	-0.69326100	-4.66631900
H	0.86321100	-5.12857500	1.07557600
H	0.24995200	-3.79170400	-1.80865600
H	1.24779900	-2.43860300	-2.36296800
H	2.50981100	-5.16696600	0.43995800
H	1.98395200	-4.02181700	-2.09032000
H	-0.73558100	2.31260800	3.98434900
H	-0.50438600	3.99464400	3.48422100
H	2.68182600	4.05076300	2.12174900
H	1.35935400	0.24087800	3.17326600
H	-2.50981100	5.16696600	0.43995800
H	0.50438600	-3.99464400	3.48422100
H	3.48990900	-1.29791400	-0.52618800
H	3.59347200	-1.77927600	1.17656900
H	1.40171600	4.67561900	1.07463500
H	2.51087200	3.44822600	0.46440900
H	2.38679000	0.38100700	1.75600000
H	2.19382800	-4.43364500	2.01482500
H	-0.86321100	5.12857500	1.07557600
H	-2.19382800	4.43364500	2.01482500
H	-4.08598900	2.90175900	-0.09955700
H	-1.98395200	4.02181700	-2.09032000
H	0.73558100	-2.31260800	3.98434900
H	-0.77584200	-3.15337000	4.36798700
H	-2.38679000	-0.38100700	1.75600000
H	-2.68182600	-4.05076300	2.12174900
H	4.08598900	-2.90175900	-0.09955700

H	-3.59347200	1.77927600	1.17656900
H	-3.48990900	1.29791400	-0.52618800
H	-1.24779900	2.43860300	-2.36296800
H	-0.24995200	3.79170400	-1.80865600
H	-1.35935400	-0.24087800	3.17326600
H	-2.70765500	-1.38285800	3.17214900
H	-1.40171600	-4.67561900	1.07463500
H	-2.51087200	-3.44822600	0.46440900
N	-1.26391900	-0.42246600	-1.33253700
N	-0.37706900	1.85044000	0.80742500
N	0.37706900	-1.85044000	0.80742500
N	1.26391900	0.42246600	-1.33253700
Si	-1.59436200	2.87675700	0.11313800
Si	-0.78108200	-2.39734300	1.98429100
Si	1.59436200	-2.87675700	0.11313800
Si	0.78108200	2.39734300	1.98429100

Co-1:

High spin

Energy: -2387.1725395 Hartree

C	0.00000000	3.54210800	-0.42916200
C	2.04758300	4.00285500	1.74001000
C	2.91700400	2.87877400	-0.97141600
C	-2.08651300	1.43586800	2.27416900
C	-0.69608600	0.26071100	-2.95263700
C	0.69608600	-0.26071100	-2.95263700
C	4.15937800	0.75550200	1.93155400
C	2.08651300	-1.43586800	2.27416900
C	-2.44327600	1.08259900	-1.66701100
C	-1.46595800	0.37153500	-4.11699700
C	2.44327600	-1.08259900	-1.66701100
C	1.46595800	-0.37153500	-4.11699700

C	-2.91700400	-2.87877400	-0.97141600
C	0.00000000	-3.54210800	-0.42916200
C	-1.85006600	-1.10258800	3.91691900
C	-2.76274400	0.87159900	-4.02886700
C	-3.26372300	1.24006600	-2.78158200
C	3.26372300	-1.24006600	-2.78158200
C	2.76274400	-0.87159900	-4.02886700
C	1.85006600	1.10258800	3.91691900
C	-4.15937800	-0.75550200	1.93155400
C	-2.04758300	-4.00285500	1.74001000
Co	0.00000000	0.00000000	0.00078900
H	-2.61904800	1.81482000	3.15686300
H	-2.44788100	-0.59624200	4.68646100
H	-3.37455900	0.96164700	-4.92161500
H	-4.26957700	1.62931200	-2.66577900
H	-2.78955800	1.33388700	-0.67122600
H	-1.06957500	0.05270800	-5.07405900
H	2.78955800	-1.33388700	-0.67122600
H	4.26957700	-1.62931200	-2.66577900
H	3.37455900	-0.96164700	-4.92161500
H	1.06957500	-0.05270800	-5.07405900
H	2.97781400	3.72656800	2.24899300
H	3.88385900	2.53536900	-0.58435000
H	2.66853700	2.24906200	-1.83611900
H	2.19386800	5.00472000	1.31506900
H	3.05056000	3.90569300	-1.33704800
H	-0.79317600	-0.92153500	4.14606300
H	-2.02666300	-2.17943900	4.01507100
H	-4.73595300	-0.25707400	2.72214700
H	-1.03461600	1.72717000	2.36166400
H	-2.19386800	-5.00472000	1.31506900
H	2.02666300	2.17943900	4.01507100

H	-0.26261800	3.07868800	-1.38605400
H	-0.87037000	3.47020300	0.23347200
H	-4.42509600	-1.81887600	1.95600600
H	-4.50588100	-0.35578600	0.96945900
H	-2.50399700	1.96004300	1.40433000
H	1.26334300	4.07875800	2.50300200
H	-2.97781400	-3.72656800	2.24899300
H	-1.26334300	-4.07875800	2.50300200
H	-0.18042300	-4.60794700	-0.62229000
H	-3.05056000	-3.90569300	-1.33704800
H	0.79317600	0.92153500	4.14606300
H	2.44788100	0.59624200	4.68646100
H	2.50399700	-1.96004300	1.40433000
H	4.73595300	0.25707400	2.72214700
H	0.18042300	4.60794700	-0.62229000
H	0.87037000	-3.47020300	0.23347200
H	0.26261800	-3.07868800	-1.38605400
H	-2.66853700	-2.24906200	-1.83611900
H	-3.88385900	-2.53536900	-0.58435000
H	1.03461600	-1.72717000	2.36166400
H	2.61904800	-1.81482000	3.15686300
H	4.42509600	1.81887600	1.95600600
H	4.50588100	0.35578600	0.96945900
N	1.19214800	-0.61336600	-1.74762200
N	-1.30861000	-1.15457000	0.92451800
N	1.30861000	1.15457000	0.92451800
N	-1.19214800	0.61336600	-1.74762200
Si	-1.55587500	-2.78033100	0.36350200
Si	2.28924700	0.45464800	2.18229400
Si	1.55587500	2.78033100	0.36350200
Si	-2.28924700	-0.45464800	2.18229400

TD-DFT calculated transitions 1-80 for **Co-1** (see Figure S23a)

Excited state	λ (nm)	f	Excited state	λ (nm)	f
1	1895.49	0.0001	41	313.21	0.0001
2	1528.98	0.0000	42	310.28	0.0009
3	1408.66	0.0002	43	308.61	0.0000
4	1171.15	0.0026	44	307.04	0.0047
5	704.59	0.0029	45	305.52	0.0003
6	671.09	0.0012	46	304.38	0.0030
7	667.40	0.0131	47	300.87	0.0001
8	659.10	0.0004	48	300.16	0.0005
9	656.30	0.0004	49	299.78	0.0003
10	626.12	0.0001	50	298.59	0.0022
11	487.63	0.0009	51	297.91	0.0003
12	468.95	0.0188	52	296.33	0.0004
13	462.48	0.0032	53	292.54	0.0031
14	462.26	0.0001	54	290.01	0.0010
15	441.98	0.0031	55	287.73	0.0366
16	439.90	0.0001	56	285.55	0.0007
17	434.73	0.0012	57	280.95	0.0002
18	424.47	0.0000	58	279.69	0.0030
19	412.59	0.0068	59	279.37	0.0163
20	407.70	0.0002	60	278.10	0.2035
21	403.50	0.0037	61	276.33	0.0009
22	395.51	0.0094	62	276.28	0.0002
23	390.94	0.0001	63	273.03	0.0001
24	389.70	0.0000	64	272.76	0.0003
25	382.68	0.0145	65	271.68	0.0024
26	377.55	0.0000	66	270.25	0.0017
27	358.25	0.0020	67	269.79	0.0005
28	357.82	0.0113	68	268.02	0.0000
29	349.32	0.0022	69	266.26	0.0006
30	347.84	0.0005	70	265.58	0.0031
31	338.91	0.0008	71	263.70	0.0036
32	337.67	0.0005	72	263.28	0.0027
33	330.35	0.0019	73	260.54	0.0000
34	324.39	0.0019	74	259.61	0.0039
35	324.13	0.0015	75	259.38	0.0000
36	323.87	0.0000	76	259.28	0.0009
37	321.11	0.0039	77	258.94	0.0013
38	316.88	0.0055	78	257.41	0.0129
39	315.67	0.0003	79	256.83	0.0003
40	313.81	0.0017	80	256.57	0.0007

Co-1/L-**1**:

Low spin

Energy: -3072.4934731 Hartree

C	4.09882600	-0.48795800	2.56282700
C	3.61140700	-1.15916200	3.67731100
C	2.24246100	-1.34483400	3.80822400
C	1.40934100	-0.88170200	2.79372000
N	1.87503700	-0.26106300	1.71184400
C	3.19437700	-0.03572100	1.60438800
C	5.03571400	2.49028500	-0.50775200
C	4.82670100	1.48027400	0.42126900
C	3.57834100	0.86343200	0.49831900
N	2.59233700	1.20234000	-0.35480200
C	2.78004200	2.20527900	-1.21284700
C	3.98444100	2.88444400	-1.32412200
Co	0.87882600	0.19561000	-0.22455400
N	1.68564800	-1.41006100	-0.97985200
Si	2.37717900	-1.48344600	-2.57497600
C	3.93357000	-2.57468700	-2.59504600
C	3.10582900	0.10003800	-3.32391300
C	1.17472000	-2.04125000	-3.92666200
Si	1.47157800	-2.98017800	-0.23101800
C	0.00218800	-3.27564200	0.92161600
C	3.01719900	-3.49688700	0.74575900
C	1.14328800	-4.37798100	-1.48054900
N	-0.01930600	1.81878800	0.05649700
Si	-1.11231500	2.16310800	-1.30189600
C	-0.96767100	3.97971100	-1.81325600
C	-2.91209900	1.79027200	-0.89691600
C	-0.62801300	1.16054100	-2.81797300
Si	0.06675700	2.91157300	1.44280100
C	-1.63852000	3.60229800	1.85384400
C	1.23767000	4.33291600	0.99930700
C	0.71104500	2.23525800	3.07047200
C	-3.20584300	-2.02537600	2.71867900
C	-3.71421500	-1.22687700	1.51821900
O	-2.78622000	-1.25037200	0.46510900
C	-1.59294800	-0.63323100	0.74551200
O	-0.81515400	-0.69886400	-0.25896500
C	-5.02062800	-1.82332700	1.00654300

O	-1.41525900	-0.12400800	1.85195100
C	-5.60426300	-0.98274700	-0.09426800
C	-6.41807600	0.10904700	0.21262400
C	-6.92098900	0.92645600	-0.79384200
C	-6.61359900	0.66016500	-2.12497300
C	-5.80172200	-0.42549600	-2.44121500
C	-5.30000000	-1.24008500	-1.43182900
O	-3.74261500	-2.10094000	3.77445600
H	5.16704500	-0.32071800	2.44935300
H	4.29796300	-1.52214700	4.43958700
H	1.81600000	-1.83960200	4.67687000
H	0.32391700	-0.96532200	2.84818300
H	6.00341500	2.98372300	-0.56954200
H	5.61781800	1.20373000	1.11275200
H	1.92409000	2.46796300	-1.83212900
H	4.08775900	3.69303700	-2.04231800
H	4.70960100	-2.08623200	-1.98469800
H	4.32028400	-2.64349400	-3.62278800
H	3.81162600	-3.59492000	-2.21458400
H	3.46039800	-0.20150000	-4.32165900
H	3.98001800	0.47294100	-2.77386300
H	2.40032500	0.92534900	-3.48034600
H	0.59846400	-2.93583800	-3.66819100
H	1.72669200	-2.24913300	-4.85569000
H	0.45850600	-1.23599000	-4.14486400
H	-0.93317500	-3.29457800	0.34804000
H	-0.13854800	-2.58197900	1.75526600
H	0.14808300	-4.27838700	1.35372000
H	3.04206100	-4.59098600	0.85735000
H	3.02167200	-3.06989300	1.75805400
H	3.94586000	-3.18807200	0.24694900
H	1.12053100	-5.31662400	-0.90581800
H	1.86577700	-4.50894700	-2.29354800
H	0.14758000	-4.25326100	-1.92861600
H	-1.62001200	4.14424700	-2.68343600
H	0.05510400	4.24039600	-2.12090200
H	-1.27500200	4.68854100	-1.03378700
H	-3.13507700	0.72284300	-1.02839100
H	-3.56058300	2.35297500	-1.58418800
H	-3.18879100	2.06943700	0.12723000

H	-1.38114100	1.34019600	-3.59981100
H	-0.62404300	0.08313800	-2.60559900
H	0.34653300	1.44133900	-3.24232600
H	-2.15075500	4.09837700	1.02037200
H	-1.53676900	4.33644700	2.66616600
H	-2.28293400	2.79070800	2.21922800
H	2.27754500	3.97733900	0.94855500
H	1.19057700	5.09350300	1.79238700
H	0.99723100	4.82325900	0.04760900
H	0.12104400	1.37366600	3.40215400
H	0.58614700	3.04037300	3.81068600
H	1.77414200	1.96392700	3.05797200
H	-3.87293200	-0.19318200	1.87222000
H	-5.71104500	-1.89036400	1.85961900
H	-4.82391600	-2.84720700	0.65719400
H	-6.65963100	0.31712600	1.25677800
H	-7.55853900	1.77154400	-0.53804400
H	-7.00921200	1.29633200	-2.91534500
H	-5.55645500	-0.63992200	-3.48038900
H	-4.65180400	-2.08170500	-1.67623900

Co-1/L-**1**:

High spin

Energy: -3073.8640162 Hartree

C	-2.29835400	4.07687900	-1.17640800
C	-1.25136100	4.59300500	-1.93506500
C	-0.16572300	3.77263000	-2.22636500
C	-0.16550700	2.47255800	-1.72463100
N	-1.16477000	1.97305700	-0.98408400
C	-2.23398900	2.75249700	-0.72459800
C	-5.57407600	2.13590600	0.95469200
C	-4.59584600	2.72960800	0.16305700
C	-3.32967800	2.13498000	0.06585000
N	-3.04478800	0.97402100	0.69147600
C	-3.99323900	0.41300800	1.45161600
C	-5.26484400	0.95698200	1.62695600
Co	-1.04064200	-0.11569800	-0.05650600
N	-1.96681000	-1.41847600	-1.24785100

Si	-3.07400500	-2.60515100	-0.61492700
C	-4.89965400	-2.18447500	-0.98428200
C	-2.92689800	-2.81954200	1.28844300
C	-2.81488200	-4.38416000	-1.25501500
Si	-1.81766300	-1.18333800	-2.97938700
C	-0.01327500	-1.01012100	-3.54299700
C	-2.79976800	0.34108300	-3.57932700
C	-2.50278900	-2.60076500	-4.05872700
N	-0.20515800	-0.59422600	1.91102300
Si	0.85386100	-2.06536300	1.97318500
C	0.35934500	-3.02193800	3.54172300
C	2.70073000	-1.65281200	2.07391400
C	0.63618200	-3.20423200	0.49120800
Si	-0.28290300	0.57449000	3.28108500
C	1.31144000	0.70048200	4.29128500
C	-1.64883200	-0.09576900	4.42860400
C	-0.75359200	2.32659800	2.76359500
C	3.44899800	3.09791000	-0.24127400
C	3.97264800	1.64569900	-0.24962300
O	2.99629400	0.76843200	-0.78142600
C	1.81811600	0.68397300	-0.04949700
O	0.97319400	-0.08285300	-0.60908100
C	5.23598800	1.55420500	-1.12487500
O	1.71777700	1.33747600	0.99918000
C	5.94096800	0.21812600	-1.01223300
C	7.07571700	0.08436600	-0.20114300
C	7.72913400	-1.14347800	-0.07968300
C	7.25379500	-2.25886000	-0.77093900
C	6.12304800	-2.13720100	-1.58239100
C	5.47178700	-0.90914600	-1.70260700
O	3.98090300	4.02972600	0.26933000
H	-3.14302000	4.70677700	-0.92478900
H	-1.28558200	5.62002700	-2.28667000
H	0.67527900	4.12483000	-2.81359500
H	0.65601100	1.79709100	-1.92290600
H	-6.55867300	2.58644600	1.03904200
H	-4.82274800	3.63646300	-0.38433100
H	-3.72415200	-0.51591900	1.93651200
H	-5.98790600	0.45448000	2.26079000
H	-5.19713700	-1.22100500	-0.55350000

H	-5.57145100	-2.95377000	-0.57968100
H	-5.08261400	-2.12656800	-2.06429300
H	-2.44850000	-3.77882500	1.51908000
H	-3.92028100	-2.84410700	1.75634900
H	-2.33412300	-2.04525900	1.78497600
H	-3.18514300	-4.54069600	-2.27164100
H	-3.35408100	-5.08106100	-0.59874000
H	-1.75594300	-4.66934800	-1.23848100
H	0.46490200	-1.99845900	-3.54925400
H	0.58655500	-0.37755000	-2.88501000
H	0.03520300	-0.61454200	-4.56659800
H	-2.82177200	0.37488700	-4.67672700
H	-2.37688500	1.28784900	-3.22965400
H	-3.83871900	0.29027700	-3.22860800
H	-2.37667700	-2.30843600	-5.11015400
H	-3.56927200	-2.80277700	-3.90654500
H	-1.95702000	-3.53927800	-3.91526000
H	0.90806700	-3.97273300	3.55182100
H	-0.70995000	-3.25815100	3.55612900
H	0.60601400	-2.48821200	4.46570800
H	3.09209800	-1.36375200	1.09393600
H	3.22561400	-2.56899400	2.37656900
H	2.94904800	-0.86816600	2.79030700
H	1.40881200	-3.98351100	0.54865400
H	0.76639700	-2.66119800	-0.44821000
H	-0.33641000	-3.70042000	0.46844600
H	1.65175700	-0.25500500	4.70335400
H	1.13727100	1.37945300	5.13643400
H	2.11360500	1.12407700	3.67948100
H	-2.62823500	-0.12015800	3.94080800
H	-1.72787200	0.57644100	5.29339200
H	-1.43129900	-1.09988000	4.80472900
H	-0.10661400	2.66471400	1.95059400
H	-0.59724600	2.99217300	3.62288100
H	-1.79885600	2.41606900	2.45872600
H	4.19363700	1.38831900	0.79305300
H	5.90909400	2.36055300	-0.81299300
H	4.94498400	1.75279700	-2.16326100
H	7.45435900	0.95140700	0.33633700
H	8.61061500	-1.22591600	0.55097600

H	7.76180700	-3.21542300	-0.68083700
H	5.74686200	-3.00025500	-2.12551000
H	4.58928200	-0.82167200	-2.32913100

TD-DFT calculated transitions 1-80 for **Co-1/ʟ-1** (see Figure S23b)

Excited state	λ (nm)	f	Excited state	λ (nm)	f
1	2536.16	0.0002	41	347.8	0.0001
2	1613.08	0.0002	42	344.09	0.0026
3	1273.34	0.0004	43	337.45	0.0149
4	1245.71	0.0125	44	336.85	0.0014
5	1202.46	0.0021	45	335.25	0.0004
6	968.05	0.0003	46	330.69	0.0017
7	861.88	0.0001	47	327.04	0.0014
8	704.86	0.0042	48	325.07	0.0087
9	666.35	0.0093	49	323.3	0
10	611.16	0.0001	50	317.97	0.0006
11	564.87	0.0048	51	316.04	0.0008
12	560.9	0.0035	52	315.97	0.0003
13	557.11	0.0046	53	314.96	0.0085
14	545.52	0.0016	54	312.58	0.0002
15	500.09	0.0007	55	310.37	0.0026
16	476.15	0.001	56	308.85	0
17	470.84	0.0011	57	308.3	0.0016
18	456.05	0.001	58	307.96	0.0001
19	446.62	0.0229	59	306.68	0.0077
20	441.71	0.0142	60	305.37	0.001
21	432.82	0.0036	61	303.38	0.0021
22	419.54	0.0028	62	302.48	0.0002
23	414.13	0.003	63	300.6	0.0045
24	408.86	0.0101	64	298.44	0.0004
25	402.4	0.0017	65	297.61	0.0015
26	399.57	0.0001	66	296.39	0.0025
27	397.4	0.0008	67	293.6	0.0004
28	395.4	0.0036	68	293.34	0.0013
29	390.08	0.0001	69	292.82	0.0002
30	386.28	0.0036	70	291.72	0.0025
31	385.66	0	71	291.3	0.0019
32	384.24	0.0026	72	290.56	0.0022
33	383.99	0.013	73	286.53	0.0014
34	378.51	0.0022	74	285.77	0.0163
35	368.89	0.0008	75	284.37	0.0005
36	366.77	0.0002	76	282.99	0.0064
37	364.02	0	77	282.72	0.0078
38	362.7	0.0349	78	281.86	0.0306
39	359.02	0.005	79	281.19	0.0062
40	358.43	0.0024	80	280.51	0

S8. References

1. Q. Yin, R. Tong, Y. Xu, K. Baek, L. W. Dobrucki, T. M. Fan and J. Cheng, *Biomacromolecules*, 2013, **14**, 920-929.
2. Y. Lu, L. Yin, Y. Zhang, Z. Zhang, Y. Xu, R. Tong and J. Cheng, *ACS Macro Lett.*, 2012, **1**, 441-444.
3. O. Thillaye du Boullay, C. Bonduelle, B. Martin-Vaca and D. Bourissou, *Chem. Commun.*, 2008, 1786-1788.
4. O. Thillaye du Boullay, E. Marchal, B. Martin-Vaca, F. P. Cossío and D. Bourissou, *J. Am. Chem. Soc.*, 2006, **128**, 16442-16443.
5. A. Buchard, D. R. Carbery, M. G. Davidson, P. K. Ivanova, B. J. Jeffery, G. I. Kociok-Koehn and J. P. Lowe, *Angew. Chem. Int. Ed.*, 2014, **53**, 13858-13861.
6. D.-Y. Lee and J. F. Hartwig, *Org. Lett.*, 2005, **7**, 1169-1172.
7. C. K. Williams, L. E. Breyfogle, S. K. Choi, W. Nam, V. G. Young, M. A. Hillmyer and W. B. Tolman, *J. Am. Chem. Soc.*, 2003, **125**, 11350-11359.
8. N. J. Brown, J. E. Harris, X. Yin, I. Silverwood, A. J. P. White, S. G. Kazarian, K. Hellgardt, M. S. P. Shaffer and C. K. Williams, *Organometallics*, 2014, **33**, 1112-1119.
9. B. M. Chamberlain, M. Cheng, D. R. Moore, T. M. Ovitt, E. B. Lobkovsky and G. W. Coates, *J. Am. Chem. Soc.*, 2001, **123**, 3229-3238.
10. A. M. Bryan, G. J. Long, F. Grandjean and P. P. Power, *Inorg. Chem.*, 2013, **52**, 12152-12160.
11. A. Panda, M. Stender, M. M. Olmstead, P. Klavins and P. P. Power, *Polyhedron*, 2003, **22**, 67-73.
12. A. J. Chmura, M. G. Davidson, C. J. Frankis, M. D. Jones and M. D. Lunn, *Chem Commun*, 2008, 1293-1295.
13. Y. Sun, Z. Jia, C. Chen, Y. Cong, X. Mao and J. Wu, *J. Am. Chem. Soc.*, 2017, **139**, 10723-10732.
14. T. K. Saha, V. Ramkumar and D. Chakraborty, *Inorg. Chem.*, 2011, **50**, 2720-2722.
15. W. J. Evans, M. A. Johnston, C. H. Fujimoto and J. Greaves, *Organometallics*, 2000, **19**, 4258-4265.
16. D. F. Evans, *J. Chem. Soc.*, 1959, 2003-2005.
17. Y. Zhong, Q. Feng, X. Wang, J. Chen, W. Cai and R. Tong, *ACS Macro Lett.*, 2020, **9**, 1114-1118.
18. R. R. Gagne, C. A. Koval and G. C. Lisensky, *Inorg. Chem.*, 1980, **19**, 2854-2855.
19. V. V. Pavlishchuk and A. W. Addison, *Inorg. Chim. Acta*, 2000, **298**, 97-102.
20. J. W. Tucker and C. R. J. Stephenson, *J. Org. Chem.*, 2012, **77**, 1617-1622.
21. D. Rehm and A. Weller, *Israel J. Chem.*, 1970, **8**, 259-271.
22. Q. Feng and R. Tong, *J. Am. Chem. Soc.*, 2017, **139**, 6177-6182.
23. R. Wang, J. Zhang, Q. Yin, Y. Xu, J. Cheng and R. Tong, *Angew. Chem. Int. Ed.*, 2016, **55**, 13010-13014.
24. T. J. Deming, *J. Am. Chem. Soc.*, 1997, **119**, 2759-2760.
25. T. J. Deming and S. A. Curtin, *J. Am. Chem. Soc.*, 2000, **122**, 5710-5717.
26. C. K. Prier, D. A. Rankic and D. W. C. MacMillan, *Chem. Rev.*, 2013, **113**, 5322-5363.
27. K. R. Dunbar and S. C. Haefner, *Inorg. Chem.*, 1992, **31**, 3676-3679.